Non-host resistance-associated proteome changes in citrus-*Xanthomonas* interactions

Thesis submitted to the University of Hyderabad for the award of

Doctor of Philosophy

by

T. Swaroopa Rani

(Regd No. 07LPPH10)

Department of Plant Sciences

University of Hyderabad

Hyderabad-500046

India

July, 2013

University of Hyderabad

(A Central University established in 1974 by an act of parliament)
HYDERABAD-500 046, INDIA

DECLARATION

I, T. Swaroopa Rani, hereby declare that this thesis entitled **"Non-host resistance-associated proteome changes in citrus-*Xanthomonas* interactions"** submitted by me under the guidance and supervision of **Prof. Appa Rao Podile** is an original and independent research work. I also declare that it has not been submitted previously in part or in full to this University or any other University or Institution for the award of any degree or diploma.

T. Swaroopa Rani
(07LPPH10)

Prof. Appa Rao Podile
(Research Supervisor)

University of Hyderabad

(A Central University established in 1974 by an act of parliament)

HYDERABAD-500 046, INDIA

CERTIFICATE

This is to certify that this thesis entitled **"Non-host resistance-associated proteome changes in citrus-Xanthomonas interactions"** is a record of bonafied work done by **Ms. T. Swaroopa Rani** a research scholar for Ph.D. programme in Department of Plant Sciences, School of Life Sciences, University of Hyderabad under my guidance and supervision.

Prof. Appa Rao Podile

(Research Supervisior)

Head,

Department of Plant Sciences

Dean,

School of Life Sciences

CONTENTS

Acknowledgement

I take immense pleasure in thanking Prof. Appa Rao Podile, who had been a source of inspiration and role model in any given way, for constant moral and personal support and guidance throughout my doctoral research. The leadership and critical assessment capabilities of Prof. Podile, allowed me to mobilize collective knowledge and capacity in the best way possible and created an enabling environment to complete this work.

I thank the present and former Deans, School of Life Sciences, Prof. R. P. Sharma and Prof. M. Ramanadham, the present and former Heads, Department of Plant Sciences Prof. Ch. Venkataramana and Prof. A. R. Reddy for allowing me to use the facilities of the School and the Department.

I sincerely acknowledge the infrastructural support provided by UGC-SAP, DST-FIST, DBT-CREBB, to the Dept. of Plant Sciences and UoH BBL, DBT-CREBB and DST-INSPIRE for the research fellowship.

This thesis is not only the result of my scientific works but the outcome of a long road and I am glad to acknowledge everyone who has contributed to the build-up of my scientific personality and therefore, to the completion of this thesis.

My heartfelt thanks are also due to my former colleagues of MPMI group Dr. Anil Kondreddy, Dr. B. Sashidhar, Dr. V. L. Vasudev, Dr. P. Purushotham, Dr. K. Suma, Dr. Ch. Neeraja, Dr. Debashish Dey and Dr. Swarnalee Dutta, for their timely help and constant encouragement.

I would like to mention my colleagues Sippy, Uma, Sharma, Das, Manjeet, Madhu, Rambabu, Papa Rao, Durgesh, Sandhya, Sravani, Dr. Sadaf, Dr. Suvarna, and Dr. Jalaja who have made the my stay always cheerful in HCU.

I would like to thank all my dearest friends who supported me in every situation and encouraged me a lot.

My heartfelt thanks to Prof. Uemura Matsuo for allowing me to carry part of research work in his lab and thank Mr. Daisuke for the help in performing non-gel-based proteomics.

I am thankful to Mrs. Monica and Mrs. Kalpana for their help in using proteomic facility.

This dissertation work at MPMI group could never run smoothly without the help I got from Narasimha, Malla Reddy, Devaiah and Seetaram for their assistance in the lab and in the green house.

I am thankful to all my batch mates and other research scholars of the School of Life Sciences for their timely help.

I highly acknowledge the efforts of Ramesh, Mohan Rao and Sudarshanam and other non-teaching staff of Dept. of Plant Sciences.

Saving the most important for the last, I would like to express my heartfelt thanks to my beloved parents Sri. T.V. Rami Reddy and Smt. Rajeshwari and my brothers Suresh, Srinivas and my grandparents for their blessings, wishes, support and constant encouragement throughout my research career.

T. Swaroopa Rani

Dedicated to

my mother

Smt. T. Rajeshwari

ABBREVIATIONS

°C	: degree centigrade/degree Celsius
µg	: microgram
µM	: micromolar
•OH	: hydroxyl radicals
2-DE	: 2-dimensional electrophoresis
A	: absorbance
ACN	: acetonitrile
APX	: ascorbate peroxidase
ATP	: adenosine tri phosphate
avr	: avirulence
BSA	: bovine serum albumin
CHAPS	: 3-[(3-cholamidopropyl)dimethylammonio]-2-hydroxy-1-opanesulfonate
CHCA	: α-cyano-4-hydroxycinnamic acid
CV	: coefficient of varience
CW	: cell wall
DAB	: 3,3'-diaminobenzidine
dai	: days after inoculation
DMSO	: dimethyl sulfoxide
DNA	: deoxy ribonucleic acid
DTT	: dithiothreitol
ECM	: extracellular matrix
EDTA	: ethylene diamine tetra acetic acid
EST	: expressed sequence tag
ET	: ethylene
ETI	: effector-triggered immunity
ETS	: effector-triggered susceptibility
FBPase	: fructose 1,6 bisphosphatase
g	: gram
GST	: glutathione S-transferase
h	: hour(s)
H_2O_2	: hydrogen peroxide
HEPES	:4-(2-hydroxyethyl)-1-piperazine ethanesulfonic acid
hpi	: hours post inoculation
HR	: hypersensitive response
HSP	: heat shock protein
IEF	: isoelectric focusing
JA	: jasmonic acid
kDa	: kilodalton
L	: litre
LC	: liquid chromatography
M	: molar
MALDI-TOF	: matrix-assisted laser desorption/ionization-time of light
MAPK	: mitogen-activated protein kinase
MDA	: malonic dialdehyde
MDH	: malate dehydrogenase
mg	: milligram
$MgCl_2$	: magnesium chloride
min	: minute(s)

MIR	: miraculin
ml	: milliliter
mM	: millimolar
MS	**:** mass spectrometry
MWt	: molecular weight
NBT	: nitro-blue tetrazolium
NH_4HCO_3	: ammonium bicarbonate
NHR	: non-host resistance
nm	: nanometers
NPs	: nuclear proteins
O.D.	: optical density
$O_2^{\cdot -}$	: superoxide radicals
OEE	: oxygen evolving enhancer
PAGE	: polyacrylamide gel electrophoresis
PAL	: phenylalanine ammonia-lyase
PAMP	: pathogen-associated molecular patterns
PCD	: programmed cell death
PEN	: penetration
PGK	: phosphoglycerate kinase
pI	: isoelectric point
PM	: plasma membrane
PMSF	: phenyl-methyl sulphonyl fluoride
PRX	: peroxidase
PR proteins	: pathogenesis-related proteins
PRRs	: Pattern recognization receptors
PTI	: PAMP-triggered immunity
PTM	: post-translational modification
PVP	: polyvinylpyrrolidone
R gene	: resistance gene
Rbcl	: rubisco larger subunit
RNA	: ribonucleic acid
ROS	: reactive oxygen species
SA	: salicylic acid
SAR	: systemic acquired resistance
SDS	: sodium dodecyl sulphate
SE	: soluble-ECM
SNARE	: soluble N-ethylmalemide-sensitive attached receptor
SOD	: superoxide dismutase
STK	: Serine/threonine kinase
TBARS	: thiobarbituric acid reactive substances
TEMED	: tetramethylethylenediamine
TFA	: trifluoroacetic acid
TFs	: transcription factors
Tris	: tris-(Hydroxymethyl) aminoethane
V	: volume
W	: weight
WE	: wall-bound ECM
Xac	: *Xanthomonas axonopodis* pv. *citri*
Xoo	: *Xanthomonas oryzae* pv. *oryzae*
XTH	: xyloglucan endotranshydrolase/glucosylase

List of figures

List of tables:

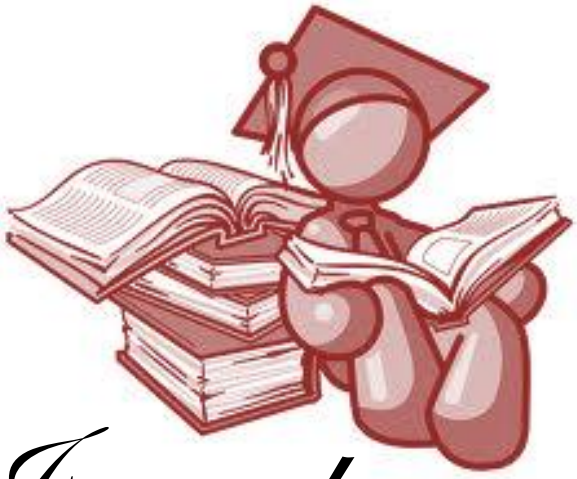

Introduction

1.1. Outcome of plant-pathogen interaction:

Unlike animals, plants are sessile and adopted many strategies to protect themselves from invading enemies. Pathogens are one of the prevalent stresses to plants. Most plant diseases are caused by fungi, bacteria, and viruses. The term disease refers to the destruction of live plants, caused by pathogens. Any environmental factor that favors the growth of parasites or disease transmitters or that is unfavorable to the growth of the plants will lead to increase in the likelihood of infection and the amount of destruction caused by parasitic disease. Parasitic diseases are spread by dissemination of the agent itself (bacteria and viruses) or of the reproductive structures (the spores of fungi). Wind, rain, insects, humans, and other animals may provide the means for dissemination.

The plant–pathogen molecular interaction provides a strong conceptual framework for understanding how these organisms coexist. Plants have evolved innate immune systems that recognize the presence of potential pathogens and initiate effective defense responses, whereas successful pathogens have evolved effector proteins that can suppress host immune responses. Furthermore, effectors can themselves act as elicitors and can be disabled by the host. Overall, the pathogenic niche is highly evolved and carefully monitored by both participants.

Plants, in nature, are generally resistant to most pathogens. The ability of a pathogen to cause disease in a host plant is usually the exception, not the rule. This is due to the specific nature of plant-pathogen interactions, where only a few well adopted microbes can infect a targeted plant species. The outcome of plant-pathogen interaction leading to disease is termed as compatible interaction and the susceptible plant species (Fig 1.1) is known as host to this pathogen. In incompatible interaction, plant resistance (R) gene products recognize avirulence gene (*avr*) products of adopted pathogen and confer narrow spectrum of resistance (Zimmerli et al. 2004; Dangl and Jones, 2001; Holub, 2001). Another less explored plant-pathogen interaction is the non-host interaction, where an entire plant species shows resistance to an entire pathogen species. The plant that is resistant to all isolates of a particular pathogen is known as non-host plant and the pathogen as non-host pathogen to all the members of a plant species, and dictates the most robust form of plant immunity (Jones and Takemoto, 2004; Mysore and Ryu, 2004; Thordal-Christensen, 2003; Heath, 2000). Multiple layers of defense responses involving

interplay of both constitutive barriers and inducible reactions are involved in non-host resistance (NHR) (Nurnberger and Lipka, 2005). The potential of NHR in conferring broad spectrum and durable resistance in plants necessitates the importance in understanding the molecular mechanisms involved in this form of resistance.

1.2. The challenging road to disease:

Plant–pathogen interactions are complex. In response to attack by pathogens, plant can mount several defense barriers. Pathogen has to overcome many obstacles, to get access in to plant, to cause disease (Fig 1.2). Initial requirement for plant disease is basic compatibility, where appropriate cues from the plant are required for inducing cell differentiation and expression of essential pathogenicity genes. For instance, surface topology and wax composition of plants determine whether plants are hosts or non-hosts. Pre-existing physical or chemical barriers, such as the presence of trichomes and waxy cuticles or toxic secondary metabolites of plant form the early obstacles for the pathogen. In most of the cases, these preformed barriers are sufficient to resist the plant from invading pathogens. However, on failure of this second obstacle, plants can activate additional defense responses, often called as induced defense.

General elicitors released during attack by pathogen induce structural and physical defenses, such as the thickening of cell walls, chemical defenses and production of antimicrobial compounds. The important hallmarks of a successful adapted pathogen are its ability to cross the above three obstacles and enter the host tissue to establish feeding structures, derive nutrition from the host and finally to complete its life cycle. If the pathogen is successful, then the next two obstacles faced by the pathogen are based on classical gene-for-gene interactions. At the 6^{th} obstacle, host pathogens are recognized on the basis of individual pairs of *avr* and *R* genes. A non-host pathogen expressing two or more *avr*-genes that mediate recognition in all genotypes of a plant species will fail to overcome the 5^{th} obstacle and never reach the 6^{th} obstacle (Thordal-Christensen, 2003). So, NHR operates at at least 5 different levels before race-specific resistance (Fig 1.2). Disease occurrence in plants is rare, mostly because of these 5 different defense layers that are involved in execution of NHR.

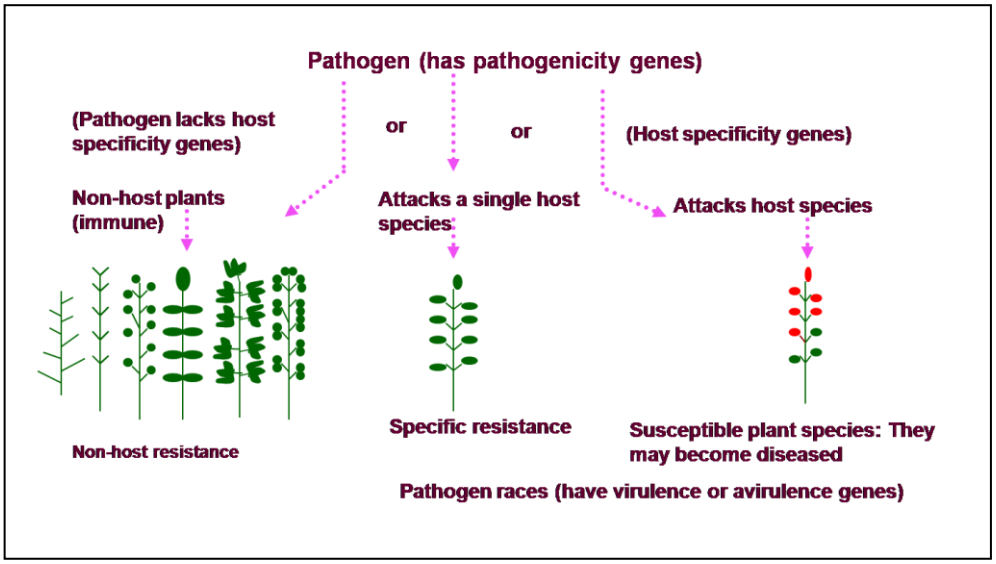

Redrawn from Sharma PD, Plant Pathol. (2004)

Fig 1.1: Schematic representation of general interactions of a pathogen with its host and non-host plants

Plants are surrounded by pathogens. All the pathogens cannot cause disease to plants, as plants have certain, but not always, levels of possible, unspecific resistance that is effective against each of their pathogens. Such resistance is called as geneeral or nonspecific or non-host resistance controlled by many genes also called as polygenic resistance. During co-evolution pathogens have evolved with virulent genes that condition growth and disease on particular plants. In turn plants have evolved with resistant (R) genes that can recognize effectors of pathogens and lead to specific resistance.

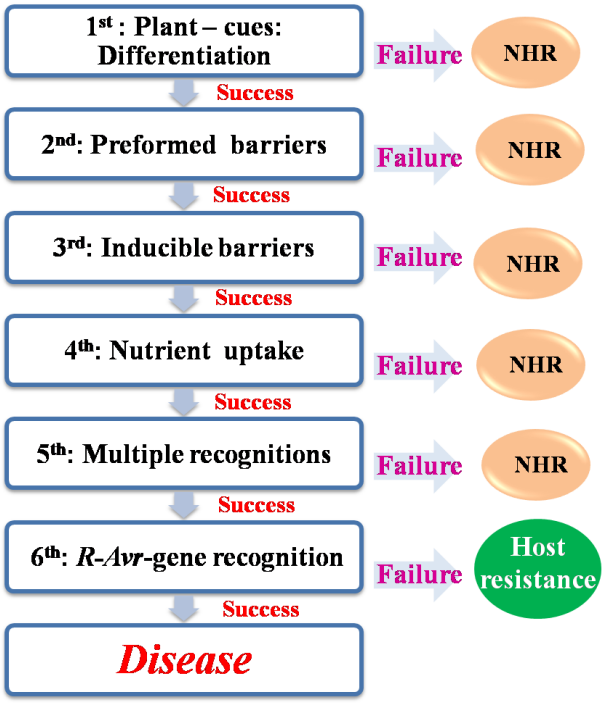

Redrawn from Thordal-Christensen, Curr. Opin. Plant Biol. (2003)

Fig 1.2: A simplified representation of the obstacles faced by of the pathogen during an attempt to cause disease

Stages at which non-host and host resistance can be manifested are indicated in the right. When a pathogen comes in contact with plant, the initial requirement for pathogen, is to obtain appropriate cues from the plant for inducing cell differentiation and expression of essential pathogenicity genes. Later pre-existing physical or chemical barriers acts as secondary obstracle. If pathogen succeeds at this second obstacle, plants can activate additional defense responses, often called as induced defense such as thickening of cell walls, chemical defenses and production of antimicrobial compounds. If pathogen fails to cross this barrier then it leads to NHR. If the pathogen overcomes the third obstacle then pathogen has to gain access to derive nutrition from the host complete its lifecycle. If the pathogen is successful then the next two obstacles faced by the pathogen are based on classical gene-for-gene interactions. At the 6th obstacle, host pathogens are recognized on the basis of individual pairs of *avr* and *R* genes.

1.3. NHR in plants to microbial pathogens:

1.3.1. Types of NHR:

NHR is a complex phenomenon in which the invading pathogen is restricted at various levels. Based on the execution of hypersensitive reaction (HR) and the layer at which the pathogen entry is restricted, NHR has been classified into two types (Mysore and Ryu, 2004). In type-I NHR, the non-host pathogens are restricted at the plant surface without HR symptoms (Fig 1.3A), while type II NHR is always associated with rapid localized necrotic HR (Fig 1.3B). Type I is most common form of NHR (Lu et al. 2001), in which the non-adapted pathogen is not able to overcome the preformed and general elicitor-induced plant defense responses such as cell wall (CW) thickening, papilla formation, accumulation of phytoalexin and other plant secondary metabolites. During type II NHR, the non-adapted pathogen is able to overcome preformed and general elicitor-induced plant defense responses, probably by producing detoxifying enzymes. Specific pathogen elicitors are then recognized by the plant surveillance system and this triggers plant defense leading to a HR. Pathogenesis-related (PR) gene expression as a component of systemic acquired resistance (SAR) can be induced by general elicitors of the non-adapted pathogen and also during type II NHR. The same plant species can exhibit both types of NHR (Peart, 2002), and the same pathogen can trigger different NHR types in different plant species (Lu et al. 2001).

1.3.2. Pathogen recognition by non-host plants:

When pathogen manages to overcome constitutive defense layers of non-host, it gets subjected to recognition at the plant cell surface and activates inducible plant defense responses. Activation of inducible plant defense responses is probably brought about by the recognition of invariant pathogen-associated molecular patterns (PAMP) that are characteristic of different classes of microorganisms or by surveillance of host cellular intactness. PAMPs are recognized at the cell surface by cognate PAMP recognization receptors (PRRs) and induce a surplus of defense responses referred to as PAMP-triggered immunity (PTI) leading to basal or NHR in plants. PTI plays a major role in NHR (Schwessinger and Zipfel, 2008). Basal disease resistance at the first glance is PTI

plus weak ETI (effector-triggered immunity) minus ETS (effector-triggered susceptibility) (Godfrey and Rathjen, 2012; Zipfel, 2009; Zhou and Chai, 2008; Jones and Dangl, 2006). General elicitors like Pep-13, N-terminal 22-mer fragment of eubacterial flagellin (flg22), a cold-shock-inducible RNA-binding protein, *Phytophthora* CW transglutaminase, lipopolysaccharide (LPS) (Felix and Boller, 2003; Nürnberger et al. 1994) and breakdown products of the plant CW (endogenous elicitors) that are probably released by attacking phytopathogenic microbes (Vorwerk et al. 2004) are able to induce innate immune responses in various plants.

Inducible structural barrier called as papilla restricts further entry of pathogen. Antimicrobial compounds are targeted to papilla by vesicle trafficking and cytoskeleton reorganization. If the pathogen overcomes inducible defense response by means of secreted effectors that suppress PTI responses, then plant respondss to pathogenic invasion by recognizing strain-specific effectors by triggering ETI. Genes involved in R-gene mediated resistance actively take part in ETI leading to the activation of defense signalling hormones and finally HR. Both PTI and ETI play in the NHR of plant species against non-adaptive or non-host pathogens. It is speculated that PTI and ETI play an increasingly major and a minor role, respectively, in conferring NHR as the evolutionary distance between the non-host and the non-host pathogen species widens (Schulze-Lefert and Panstruga, 2011), and *vice versa*.

1.3.3. Signal transduction during NHR:

Recognition of the pathogen triggers activation of signal transduction cascade and transcriptional changes. Early events in the cascade involve ion fluxes, protein phosphorylation, enhanced cytosolic Ca^{2+} concentrations, Ca^{2+}-dependent protein kinases, mitogen-activated protein kinase (MAPK), extracellular adenosine triphosphate (eATP), and reactive oxygen species (ROS) accumulation (Huckelhoven, 2007). Ca^{2+} influx is essential for alkalinization of apoplast and initial ROS accumulation (Blume et al. 2000; Grant et al. 2000). MAPKs are important in cross-talk during stress signalling that result in protection against microbial invasion (Meng and Zhang, 2013; Jonak et al. 2002; Nurnberger and Scheel, 2001; Zhang and Klessig, 2001). A set of loss and gain-of-function experiments performed in tobacco or *Arabidopsis*, revealed the causal links between MAPK activation, expression of PR genes and the initiation of programmed cell

death (PCD) (Nürnberger et al. 2004; Jonak et al. 2002; Ren et al. 2002; Zhang and Klessig, 2001). In *Nicotiana benthamiana*, virus-induced gene silencing of NbSIPK and NbWIPK (orthologues of AtMPK6 and AtMPK3, respectively) allowed multiplication of non-host bacterium *Pseudomonas cichorii*, revealing the importance of MAPK in NHR (Sharma et al. 2003). High-throughput over expression and NbMKK1-silencing in *N. benthamiana* further confirmed the role of MAPKs in controlling NHR (Takahashi et al. 2007).

1.3.4. Role of plant hormones in NHR:

Plant hormones like salicylic acid (SA), jasmonic acid (JA) and ethylene (ET) appear to be involved in later signaling events of induced immune response. Mutant analysis of *Arabidopsis*, defective in SA (sid2), JA (jar1) and ET-mediated defense signalling pathways, has demonstrated the role played by hormones in non-host interactions (Zimmerli et al. 2004; Knoester et al.1998). Microarray analysis in *Arabidopsis* has illustrated that the host powdery mildew and the non-host barley powdery mildew elicits different JA/ET responses (Zimmerli et al. 2004). In *Arabidopsis*, SA signalling pathway mutants like *eds1*, *pad4*, and *eds5* compromised resistance against *Xanthomonas citri* subsp. c*itri*, indicating the critical role of SA signalling pathway in regulating non-host defense (An and Mou, 2012). Sunflower rust fungus (*Puccinia helianthi)* failed to form haustoria on any of the *Arabidopsis* mutants lacking the production of SA and JA/ET. Different non-host *Uromyces* sps. displayed different penetration frequencies on these *Arabidopsis* mutants. This was attributed to strong expression of wall-associated defense responses which are not induced by *Uromyces* species (Mellersh and Heath, 2003). Mysore and Ryu (2004) showed the crucial importance of JA, ET and SA not only in cultivar specific resistance, but also in maintenance of NHR in specific plant-non-host microbe interactions.

1.3.5. Role of cytoskeleton and vesicle trafficking in plant defense:

During non-host plant-pathogen interactions, polarized accumulation of defense compounds at the pathogen intruding site depends on cytoskeletal rearrangements and secretory processes (Lipka and Panstruga, 2005; Schmelzer, 2002). Secretory vesicles are involved in poisoning of apoplast by transporting secondary metabolites to sites of incipient pathogen ingress. A striking example supporting this hypothesis comes from

studies of non-host interaction between sorghum (*Sorghum bicolor*) and *Colletotrichum graminicola*, wherein accumulation of red-colored 3-deoxyanthocyanidin phytoalexin takes place at pathogen ingression areas (Snyder et al.1991; Snyder and Nicholson, 1990). The polarized transport correlates with a reorganization of the actin cytoskeleton and results in a chemical CW reinforcement that involves binding by ether linkages of vesicle-transported hydroxycinnamic acid amides (McLusky et al. 1999). It is thought that the actin cytoskeleton plays a pivotal role for cell polarization process by providing tracks for organelle and vesicle traffic during compatible, incompatible and non-host interactions (Takemoto et al. 2003). By the inhibition of actin polymerization using cytochalasins, *Erysiphe pisi* penetrated and formed haustoria in non-host plant barley, but there was no disease because of HR (Kobayashi et al. 1997).

A meticulous screening of *Arabidopsis* mutants defective in pre-haustorial responses, led to the identification of penetration (PEN) genes encoding secretion-associated and efflux-associated proteins like plasma membrane (PM) -resident PEN1 syntaxin, PEN2 myrosinase, and PM-resident PEN3 ABC transporter (Underwood and Somerville, 2013; Stein et al. 2006; Lipka et al. 2005; Collins et al. 2003). All three PEN genes are also involved in secretion and accumulation of anti-microbial components to the papillae (Fig 1.4). In *Arabidopsis*, at sites of attempted penetration by non-adapted *Blumeria graminis* pv. *hordei*, soluble N-ethylmalemide-sensitive attached receptor (SNARE) domain-containing PEN1 syntaxin, SNAP33 and VAMP721/722 assemble into a ternary SNARE complex bind secretory vesicles containing unknown cargo to the plant PM and secretes the cargo to the site of pathogen invasion (Fig 1.4) (Kwon et al. 2008). Accumulation and sequential action of PEN-2-derived indole glucosinotes (group of tryptophan-derived compounds), hydrolysis products and camelexin were important in NHR (Sanchez-Vallet et al. 2010; Bednarek et al. 2009).

In *pen1* mutants delay in papillae formation resulted in decreased penetration resistance but without disease development indicated that, PEN1/*Hv*ROR2 is not the only component of complex NHR mechanisms (Assaad et al. 2004). Entry rates of pathogen were twice in double mutant of *pen1pen2*, when compared to single mutants of either *pen1* or *pen2* (Lipka et al. 2005) suggesting that *PEN1* and *PEN2* act in separate defense pathways. PEN3/PDR8 may be involved in exporting toxic materials to attempted invasion sites, and intracellular accumulation of these toxins in *pen3* mutants may

secondarily activate the SA pathway (Stein et al. 2006). Vesicle trafficking-mediated extracellular accumulation of toxic antimicrobial compounds, though, could be contained within the papillary CW scaffold, might form a fine-tuned chemical and structural barrier against microbial intruders together with chemical cross-linking of the newly synthesized cell wall polymers (Kwon et al. 2008).

1.3.6. Oxidative burst restricts the entry and growth of non-host pathogens:

Inhibition of secretory system by the inhibitors like monensin, brefeldin A and N-ethylmaleimide shows differential inhibition of ROS production, suggesting the involvement of secretory components in generation of apoplastic H_2O_2 (Davies et al. 1991; Bolwell et al. 1999). CW or extracellular matrix (ECM) responds to environmental clues like biotic and abiotic stress through the release of signalling molecules like H_2O_2. The production of ROS like O_2^-, H_2O_2 and $HO\cdot$ in the cell, known as the "oxidative burst", is one of the earliest events detectable during the incompatible and non-host plant-pathogen interactions (Yoshioka et al. 2008). The ROS production modifies CW components by the process of CW softening/stiffing and antioxidative status of the cell initiating downstream signalling, to control plant growth and restrict the growth of pathogens. The major sources of ROS could be PM-localized NADPH/NADH-dependent, generating superoxide, or CW-localised peroxidase-dependent, generating H_2O_2 (Bolwell, 1999). Subcellular production of ROS also plays a role in NHR (Zurbriggen et al. 2009). Several lines of evidence from various plant species suggest that the sources of ROS are different during NHR and during incompatible interaction, but may interact with each other. Different plants exhibit different oxidative burst phases with an early production of ROS in both compatible and incompatible interactions (Apel and Hirt, 2004; Grant et al. 2000). Despite the similarities to host resistance, the involvement of ROS in non-host interactions may vary in terms of the intensity and timing of ROS bursts (Able et al. 2003; Huckelhoven et al. 2001).

1.3.7. The NHR and gene-for-gene interactions appear to have links:

Accumulated evidences support the hypothesis that NHR is also determined by gene-for-gene interactions (Kobayashi et al. 1990; Whalen et al. 1988). Some non-host pathogens escape or overcome the preformed and inducible barrier, and further intrude in to the cell where the ingression of such pathogens is halted by the HR-mediated cell death (Fig

1.3B). This form of resistance is dependent on genes like *PAD4, EDS1, SAG101* linked to R-gene-mediated resistance (Lipka et al. 2005). Multiple *R* genes present in non-host plants may simultaneously recognize their corresponding *avr* gene-encoded products and thereby activate the plant surveillance system (Mysore and Ryu, 2004). *HSP70, HSP90* and *SGT1* stabilize R proteins and upstream of *EDS1* and also contribute to NHR in *N. benthamiana* (Kanzaki et al. 2003; Peart et al. 2002). The genes like *EDS1, PAD4, SAG101,* and *NHO1* are likely to participate in various non-host responses after penetration resistance has been breached.

Complete compromise of NHR was evident in *pen2 pad4 sag101* triple and *pen3eds1* double mutants but not in *pad4sag101* double mutant (Stein et al. 2006; Lipka et al. 2005; Zimmerli et al. 2004). NHR is severely compromised in *Arabidopsis* against *Bgt* when the actin cytoskeleton functions in combination with *eds1* (Yun et al. 2003). The silencing of SGT1 also compromised NHR against *Pseudomonas syringae* pv. *maculicola* and *Xanthomonas axonopodis* pv. *vesicatoria* (Peart et al. 2002). In Hsp70 and Hsp90 silenced plants, NHR was severely reduced against non-host pathogen *Pseudomonas cichorii* due to reduction in expression and HR (Kanzaki et al. 2003). Another mutational analysis of *Arabidopsis* indicated the involvement of specific gene NHO1 (glycerol kinase) in NHR against bacteria (Kang et al. 2003).

The absence of known *R* genes in plants does not result in susceptibility to non-host pathogens. *R* gene–mediated resistance certainly contributes to resistance in non-host interactions. In addition to gene-for-gene recognition, other mechanisms are likely to be involved. The basic compatibility associated with many potential pathogens reinforces the importance of plant defense mechanisms in non-host interactions. The major difference between NHR and incompatible interactions could be at the first barrier of the plant during pathogen recognition. The initial contact of the pathogen with ECM triggers a series of downstream signalling cascades. This contact point appears as the most crucial interacting platform for NHR.

1.3.8. Involvement of conventional cell death regulators in execution of NHR:

Cell death regulators play a crucial role in regulation of HR-mediated cell death in NHR. The identified cell death regulators involved in NHR are NbCD1, BAX inhibitor-1 (BI-1) and caspases (Fig 1.3B). NbCD1, a novel class II ethylene - responsive element

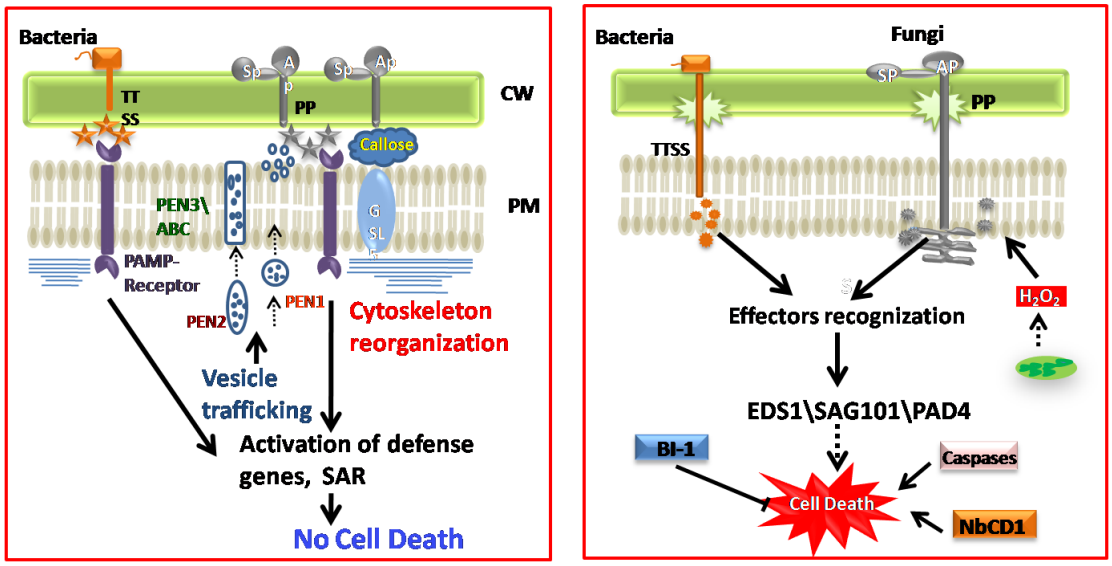

Adopted from Uma et al. J. Plant Physiol. (2011)

Fig 1.3: Schematic representation of types of NHR

A) In type I NHR- Receptors present at the of plant cell surface (e.g. PAMP, represented as stars) perceive exogenous signals and initiates downstream signalling events, like callose deposits, cytoskeleton reorganization and polarization of secretory components (PEN1, PEN2 and PEN3) to the pathogen entry site further restricting its entry without occurrence of cell death.

B) In type II NHR-The non-host pathogen overcome preformed and general elicitor induced plant defense responses, probably by producing detoxifying enzymes. Specific pathogen elicitors are then recognized by the plant's surveillance system, and this triggers plant defense reactions leading to cell death. EDS1, SAG101 and PAD4 genes, which are involved in R-gene mediated resistance, can also function in perceiving effector molecules (represented as stars below the PM) secreted by the non-host pathogen. H_2O_2 produced from suborganelles like chloroplasts can also restriction pathogen survival. Cell death regulators like BI-1 (Bax inhibitor 1), caspases and NbCD1 also play a role in triggering cell death.

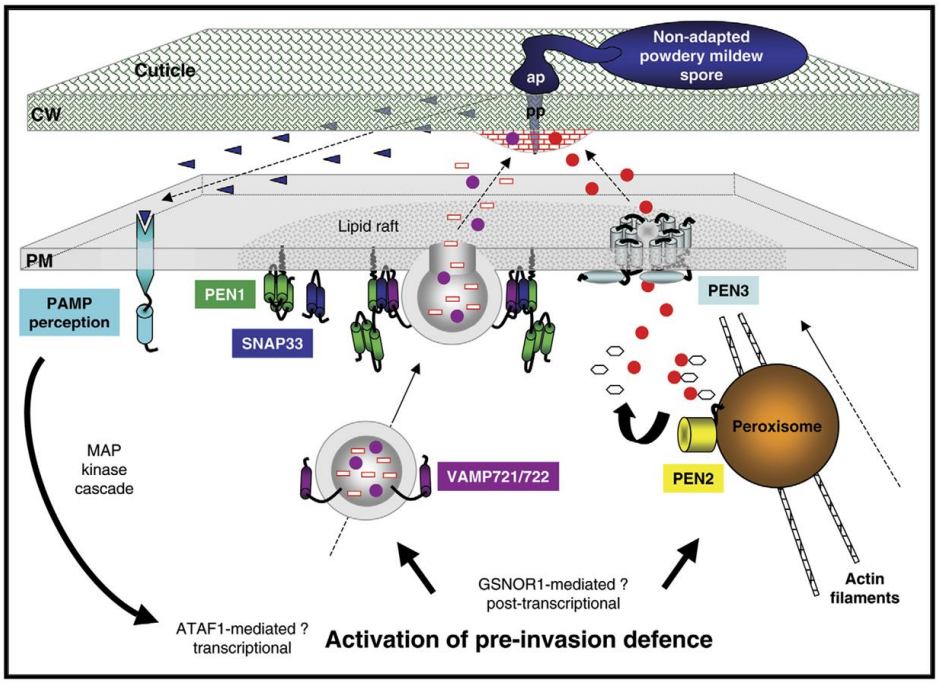

Adopted from Lipka et al. Curr. Opin. Plant Biol. (2008)

Fig 1.4: Schematic overview of mechanism of PEN genes in NHR

When a non-adopted Barley powdery mildew spores try to penetrate the cuticle and CW of non-host plant by means of appressorium (ap) and penetration peg formation (pp). PRR-mediated recognition of fungal PAMPs (blue triangles) is likely to induce MAP-kinase signalling and ATAF1-mediated (?) transcriptional activation of the pre-invasion defence machinery. Post-translational control (e.g. via GSNOR1-mediated S-nitrosylation) represents another regulatory layer. The PM-localised syntaxin PEN1 and ABC-transporter PEN3 accumulate in a lipid raft-like microdomain. PEN1 forms a SNARE complex with the membrane-anchored adaptor SNARE SNAP33 and endo-membrane-compartment-associated R-SNAREs VAMP721/722. SNARE complex formation drives secretion of cell wall precursors (red rectangles) and/or antimicrobial compounds (purple dots) at sites of attempted fungal invasion. PEN3 discharges potentially toxic aglycons (red dots) that were catalytically released from non-toxic glycosidic (black hexagons) precursors by PEN2 enzyme activity. PEN2 is associated with the periphery of peroxisomes. These are known to shuttle along a focally reorganised actin cytoskeleton. Together, PEN1/SNAP33/VAMP721/722- and PEN2/PEN3-mediated defence mechanisms contain the majority of fungal invasion attempts.

binding factor, is a potent inducer of the HR-like cell death and was expressed by treatments with non-host pathogen *P. cichorii* (Nasir et al. 2005). BI-1 proteins, suppressors of PCD, on overexpression of HvBI-1 in barley epidermal cells weakened CW–associated H_2O_2 formation, penetration resistance to appropriate and inappropriate *Blumeria graminis*, and *MLA12*- mediated post-penetration resistance (Eichmann et al. 2006; 2004). Inhibition of caspases, key executers of PCD, delayed HR in non-host plants like cowpea, french bean and in tobacco- *P. syringae* pv. *phaseolicola* non-host system but not in cowpea-rust fungus interaction. Cell death during non-host interactions requires caspase-like activity in several non-host combinations but not in incompatible host resistance (Christopher-Kozjan and Heath, 2003). These observations indicate the involvement of conventional cell death regulators in incompatible as well as non-host interactions.

The nature of NHR implies that it is broad-spectrum and durable; thus, it is of great interest to agriculture. Unraveling the mechanisms of NHR is also crucial for our understanding of host-specificity and the pathogenesis of phytopathogens. Though the involvement of different components in NHR is known, the mechanisms involved in the recognition of non-host pathogen, at the early stage of interaction and the execution of NHR, are not well understood. Most of the studies on NHR are focused at the gene expression level, where there is far less information available on their functional products. The possibility to use proteomics-based approaches to understand the network of the significant factors that would allow gain insights into the most neglected form of disease resistance, (NHR) is attractive.

1.4. Proteomics as a tool to study plant-pathogen interaction:

Proteomics has been used to gain an in-depth understanding of many aspects of the plant defense against pathogens. It has allowed monitoring the differences in abundance of proteins as well as posttranscriptional and post translational processes, protein activation/inactivation, and turnover (Zimaro et al. 2011). Proteomics also offers a window to study protein trafficking and routes of communication between organelles. Proteome of a particular cell represents a subset of all gene products. Proteomes are physicochemically highly heterogeneous, structurally complex and are modified both

spatially as well as temporally during interaction with the biotic and abiotic environments. An understanding of the mechanisms by which plants resist pathogen infection or mount a successful defense response is vital for a better and more detailed understanding of the molecular mechanism of these interactions. The information, thus obtained, will eventually enable alternative approaches to increase plants' immunity.

To gain an in-depth understanding of plant defense systems, there is a need to identify the diverse and complex signalling cascades and the multiple interacting biochemical pathways activated by the pathogen. Although, microarray provides the snapshot of all the genes at one time point, the level of specific mRNA does not necessarily predict the level of corresponding proteins. Proteomics is used as an ideal tool for understanding how complex biological processes occur at the molecular level, how they differ in various cell types, and how they are altered during interaction with microbes (Afroz et al. 2013; Mehta et al. 2008). The increasing genome sequences, expressed sequence tag (ESTs) databases, and the advancement of the mass spectrometry (MS) have benefied in the protein analysis and comparative proteomics. It has become a reliable approach to study the complex molecular phenomena mediating the resistance reactions of the plant against pathogen invasion.

1.4.1. Proteome profiling techniques:

Global patterns of gene expression can be analysed by performing protein analysis of cells or cell fractions by gel-based (such as 2DE, and 2DIGE) or gel- free approaches (liquid chromatography-based proteomics using isotopic labeling (such as ICAT and iTRAQ), followed by identification of proteins by MS (Fig 1.5). The work flow of gel-based comparative proteomic analysis principally consists of the extraction of desired proteomes, separation by gel electrophoresis, comparison of their differential expression with respect to pathogen attack, and the identification of the desired protein with matrix-associated laser desorption ionization time of flight (MALDI-TOF), electrospray ionization (ESI) and MS (Fenn et al. 1989; Karas and Hillenkamp, 1988). In gel-free approaches, protein identification and relative protein abundance are determined after protein identification using mass spectrometer in combination with software (Moresco et al. 2008). Gel-free techniques consist of two-dimensional liquid-phase chromatography that is based on a high-performance chromatofocusing in the first dimension followed by high-resolution reversed-phase chromatography in the second (Pirondini et al. 2006). In

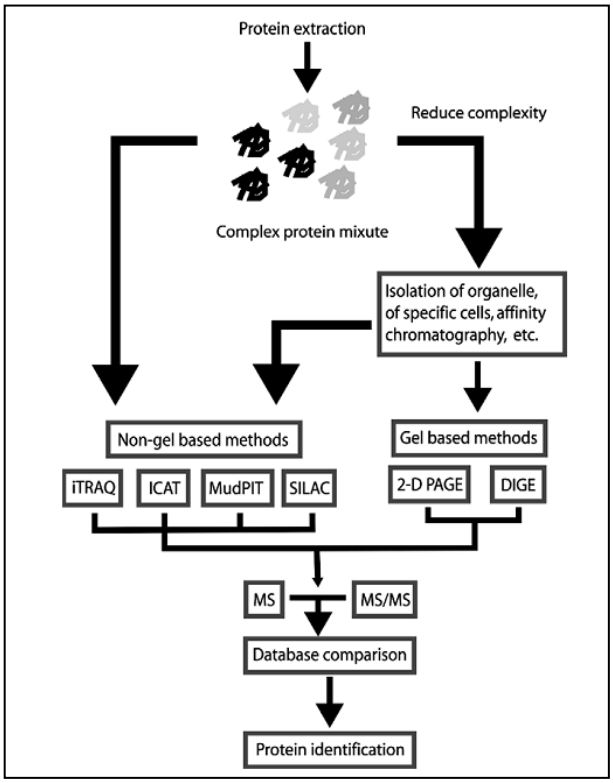

Adopted from Quirino et al. Phytochemistry (2010)

Fig 1.5: Schematic representation of the different approaches used in proteomic studies

Independent protein separation technologies (*i.e.*, non-gel based) are complementary to gel-based ones and together the different techniques allow for improved proteomic coverage. Complex proteome can be analysed by either gel-based or non-gel based protein separation methods followed by MS or MS/MS analysis. In 2-D PAGE and DIGE proteins are separated based on pI and molecular weight and they the most commonly used methods. In MudPIT, iTRAQ, SILAC and ICAT the proteomes analysis is dependent on liquid chromatography (*i.e.*, a strong cation exchange phase followed by a reversed phase chromatography).

an alternative technique, 1-DE-nanoscale capillary LC-MS/MS, namely, GeLC-MS/MS, that combines a size-based protein separation with an in-gel digestion of the resulting fractions. Between the LC-based strategies, there is a particular methodology, 'Multidimensional Protein Identification Technology' (MudPIT) that allows the detection of a much larger number of proteins compared to gel-based methods (Ye et al. 2007). Even though gel-based and gel-free techniques are powerfull in profiling proteome of the cell, each of the methods has its own limitations. Therefore, to have a comprehensive analysis of proteome changes, a combination of both the methods is preferable.

1.5. Total proteome analysis:

To investigate the role of defense-responsive proteins in the rice–*Xanthomonas oryzae* pv. *oryzae* (*Xoo*) interaction, a total leaf proteomic approach was applied (Mahmood et al. 2006). These analyses revealed differential induction of four defense-related proteins [PR-5, probenazole-inducible protein, superoxide dismutase (SOD) and peroxredoxin] during interaction with compatible and incompatible *Xoo* races. In another study, 26 differentially regulated defense proteins were identified in wild tomato species *Lycopersicon hirsutum* in response to the causal agent of bacterial canker (*Clavibacter michiganensis* ssp. *michiganensis*) by comparing two partially resistant lines and a susceptible control line (Coaker et al. 2004). The role of *X. axonopodis* pv. *citri* (*Xac*) plant-natriuretic-peptide in counteracting the shutdown of host photosynthesis during infection and the consequent maintenance of the host carbohydrate supply enabling prolonged biotrophic pathogen survival and colonization has been established in citrus through total leaf proteomics (Zimaro et al. 2011; Garavaglia et al. 2010).

Proteomic approach for analysis of NHR in plants was limited to a few studies. In NHR interaction of *Oryza sativa* against wheat leaf rust fungus, *Puccinia triticina*, proteins that participate in defense/stress responses, energy/carbohydrate metabolism, oxidation–reduction processes, protein folding/turnover, signal transduction and cell death regulation have been identified (Li et al. 2012).

1.6. Subcellular proteome analysis:

Proteomics studies at the sub-cellular level contribute to the elucidation of new

metabolic pathways as well as to functional differentiation of cells (Reumann et al. 2007; Majeran et al. 2005). New roles for organelles are emerging from sub-cellular proteomic studies (Reumann et al. 2007; Chivasa et al. 2002). A number of studies have examined proteins that are resident in different plant cell compartments, such as the chloroplast (Arai et al. 2008), mitochondria (Brugiere et al. 2004), nucleus (Bae et al. 2003), peroxisomes (Reumann et al. 2007), vacuole (Jaquinod et al. 2007), tonoplast (Schmidt et al. 2007), the PM (Santoni et al. 2000), endoplasmic reticulum (Maltman et al. 2007) and plant cell-wall (Robertson et al. 1997). The specific role of sub-organelles in defense response can also be understood through sub-organelle proteomics. One way to minimize some of the problems in profiling proteins during proteomic studies is to reduce the complexity of the protein sample, through sub-cellular proteomics. The identification of proteins recruited to subcellular compartments during stress will confer specific function of the organelle and gives an additional dimension to the proteome analysis.
Thus, complementary approaches such as total cell and sub-organelle proteome-based expression profiling provides a comprehensive picture of plant-pathogen interactions.

1.6.1. Extracellular matrix (ECM)-associated defense responses:

The ECM is a primary barrier and frontline of defense for pathogen entry and environmental changes, as it serves as a repository for most of the enzymatic, non-enzymatic and cell signalling-related components (Uma et al. 2011). The involvement of ECM as one of constitutive and inducible defense barriers through its structural and secretome changes during interactions with pathogens has been demonstrated (Jamet et al. 2008a).

Wang et al. (2012) demonstrated the importance of restricting nutrient availability in the apoplast during non-host-pathogen infection in order to arrest bacterial growth. Inducible non-host defense responses can occur through PTI or through ETI (Senthil-Kumar and Mysore, 2013). Inducible NHR responses are more efficient than preformed defenses and, therefore, understanding them is important to engineer durable disease-resistant crops (Heath, 2000). Mutants of *Arabidopsis* like *eds1, pad4*, and *eds5*, involved in SA signalling pathway, exhibited compromised resistance against *Xanthomonas citri* subsp. *citri*, indicating the role of SA signalling pathway in regulation of NHR (An and Mou 2012).

Activation of inducible plant defense responses is brought about by the recognition of invariant PAMPs at the plant cell surface including the ECM. The ECM is a primary barrier that functions as a frontline of defense strategy against pathogen entry. The ECM or apoplast is the total extracellular space external to the plasma membrane and comprises cell wall and the intercellular spaces (Agrawal et al. 2010). The fluid moving in the extracellular space is usually named apoplastic fluid. ECM is also a repository for most of the enzymatic, non-enzymatic and cell signalling-related components (Ringli 2010). The ECM-plasma membrane continuum-associated molecules are engaged in pathogen recognition and execution of plant defense responses (Uma et al. 2011). ECM is one of the constitutive and inducible defense barriers through structural and secretome changes during interactions with pathogens (Carpita and McCann 2000, Casasol et al. 2008, Dahal et al. 2010, Jamet et al. 2008a).

The plant CW is one of the distinguishing features and a dynamic structure that consists predominantly of polysaccharides. Plants possess less than 10% proteins of the total CW mass, relative to 90% polysaccharides, but still constitute several hundred in number (Jamet et al. 2008b). The structure and architecture of the primary cell wall describes the existence of interwoven networks of polysaccharides and proteins (Cosgrove, 2005). Histochemical analysis showed various differences on the constitutive level and changes after pathogen interaction on the level of pectic polysaccharide, though the differences could not conclusively explain the entire background of the resistance reactions (Wydra and Beri, 2006). Since proteins perform the enzymatic, regulatory and structural functions in biological systems the role of proteins secreted in to the plant CW by the plants and pathogen during the host-pathogen interactions can play vital roles in deciding the outcome of plant–microbe interactions.

In plant cells, many proteins undergo secretion or exocytosis to the ECM in order to maintain cell structure, regulate the external environment and as a part of signalling and defense mechanisms. In “classical” or “conventional” protein secretion, proteins containing a signal peptide are transported *via* the Golgi apparatus. In *Arabidopsis* genome, 18% of proteins are predicted to be secreted (the *Arabidopsis* Genome Initiative, 2000), but recurrently between 40 and 70% of the proteins identified in the secretome studies lack a signal peptide. Such proteins putatively belong to the class of leaderless secreted proteins (Ding et al. 2012). Extraction of wide range of ECM –

associated proteins to a substantial purity is a challenging task due to the structural complexities of the ECM and the nature of ECM-associated proteins (Jamet et al. 2008b).

Secretome analysis of *A. thaliana* has identified GDSL LIPASE1 (GLIP1) involvement in defense against *Alternaria brassicicola* (Oh et al. 2005). A stem cell wall proteomics of susceptible and resistant varieties of tomato, during interaction with *Ralstonia solanacearum,* has unveiled the understanding of the molecular basis of the host-pathogen interactions (Dahal et al. 2010). The extracellular proteome changes in *Arabidopsis* suspension cells during interaction with different genotypes of *P. syringae* has provided the possibility to directly compare the interactions resulting in basal resistance, susceptibility, and gene-specific resistance (Kaffarnik et al. 2009). *A. thaliana* apoplastic proteomics has led to the identification of key molecules involved in perception of pathogens and candidate proteins involved in response to oligogalacturonides (Casasoli et al. 2008). Thus, the plant ECM responds to pathogen invasion but the variation of ECM response towards host/non-host pathogen has not been explored. Understanding the variation of ECM response will provide clues regarding the mechanisms involved during compatible and non-host interactions. As proteins perform the enzymatic, regulatory and structural functions in a biological system, a time course study of comparative proteomic changes occurring at the ECM, during interaction with host and non-host pathogen interaction, will decipher the role of ECM-associated secretome in establishing the outcome of plant–microbe interactions.

1.6.2. Nucleus-associated defense responses:

Nucleus, the regulatory hub of the eukaryotic cell, is a dynamic system and a repository of various macromolecules that serve as modulators of cell signalling, dictates the cell fate decision. A constant flux of molecules with distinct regulatory functions through the envelope, make the nucleus one of the most important regulatory organelle within the cell, acting as the maestro in an enormous cell orchestra (Erhardt et al. 2010). The nucleus contains nearly all the genetic information required for the regulated expression of cellular proteins. It helps in shuttling of regulatory factors and gene product via the nuclear pore, aids in the production of mRNAs and ribosomes and organizes the uncoiling of DNA to replicate key genes. It coordinates innumerable pathways to achieve

growth, division and differentiation of the cell (Fink et al. 2008). It serves as the regulator in cell signalling for perceiving and transmitting extra- and inter-cellular signals in many cellular pathways. Communication between the cytoplasm and the nucleus is necessary and evident because of events such as apoptosis (Broers et al. 2002), mechanical stress (Dahl et al. 2008), environmental perturbation (Cheung and Reddy, 2012) and pathogen infection (Rivas, 2012), which lead to altered biosynthesis and modification of nuclear architecture and downstream cytoplasmic events. The dynamic nuclear organization, orchestrated by a complex network of nuclear proteins (NPs), is fundamental to an understanding of cellular development and physiology (Moriguchi et al. 2005).

Several hundred plant and animal NPs include both predicted and non-canonical candidates, are presumably associated with a variety of functions; *viz*., nucleoskeleton structure, development, DNA replication/repair, chromatin assembly/remodelling, signal transduction, mRNA processing, protein folding, transcription and splicing regulation, transport, metabolism, cell defense and rescue; all of which impinge on the complexity of NPs in plant and animal (Narula et al. 2013). Increasing evidence suggests that nearly $1/4^{th}$ of total cellular proteins are localized in the eukaryotic nucleus, implying a variety of functions (Pandey et al. 2006; Moriguchi et al. 2005). This indicates that an unexpectedly large number of proteins function in the nucleus. Changes in the nuclear proteome in varied cellular events (Abdalla and Rafudeen, 2012; Repetto et al. 2012, 2008; Cooper et al. 2011; Varma and Mishra, 2011; Abdalla et al. 2010; Choudhary et al. 2009; Buhr et al. 2008; Pandey et al. 2008; Henrich et al. 2007; Lee et al. 2006; Salzano et al. 2006; Bae et al. 2003) demonstrate that, the nuclear proteins are involved in diverse protective and signalling pathways with the protein function linked to the investigated stress condition. However, no nuclear or other organellar proteome information is available with respect to non-host pathogen interaction in plants. This nuclear proteome is of particular interest as it will provide a foundation for future investigation of the mechanisms involved in the execution of NHR.

1.7. Model system used to study NHR:

To learn more about the molecular mechanism involved in execution of NHR, citrus-*Xanthomonas* interactions were selected. Citrus canker is one of the most devastating

diseases of citrus, affecting many important citrus species such as grapefruit (*Citrus paradisis* Macf.), certain sweet oranges (*C. sinensis* (L.) Osbeck), Key lime (*C. aurantifolia* Swingle), and lemons (*C. limon* (L.) Burm. F.) (Gottwald et al. 1993). Citrus canker is caused by the Gram negative bacterium *Xanthomonas axonopodis* pv. *citri* (*Xac*) (Graham et al. 2004). Canker is a leaf spotting and rind blemishing disease and severe infection causes defoliation, shoot dieback and premature fruit drop, reducing yields by as much as 30% (Gottwald et al. 2002). Limited resistant scion germplasm resources and their interference in expression of optimum traits related to fruit quality and production is a major hurdle in development of canker-resistant citrus varieties (Viloria et al. 2004). In contrast, transgenic approach can quickly incorporate resistance into citrus without interfering with the expression of optimum varietal traits. The compatible interaction between citrus and *Xac* is a well established pathosystem, but the details of non-host interaction of citrus are less known. Here, an attempt was made to unravel NHR in citrus against rice pathogen *Xanthomonas oryzae* pv. *oryzae* (*Xoo).* To understand NHR, anatomical, biochemical and proteome-level changes occurring during citrus-*Xanthomonas* interaction were assessed. The proteome changes occurring in the whole cell and sub-organelles like ECM and nucleus were studied.

1.8. Objectives:

The work done in this study is sub-divided into four parts and described accordingly.

- ### Anatomical and biochemical changes during non-host interactions of citrus:

  We characterized citrus-*Xanthomonas* pathosystem using cytological staining methods to know, at what time point citrus is establishing defense response against *Xoo*. We performed aniline blue, trypan blue and DAB staining to investigate callose deposition, cell death and H_2O_2 accumulation during non-host interactions of citrus. The redox status of the cell during citrus-*Xanthomonas* interaction was also compared by performing enzyme assays for ROS generating and scavenging enzymes.

- ### Whole cell proteome changes during compatible and non-host interactions:

  A gel-based and non-gel-based proteomic approaches were adopted to identify and characterize the changes in abundance of whole cell proteins during NHR.

- ECM-associated proteome changes during citrus-*Xanthomonas* interaction:

  To have a comprehensive analysis ECM-proteome both disruptive and nondisruptive methods were followed to extract wall-bound and soluble ECM proteins. A gel based 2-DE complemented with MALDI-TOF MS/MS coupled with protein database searches was implemented to identify differentially induced citrus ECM proteome during *Xac* and *Xoo* interaction.

- Nuclear-associated proteome changes during non-host interaction of citrus:

  A 2-DE nuclear proteome maps image analysis and nano-LC-MS/MS analysis of citrus during both host and non-host interaction was analysed and differentially expressed proteins were identified.

Materials & Methods

2.0. Plant material and pathogen inoculations:

Citrus *sinensis* (L.) Osbeck sweet orange grafted on Rangpur lime (*C. limonia* Osb.) plants were obtained from a commercial Government certified nursery (Shiridi Sai Baba Nursery, Sangareddy, Andhra Pradesh, India) and maintained in green house at 26° C with a photoperiod of 16 h and controlled relative humidity. Plants were pruned for emergence of new flush and 22-28 day-old leaves were used in all experiments. *Xanthomonas* cultures were grown in peptone/sucrose broth (20 g/L sucrose, 5 g/L peptone, 0.5 g/L K_2HPO_4, 0.25 g/L $MgSO_4.7H_2O$, pH-7) at 28° C for 24 h. Log phase cells were harvested. The cell pellet was washed twice with 10 mM $MgCl_2$ and diluted to optical density (OD_{600}) 0.2 was used for leaf inoculation. Bacterial suspensions of *Xac*, *Xoo* and 10mM $MgCl_2$ (as mock) were infiltrated into abaxial surface of the leaf on both sides of the midrib with a needle less 1ml tuberculin syringe.

2.1. Anatomical and biochemical changes:

2.1.1. *In planta* bacterial growth:

For vesicle trafficking inhibition experiments 0.2 mM brefeldin A (Invitrogen) in 0.5% DMSO or 0.5% DMSO (Cernadas et al. 2008) was pre-infiltrated in citrus leaves. After 24 h, *Xac* and *Xoo* cultures of 0.2 (OD_{600}) were infiltrated in the pre-infiltrated regions. *In planta* bacterial growth was assessed by grinding 0.6 cm of bacterial infiltrated leaf discs in sterile water and serial diluted and plated on peptone/sucrose agar plates and incubated at 28°C for 3 days after inoculation (dai).

2.1.2. Callose deposition and cell death assay:

To examine callose deposition and cell death in *Xac*- or *Xoo*- challenged citrus leaves, aniline blue or trypan blue staining was performed. Callose deposition was analysed by destaining leaves in alcoholic lactophenol followed by staining in 0.01% aniline blue for 30 min and analyzed by Leica fluorescent microscope. Dead cells were stained according to Koch and Slusarenko (1990), by boiling leaves in lactophenol-trypan blue solution (10 ml lactic acid, 10 ml glycerol, 10 g phenol and 0.1% trypan blue dissolved in 10 ml of distilled water) for 30 min followed by decolorization in chloral hydrate solution (2.5 g dissolved in 1 ml of water) and visualized under light microscope.

2.1.3. Staining of H_2O_2 deposition:

H_2O_2 was detected *in situ* by 3,3'-diaminobenzidine (DAB) staining as described (Thordal-Christensen et al. 1997). Leaves collected at different hours post inoculation (hpi) after pathogen challenge were vacuum infiltrated with the DAB solution (1 mg/mL, pH 3.8; Sigma, St. Louis, MO). The sampled leaves were placed in a plastic box under high humidity until brown precipitate was observed (6 to 8 h) and then fixed with a solution of 3:1:1 ethanol:lactic acid:glycerol and photographed under light microscope.

2.1.4. Assay of H_2O_2 generation:

Leaf samples (0.5 g) were homogenised in ice-cold 0.1% trichloroacetic acid (TCA) and centrifuged at 12,000 g for 15 min at 4 °C. To 0.3 ml of supernatant 1.7 ml potassium phosphate buffer (pH 7.0) and 1ml of 1M potassium iodide (KI) solution were mixed and incubated for 5 min before measuring oxidation product at A_{390}. H_2O_2 concentration was calculated from a standard curve prepared from known concentrations of H_2O_2 and expressed as µmol g^{-1} fw (Velikova et al. 2000).

2.1.5. Lipid peroxidation:

Lipid peroxidation was measured in terms of malonic dialdehyde (MDA) content, a thiobarbitutric acid reactive substance (TBARS) as described by Heath and Packer (1968). Citrus leaf tissue (0.5 g) was homogenized in 0.25% thiobarbituric acid (TBA) in 10% TCA using mortar and pestle. The samples were heated at 95 ºC for 30 min and quickly cooled in an ice bath for 10 min and centrifuged at 10,000 g for 10 min. The A_{532} of the supernatant was read and interfering substances were corrected by subtracting A_{600}. Total TBARS were expressed in terms of nmol g^{-1} fresh weight using an extinction coefficient of 155 mM^{-1} cm^{-1}.

2.1.6. Leaf protein extraction for enzyme assays:

Leaf samples (0.5 g) were homogenised in 100mM potassium phosphate buffer pH 7.0 containing 0.5mM EDTA, 0.1mM phenyl-methylsulphonyl fluoride (PMSF) and 2% polyvinylpyrrolidone (PVP) in a pre-chilled pestle and mortar. The homogenate was centrifuged at 4 ◦C for 30 min at 15,000 g. The supernatant was collected and used for

enzyme assays.

2.1.7. Superoxide dismutase (SOD) activity:

Inhibition of photochemical reduction of nitroblue tetrazolium (NBT) by SOD was measured at A_{560} (Beauchamp and Fridovich, 1971). Briefly, 1 mL reaction mixture contained 50 mM phosphate buffer (pH 7.8), 13 mM methionine, 63 µM NBT, 1.3 µL riboflavin, 0.1 mM EDTA, 10 µg protein. The reaction was initiated by switching on 15 W fluorescent lamps for 10 min. The tubes covered with a black cloth served as blanks. One unit of the SOD was defined as amount of enzyme required to inhibit reduction of NBT by 50%.

2.1.8. Peroxidase (PRX) activity:

PRX was assayed in a reaction mixture consisting of 0.1 mM acetate buffer (pH 5.0), 5 mM guaiacol, 0.03% H_2O_2 and 10 µg of protein. Increase in absorbance due to oxidation of guaiacol to tetraguaiacol was measured at A_{470} as described by Chance and Maehly (1955). The PRX activity was calculated using molar extinction co-efficient 26.61 $mM^{-1}cm^{-1}$for tetra-guaiacol at 470 nm.

2.1.9. Ascorbate peroxidase (APX) activity:

The APX was assayed by measuring the decrease in absorbance at 290 nm due to reduction of ascorbate (Nakano and Asada, 1987). Briefly, the reaction mixture contained 50 mM potassium phosphate buffer (pH 7.0), 0.5 mM ascorbate, 0.5 mM H_2O_2, and 10 µg of protein. The APX activity was calculated using extinction co-efficient 2.8 mM^{-1} cm^{-1} for reduced ascorbate and expressed as mM min^{-1} mg^{-1} protein.

2.2. Whole leaf proteome changes during citrus-*Xanthomonas* interactions:

2.2.1. Total leaf protein isolation:

Citrus leaves of mock, *Xac*- and *Xoo*- challenge were collected after different hpi were immediately frozen in liquid nitrogen and stored at -80°C untill further use. Total leaf proteins were extracted as described by Issacson et al. (2006) with minor modifications. One gram of the frozen leaf tissue was ground to fine powder in liquid nitrogen and

suspended in 4 ml of the extraction buffer [0.5 M Tris–HCl (pH 7.5), 0.7 M sucrose, 0.1 M KCl, 50 mM EDTA, 2% β mercaptoethanol and 1 mM PMSF]. Equal volume of phenol saturated with Tris–HCl (pH 7.5) was added, mixed for 30 min at 4°C and centrifuged at 5,000 g for 30 min at 4°C. The upper phenolic phase was collected and an equal volume of extraction buffer was added to it. The above step was repeated and the upper phenolic phase was re-extracted. Four volumes of 0.1 M ammonium acetate in methanol was added to the collected phenolic phase and kept over-night at -20°C for protein precipitation. The samples were then centrifuged at 10,000 g at 4°C for 30 min and the precipitate was washed thrice in ice cold methanol and twice in ice cold acetone and air dried for few minutes. The final pellet was solubilized in 200 µl of the rehydration solution [8 M (w/v) urea, 2 M (w/v) thiourea, 4% (w/v) CHAPS, 30 mM dithiothreitol (DTT), 0.8% (v/v) immobilized pH gradient (IPG) buffer pH range 4–7 (GE Healthcare, Uppsala, Sweden)] and the protein concentration was determined by using amidoblack method using BSA as standard. Aliquots of 600 µg protein were mixed with rehydration solution (8 M urea, 2 M thiourea, 4% CHAPS, 30 mM DTT, 0.8% IPG buffer pH range 4–7 and 0.004% bromophenol blue) to a final volume of 320 µl and used for 2-DE.

2.2.2. 2-D Electrophoresis:

Concentration of proteins was measured by amidoblack method with bovine serum albumin as standard (Henkel and Bieger, 1994). Isoelectric focusing (IEF) of toal leaf protein was performed at 20°C in an Ettan IPGphor III electrophoresis unit (GE Healthcare) using 18 cm IPG strips (4–7 pH linear gradient; GE Healthcare). The IPG strips were rehydrated with 350 µl rehydration buffer (8 M urea, 2 M thiourea, 4% (w/v) CHAPS, 30 mM DTT, 0.8% IPG buffer pH range 4–7 and 0.004% bromophenol blue) containing 600 µg protein for 12 h at 20°C. The IEF was carried out at 500 V for 30 min, followed by a gradient increase to 10,000 V over 3 h, and 6 h at 10,000V. Whereas, for nuclear proteins IEF was performed in 11 cm IPG strips. After first dimension separation of proteins, the strips were stored at -80°C until 2-D analysis. Proir to SDS-PAGE analysis, the IEF strips were equilibrated twice for 15 min in a buffer containing 6 M urea, 50 mM Tris–HCl buffer (pH 8.8), 30% (w/v) glycerol, 2% (w/v) SDS and 0.002% bromophenol blue. Initial equilibration was performed for 15 min with the buffer containing 2% DTT, followed by another step for 15 min with 2.5% (w/v)

iodoacetamide. The strips were placed on 12.5% SDS-PAGE gel and 2-D electrophoresis was carried in EttanDalt6 chamber (GE Healthcare) at 40 V for 1 h and then 60 mA gel^{-1} for 6 h. Protein spots on 2-DE gels were visualized with colloidal coomassie staining (Wang et al. 2007) and gel images were acquired in Imagescanner (GE Healthcare).

2.2.3. 2-DE gel image and data analysis:

The differentially expressed proteins in 2-D gels were analysed using Image Master 2-D Platinum version 6 image analysis (GE Healthcare). The 2-DE images were aligned, spots were automatically detected and match sets were created. Spots were also edited manually to include a few spots missed by the software and to eliminate artefacts. Based on the position, spots selected as landmark spots in the match set were further adjusted and aligned. The quantity of spots was automatically normalized by considering the volume of each spot percentage relative to the total volume of all spots in the gel. The relative change in protein levels between the pathogen-challenged and mock gels was considered based on the ratio between them. The protein spots with differential expression levels of ≥1.5-fold between treated and mock, at least at one time point, of any of pathogen challenge were considered as upregulated and ≤0.5 as downregulated. The differentially expressed protein spots were selected for further analysis after the Student's t test ($p < 0.05$).

2.2.4. Trypsin digestion:

Differentially expressed protein spots were excised from the colloidal coomassie-stained gels. Gel pieces were washed with 50% acetonitrile (ACN) in 25 mM ammonium bicarbonate (NH_4HCO_3) until the gel pieces were destained. Later, the gel pieces were reduced and alkylated by incubating in a solution containing 10 mM DTT in 25 mM NH_4HCO_3 at 56°C for 1 h followed by 55 mM iodoacetamide in 25 mM NH_4HCO_3 for 45 min at 28°C. The gel pieces were then washed with 25 mM NH_4HCO_3 and dehydrated in ACN for digestion with 12.5 ng μL^{-1} trypsin (sequencing grade, Promega, Wisconsin, USA) in 25 mM NH_4HCO_3 solution for 16 h at 37°C. The trypsin-digested peptides were collected and gel pieces were re-extracted by sonication with 1% trifluoroacetic acid (TFA) and ACN (1:1) in two steps of 10 min each. The trypsin-digested solution collected from these two steps was pooled and vacuum-dried. The peptides were dissolved in 5µL of 1:1 ACN and 1% TFA. To 1 µL of this mixture, 1 µL of freshly

prepared α-cyano-4-hydroxycinnamic acid (CHCA) matrix in 50% ACN and 1% TFA (1:1) were added. Finally 1µL was spotted on target plate.

2.2.5. Protein identification:

Protein identification was performed by searching the MALDI -TOF mass spectral data in EST-other and NCBIInr databases using MASCOT program (http://www.matrixscience.com) employing Biotools software (Bruker Daltonics). The taxonomic category was set to *Viridiplantae* (green plants) and other search parameters were: fixed modification of carbamidomethyl (C), variable modification of oxidation (M), enzyme trypsin, peptide charge of 1^+ and monoisotropic. The protein identity was accepted only if the MASCOT probability was at significant threshfold level (P<0.05) and at least two peptides matched.

2.2.6. Sample Preparation for Nano-LC–MS/MS Analysis:

All of the sample preparation steps for nano-LC–MS/MS analysis were performed carefully on a clean bench to avoid contamination from keratin, dust and other materials. First, protein (approximately 30 µg protein) was mixed with equal volume of SDS sample buffer (2% [w/v] SDS, 50 mM Tris-HCl [pH 6.8], 6% [v/v] β-mercaptoethanol, 10% [w/v] glycerol and bromophenol blue). Samples were heated at 35 °C for 20 min in the SDS sample buffer to dissolve proteins, separated on a 10% polyacrylamide gel with 4.5% stacking gel at 100 V until the upper end of sample dye band enters 2 mm from the well. Gel slices from the well to 2 mm in front of the dye were cut in to four equal pieces and kept in 1.5 ml microtubes and in gel tryptic digestion for nano-LC-MS/MS was performed according to Takahashi et al. (2012). The peptide samples were desalted with SPE C-TIP (AMR, Tokyo, Japan) and the volume was adjusted to 15 µL.

2.2.7. Nano-LC–MS/MS Analysis of whole cell Proteins:

Digested peptide solutions were subjected to nano-LC–MS/MS analysis. Peptide solutions were trapped and concentrated in a trap column (L-column Micro 0.3 × 5 mm; CERI, Japan) using an ADVANCE UHPLC system (MICHROM Bioresources, Auburn, CA). After elution from the trap column, with 0.1% (v/v) formic acid in acetonitrile, concentrated peptides were separated with a Magic C18 AQ nano column (0.1 × 150

mm; MICHROM Bioresources) using a linear gradient of acetonitrile (from 5% [v/v] to 45% [v/v]) at a flow rate of 500 nL/min. Ionization of peptides was performed at a spray voltage of 1.8 kV using an ADVANCE spray source (MICHROM Bioresources). Mass analysis was performed using an LTQ Orbitrap XL mass spectrometer (Themo Fisher Scientific, Waltham, MA) equipped with Xcalibur software (version 2.0.7, Themo Fisher Scientific). Under the data-dependent scanning mode, full scan mass spectra were obtained in the range of 400 to 1800 m/z with a resolution of 30000. Collision-induced fragmentation was applied to the five most intense ions at a threshold above 500. These experiments were repeated four times with samples collected from biologically independent plants.

2.2.8. Analysis of Nano-LC–MS/MS Data:

Raw files of MS/MS spectra were obtained from nano-LC−MS/MS and converted to the mgf format using Proteome Discoverer (ver. 1.1.0.263, Thermo Fisher Scientific). The parameters for the conversion from raw files to mgf files were as follows: precursor mass range, m/z 350−5000; highest and lowest charge state, 0; lower and upper RT limit, 0; the minimum total intensity of a spectrum, 0; and the minimum number of peaks in a spectrum, 1. Using mgf files, peptide data were searched and proteins were identified using the MASCOT search engine (version 2.3.02, Matrix Science, London, UK) searching against the NCBInr Green Plants database (version 20110131 comprising 12852469 sequences). One missed cleavage was allowed. Fixed and variable modifications were set as carbamidomethylation of cysteines and oxidation of methionine, respectively. Peptide mass tolerance was 5 ppm. The MS/MS tolerance was 0.6 Da. Peptide charges were set to +2, +3 and +4. As a result, the false discovery rate (FDR) of peptide identification, which was based on a search of the Mascot decoy database, was less than 5%. To generate a representative list of proteins with increased reliability, the proteins were defined as "identified" if the protein matched at least one unique top-ranking peptide with an expect value ≤ 0.05. In addition, proteins identified two or more times in four repeated experiments were recruited into the protein lists. If a peptide was assigned to multiple proteins, the highest scoring protein was selected in the list. For semiquantitative analysis of differentially expressed proteins, during pathogen challenge at 2, 8 and 48 hpi, Progenesis LC−MS software (version 2.5, Nonlinear Dynamics, New Castle, U.K.) was applied to experimental raw data files. Acquired

profile data were processed according to the software's instructions. In this process, peptides that were compared between mock and pathogen challenge proteins were filtered with ANOVA ($p < 0.05$) and max fold change (>2). The resultant peptides were reanalyzed and identified with the Mascot search engine as described above.

2.2.9. Lignin deposition:

Leaves harvested at different time points after pathogen challenge were stained for lignin deposition by phloroglucinal-HCl method (Vallet et al. 1996). Mock- and pathogen-challenged leaves were incubated in a solution of 1% phloroglucinol in 100% methanol overnight. The leaf tissue was cleared by incubating in chloral hydrate and then they were subsequently mounted on slides. A few drops of concentrated hydrochloric acid were added and finally the tissues were covered with a cover slip. Tissues were viewed immediately. After ~10 min, lignified structures appeared cherry red-orange, but colour faded within 4 h.

2.2.10. Cell wall bound phenol extraction and profiling:

Leaves (0.1g) of mock and pathogen challenge, harvested at different time points were ground in liquid nitrogen and then extracted with 1 ml 80% aqueous methol (Torti et al. 1995). The suspension was homogenised for 1 min before being centrifuged at 12000 g for 10 min. After centrifugation the supernatant was decanted. The remaining precipitate was rehomogenised and centrifuged as above. The supernatant was removed and prior to extraction of cell wall phenolics, the cell wall material was further extracted with hot ethanol. To remove any alcohol soluble phenolics, washed three times with acetone and then air dried. Wall-bound phenolics were released by alkaline hydrolysis of isolated cell wall material as described by Hartley et al. (1992). Cell wall material (30 mg) was extracted with 0.1M NaOH for 24 h at 25ºC. The solutions were then acidified to pH <2 with concentrated HCl and extracted three times with 3 volumes of ethyl acetate. The phenolic ethylacetate extracts were evaporated to dryness and the samples redissolved in 200 µl 50% (v/v) aqueous methanol prior to analysis by HPLC. A C18 reverse phase column (Shimadzu LC-10AT HPLC system), and the flow rate was maintained at 1.5 ml min^{-1}. Elution was performed using a gradient system which increased the relative amounts of 0.1 % acetic acid and acetonitrile and phenolics were detected at 280 nm. Quantification was by integration of peak-areas at 280 nm, with reference to calibration

made using known amount of pure compounds.

2.3. ECM protein extraction and solibulization for 2-DE:

2.3.1. *Destructive method:*

Wall-bound ECM (WE) proteins were isolated by following a destructive method (Watson et al. 2004) with few modifications. In brief, the leaf tissues were ground to powder in liquid nitrogen with 0.3% (w/w) polyvinylpolypyrrolidone and tissue powder was transferred into a beaker containing ice-cold homogenizing buffer (5mM K_3PO_4, pH-6, 0.5 mM DTT, 1 mM PMSF) and stirred at 4°C for 30 min. The cell wall fraction was recovered by centrifugation at 1000 *g* for 5 min at 4°C. The pellet was washed with excess of deionized water and the purified ECM fraction was suspended in 3 volumes (w/v) of extraction buffer (200 mM $CaCl_2$, 5 mM DTT, 1 mM PMSF in 5mM K_3PO_4) and stirred at 4°C for 45 min. Proteins were separated from the insoluble ECM fraction at 10000 *g* for 10 min at 4°C. The step was repeated by suspending the ECM fraction in 3 M LiCl, 1 M NaCl, 1 mM PMSF. The two filtrates were combined and dialysed for 24 h against 1000 ml of water with 8 changes for every 4 h. Dialysed filtrate was vacuum-dried in centrivap concentrator (Labconco). Final WE protein pellet was solubilized in lysis buffer [9M (w/v) urea, 2M (w/v) thiourea, 4% (w/v) CHAPS, 30 mM DTT] and vortexed overnight at 4°C. Acetone precipitation was performed by adding 5 volumes of ice-cold acetone, incubated at -20°C for 16 h and pelleted at 12000 *g* for 15 min at 4°C. The pellet was air-dried, resuspended in lysis buffer and stored at -80°C till further use.

2.3.2. ***Non-destructive method:***

Soluble-ECM (SE) fraction was extracted by following vacuum infiltration and centrifugation method (non-destructive method) as described by Kocal et al. (2008). Leaves were washed thoroughly with water and vacuum-infiltrated with 50 mM HEPES [4-(2-hydroxyethyl)-1-piperazine ethane sulfonic acid]-KOH (pH-6.8) buffer with a reduced pressure of ~20 kPa. Later, leaf pieces were dried with a paper towel and inserted into a 50 mL falcon tube with tips placed at the bottom of the tube. SE fraction was collected by centrifugation for 20 min at 10°C. For 2-DE, proteins from SE fraction, were extracted in tris-saturated phenol (Isaacson et al. 2006), solubilised in lysis buffer for 16 h at 4°C and stored at -80°C till further use.

2.3.3. Enzyme assays:

Cytosolic contamination in WE protein fraction was analysed by performing catalase assay (Bhushan et al. 2006). Malate dehydrogense (MDH) assay was done for SE fractions collected at 1000, 1200, 2000, 5000 and 10000 *g* (Dani et al. 2005; Pirovani et al. 2008) to assess the influence of centrifugal force on cytosolic contamination in SE fraction.

2.3.4. Immunoblotting:

Proteins were resolved on 12.5% SDS-PAGE Laemmli buffer system and electrotransferred onto nitrocellulose membrane at 150 mA for 30 min. Rabbit polyclonal fructose 1,6 bisphosphatase (FBPase) (Agrisera, UK) in 1:5000 was used to detect the protein in the WE protein fraction with a chemiluminescent (ECL) assay. For SE protein fraction, 1:2000 dilution of rubisco (Rbcl) antibody (kind gift by Dr. K. Padmasree, University of Hyderabad, India) was used. Antibody bound protein was detected by NBT/5-bromo-4-chloro-3-indolyl phosphate method.

2.3.5. 2-D Electrophoresis and protein identification:

ECM-associated proteins of both WE and SE fractions, isolated at 8, 16, 24 and 48 hpi of citrus-*Xanthomonas* interactions, were profiled separately on 2-DE gels in biological triplicates and differentially expressed proteins were identified as mentioned in section 2.2.2 – 2.2.5.

2.3.6. Cluster analysis:

Hierarchical clustering was performed for $\log_2$ transformed average fold-change expression values of the four time points of *Xac* and *Xoo* challenge using PermutMatrix software (Caraux and Pinloche, 2005; Meunier et al. 2007). The data were clustered with the Euclidean distance similarity metric and complete linkage method.

2.4. Nuclear protein isolation:

Citrus leaves (20g) were finely powdered in mortar and pestle with 0.3% (W/W) polyvinylpyrrolidone and transferred into a beaker containing 200 ml of ice-cold

hyperosmatic buffer (10 mM Trizma base, 80 mM KCl, 10 mM EDTA, 1mM spermidine and 0.5 M sucrose, pH 9.5), 0.15% 2-mercaptoethanol and 0.5% triton X-100 and gently stirred for 30 min. Suspension was filtered through four layers of cheese cloth. The homogenate was pelleted without triton X-100. Nuclei were pellet down by centrifugation at 1800 *g* for 15 min in a swing bucket rotar. The nuclear proteins were extracted by using tri-reagent by following manufacturer's guidelines. The final protein pellet was resuspended in isoelectric focusing (IEF) sample buffer [8 M urea, 2 M thiourea, and 4% (w/v) CHAPS]. The protein concentration was determined by amidoblack method (Henkel and Bieger, 1994).

2.5.1. Assessment of integrity, enrichment and purity of nuclear fraction:

2.5.1.1. Microscopy:

The nuclear fraction was stained for 15 min with 0.1 íg/mL 4′,6′-diamidino-2-phenylindole hydrochloride (DAPI) in 0.1 M potassium phosphate buffer (pH 7.4) and then washed twice with phosphate buffer saline. For microscopy, a small volume of suspension was placed on a slide and covered with a cover glass. The images were taken with and without a UV filter.

2.5.1.2. One-dimensional SDS-PAGE analysis:

To check the enrichment and purity of nuclear fraction, cytosolic and nuclear protein samples were suspended in SDS sample buffer. Samples were incubated at 35 °C for 20 min in the SDS sample buffer to dissolve proteins, separated on a 12.5% polyacrylamide gel with 4.5% stacking gel, and electrophoresis was carried out at 100 V for 4−5 h. To check for enrichment of nuclear proteins, 30 µg of cytosolic and 10 µg of nuclear fraction proteins were run on SDS-PAGE and bands were observed by coomasie staining.

To check the purity of nuclear fraction, equal amount of cytosolic and nuclear proteins were profiled on SDS-PAGE and immunoblot was performed with rabbit polyclonal FBPase antibody (Agrisera, UK).

2.5.5. Nuclear proteome Profiling and identification of differentially expressed proteins:

Nuclear proteins isolated at 2, 8, 16 and 48 hpi of citrus-*Xanthomonas* interactions, were profiled by both gel based and non-gel based methods as mentioned in sections 2.2.2 – 2.2.8.


Results

3.0. Insights in to NHR during citrus-*Xanthomonas* interaction:

NHR is general, durable, and broad-spectrum resistance exhibited by plant species to a wide variety of microbial pathogens. Although NHR is an attractive breeding strategy, the molecular basis of this form of resistance remains unclear for many plant pathosystems, including interactions with the bacterial pathogens. The discovery of molecular mechanisms responsible for NHR may provide valuable information in the search for disease control alternatives. To better understand the complex phenomenon of NHR, we have selected citrus-*Xanthomonas* as a model system. In the present study, we compared citrus-*Xac* compatible and citrus-*Xoo* non-host interactions by performing anatomical and biochemical, studies and total cellular and sub-organelle proteomic analyses.

3.1.1. Anatomical changes in citrus-*Xanthomonas* interactions:

During plant-pathogen interactions, pathogen has to overcome constitutive and inducible defense responses of plants which include synthesis and accumulation of ROS, papillary callose and phytoalexins with or without formation of the HR. To compare the pathogenicity of *Xac* and *Xoo* on citrus leaves, 0.2 O.D. of bacterial culture, re-suspended in 10 mM $MgCl_2$, was infiltrated in to citrus leaves with a needleless syringe. During citrus-*Xoo* interaction the *in planta* growth of the bacteria declined by 10-fold at 2 days after inoculation (dai), and further decline in growth occurred at 3 dai. Whereas, growth of *Xac* increased by 100-fold at 3 dai (Fig 3.1). Water-soaked lesions, typical of a canker disease appeared in *Xac*-infiltrated areas at 48 h post inoculation (hpi) (Fig 3.2A), while in *Xoo* challenge, a typical HR symptom *i.e.*, slight yellowing at the site of bacterial infiltration, was observed (Fig 3.2A). To evaluate cellular defense responses in citrus during interaction with the two Xanthomonads, cell death and callose deposition were assessed microscopically by staining the leaves with trypan blue and aniline blue, respectively (Fig 3.2B and C). In *Xoo*-challenged leaves, the cells in and around the bacteria-infiltrated zone exhibited cell death and callose deposition at 24 hpi and 16 hpi, respectively. In citrus-*Xoo* interaction, ROS accumulation was detectable at 24 hpi through DAB staining (Fig 3.2D). However, in mock- and *Xac*-challenged leaves, cell death, callose and ROS deposition were not detectable (Fig 3.1B, C and D).

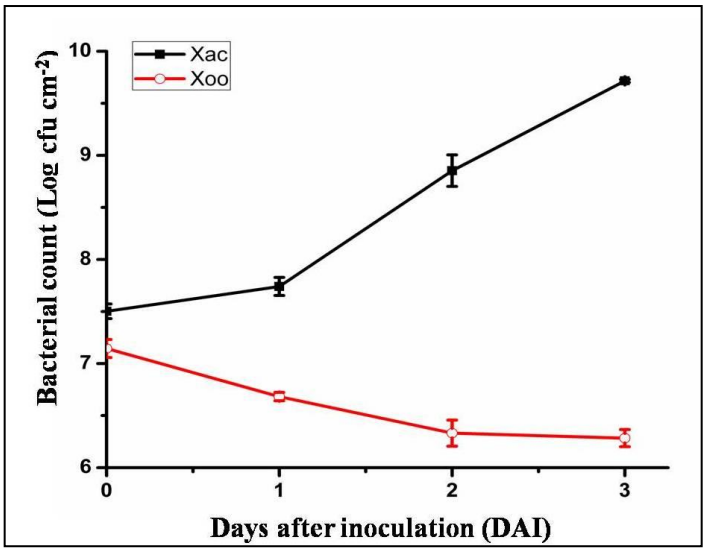

Fig 3.1: *In planta* growth of *Xac* and *Xoo* in citrus leaves

Bacterial growth in citrus leaves was assessed from 0.6 cm leaf discs of *Xac* and *Xoo* infiltrated regions and bacterial number expressed as CFU cm^{-2} leaf tissue. Lines with closed square represent *Xac* growth pattern and open circle represents growth pattern of *Xoo* in citrus leaves. Values represent means of three samples; error bars represent standard deviations.

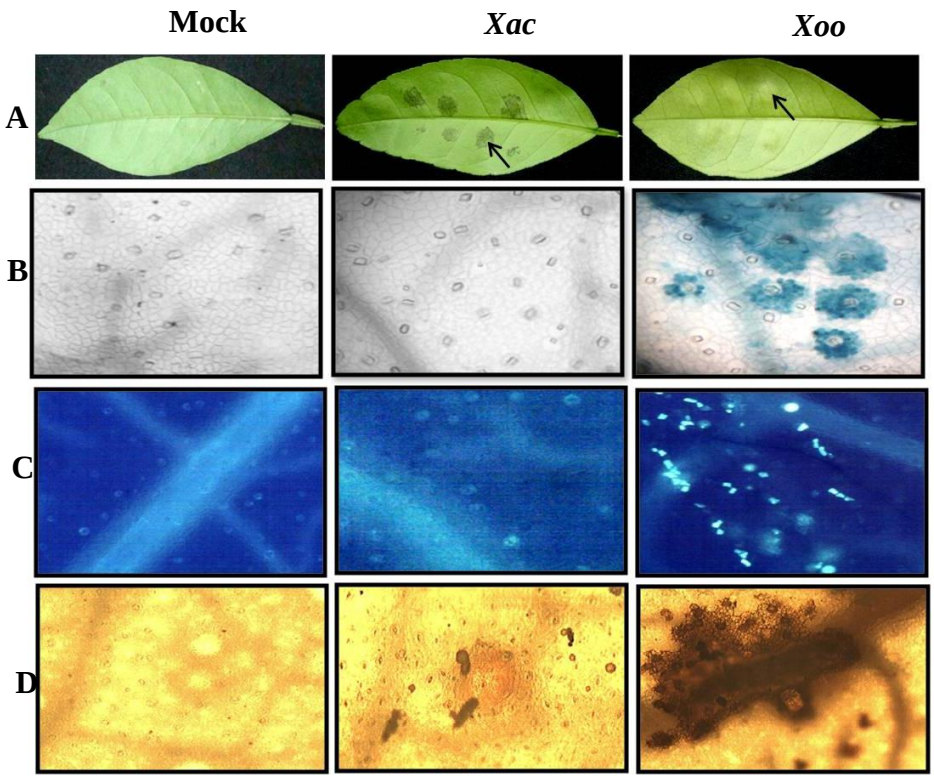

Fig 3.2: Micro- and macroscopic changes in citrus leaves following *Xac* and *Xoo* inoculations

Citrus leaves were infiltrated with 0.2 O.D. of *Xac* or *Xoo* cells suspended in 10 mM $MgCl_2$ or 10 mM $MgCl_2$ (mock) only. Mock (left panel), *Xac* (middle panel) and *Xoo* (right panel) challenged leaves: A) at 48 hpi, B) cell death was determined by trypan blue staining at 24 hpi, and C) callose deposition was examined at 16 hpi with aniline blue staining, D) ROS accumulation was determined by DAB staining at 24 hpi.

Thus, the defense response in citrus was visible at 16 hpi against *Xoo,* whereas in *Xac*-challenge, disease symptoms appeared at 48 hpi. Therefore, we selected 8, 16, 24 and 48 hpi to study the biochemical changes in citrus.

3.1.2. Biochemical changes:

ROS metabolism is one of the critical components of biotic stress response of plants, and is poorly understood. In response to pathogens, oxidative metabolism is altered in plants to produce ROS, including superoxide radical ($O_2^{-\bullet}$), hydrogen peroxide (H_2O_2), and hydroxyl radical ($OH^{\bullet}$), to kill pathogens. We have analysed ROS metabolism- related enzyme activities during citrus-*Xanthomonas* interactions.

3.1.2.1. Accumulation of ROS:

ROS production during citrus-*Xanthomonas* interactions was measured using a sensitive xylenol orange method, for the detection of low levels of soluble hydroperoxides. Inoculation of citrus leaves with non-host pathogen *Xoo* has resulted in accumulation of ROS at 24 hpi. A marginal increase in ROS was also observed during *Xac* challenge at 16 hpi. At 24 hpi during interaction with *Xoo* H_2O_2 increased, whereas during interaction with *Xac* a marginal increase in H_2O_2 occurred at 16 hpi. A 2.6-fold rise in ROS accumulation in citrus leaves occurred by 24 hpi, upon *Xoo* challenge and 1.6-fold upon *Xac* challenge in comparison with mock challenge (Fig 3.3A).

3.1.2.2. Lipid peroxidation:

ROS produced during plant-pathogen interaction can also be measured by estimating lipid peroxidation, where H_2O_2 reacts with TBA and forms TBARS. Lipid peroxidation was higher in *Xoo*-challenged leaves compared to the mock- and *Xac*-challenge during pathogenesis as evidenced by the higher MDA concentrations (Fig 3.3B). MDA concentrations peaked at 24 hpi during *Xoo* interaction, whereas during *Xac* interaction, MDA levels increased marginally at 24 and 48 hpi.

3.1.2.3. Peroxidase (PRX):

PRX appeared as a major H_2O_2 metabolizing enzyme. PRX utilizes phenolic compounds as substrates to cross-link cell walls. The PRX activity was high during *Xoo* interaction

from 16 to 48 hpi, in comparison with *Xac*- and mock-challenge. The increase in PRX activity was 2.6-fold in *Xoo*-challenge at 24 hpi, compared to *Xac*- and mock-challenge (Fig 3.4A). A marginal increase in PRX activity *i.e.*, 1.6-fold, occurred at 48 hpi during *Xac*-challenge.

3.1.2.4. Superoxide dismutase (SOD):

One of the key components of ROS metabolism is SOD, which converts superoxide radicals into H_2O_2. SOD activity was more in *Xoo*-challenge compared to *Xac*- and mock-inoculated leaves. During *Xac*-challenge, SOD activity increased marginally from 16 to 48 hpi, compared to mock-challenge (Fig 3.4B). At 24 hpi during *Xoo* interaction, SOD activity was maximum and was 4-fold higher compared to mock-challenge, while it was only 1.8-fold higher in *Xac* interaction.

3.1.2.4. Ascorbate peroxidase (APX):

APX activity was more in both *Xac* and *Xoo* interactions compared to mock-challenge. APX activity was at its peak at 16 hpi during *Xac* interaction (Fig 3.4C). Upon *Xac* challenge, APX activity was high from 8 to 48 hpi, but maximum of 5.5-fold increase was observed at 16 hpi. Whereas, a 3-fold increase was observed during *Xoo* challenge at 16 hpi.

3.2. Comparative analysis of total leaf proteome changes during *citrus-Xanthomonas* interactions using gel-based and LC MS/MS-based proteomics approaches:

LC MS/MS-based proteomics is an alternative method in which a wide range of proteins including very basic or acidic, low-abundance or hydrophobic proteins can be identified. In the present study, gel-based and non-gel-based proteomic approaches were adopted to analyse the changes in whole leaf proteome during citrus-*Xanthomonas* interactions. Two time points (an early hour of interaction *i.e.*, 8 hpi, and a late hour interaction *i.e.*, 48 hpi) were selected.

3.2.1. Gel-based proteomics of citrus leaf proteome:

A total of 310-380 protein spots were resolved in a pI-range of 4–7 and a molecular mass

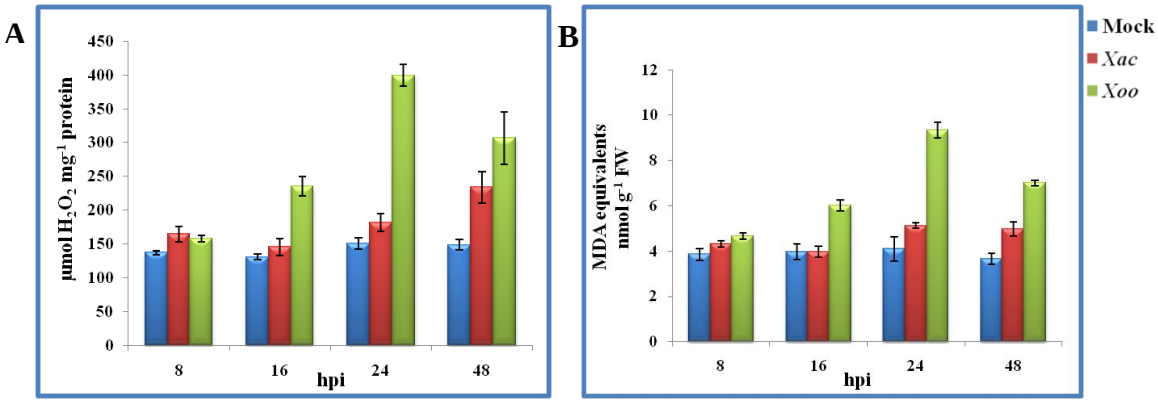

Fig 3.3: Estimation of H_2O_2 levels and lipid peroxidation during citrus-*Xanthomonas* interaction

A) H_2O_2 accumulation and, B) Lipid peroxidation levels were measured during time course of interaction of citrus with *Xac* and *Xoo*. Error bars indicate standard deviation of the mean from three independent experiments. hpi-hours post inoculation.

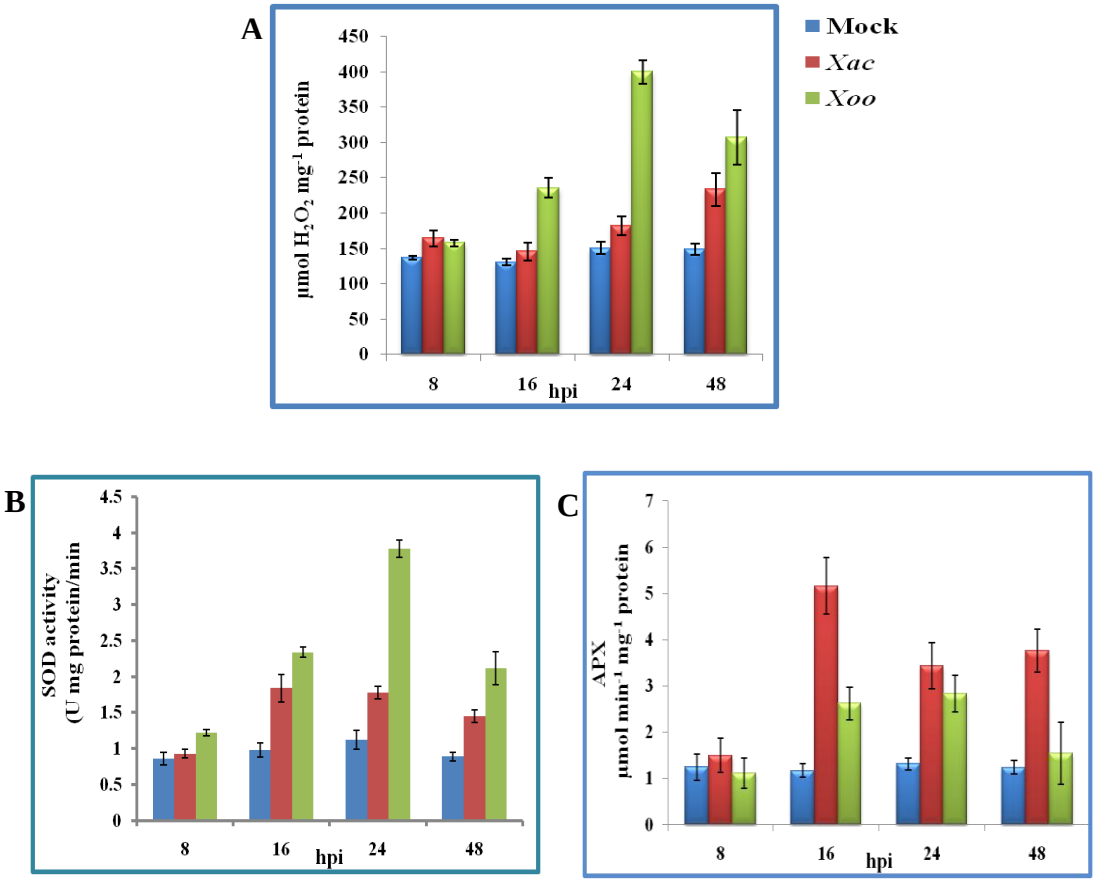

Fig 3.4: Activity of ROS metabolizing enzymes during citrus-*Xanthomonas* interaction

A) Peroxidase (PRX), B) Superoxide dismutase (SOD) and C) ascorbate peroxidase (APX), activities in citrus during interaction with *Xac* and *Xoo* were compared to mock challenge. Error bars indicate standard deviation of the mean from three independent experiments. hpi-hours post inoculation.

range between 10 and 100 kDa on 2-DE gels stained with coomassie brilliant blue dye. The protein spots differentially expressed in response to *Xanthomonas* were selected by using ImageMaster 2-D platinum version 6 software. Gel to gel variation was analysed by performing coefficient of variance analysis (CV). % CV for 50 randomly selected spots of whole leaf proteome 2DE gels was 23 % indicating minimum gel to gel variation. Proteins were considered differentially expressed, if relative % of spot volume at any one time point in all the three independent experiments, increased/decreased by at least factor of 1.5 between pathogen challenge and mock challenge. Such polypeptides were considered to be up/down-regulated.

Upon *Xac* and *Xoo* challenge, 23 proteins appear to be differentially regulated. Seven (30.4%) proteins were up-regulated and three (13%) proteins were down-regulated by *Xac*, while two (8.6%) proteins were up-regulated, and three (13%) proteins were down-regulated by *Xoo*. Seven proteins (30.4%) were up-regulated and three (13%) were down-regulated during both *Xac* and *Xoo* interactions. Protein spots 3, 4 and 17 were clearly up-regulated in citrus-*Xac* interaction, while protein spots 5 and 9 were up-regulated in citrus-*Xoo* interaction. On the other hand, *Xac* significantly down-regulated protein spots 6, 15, 16, 18 and 23, while spots 10, 11, and 14 were clearly down-regulated by *Xoo* (Fig 3. 5). Overall, the number of up/down regulated proteins was higher in *Xac* challenge compared to *Xoo* challenge in citrus.

All the 23 differentially expressed protein spots were identified through MALDI-TOF MS/MS analysis (Table 3.1). The fold-change of the differentially expressed proteins during pathogen challenge and mock, matched peptide sequence, accession number, source organism, sequence coverage, experimental and molecular weight and *pI*, and the MS/MS score of individual proteins were shown in Table 3.1. In some cases, more than one spot were identified as the same protein. For example, chlorophyll a,b protein (spot 20 and 21) and phosphoribulokinase (spot 15 and 23). The protein identification results suggest that photosynthesis and carbon metabolism related proteins were highly affected during citrus-*Xanthomonas* interaction.

3.2.2. Non-gel-based proteomics of citrus total proteome:

To have a comprehensive analysis of the total citrus leaf proteome during host and non-

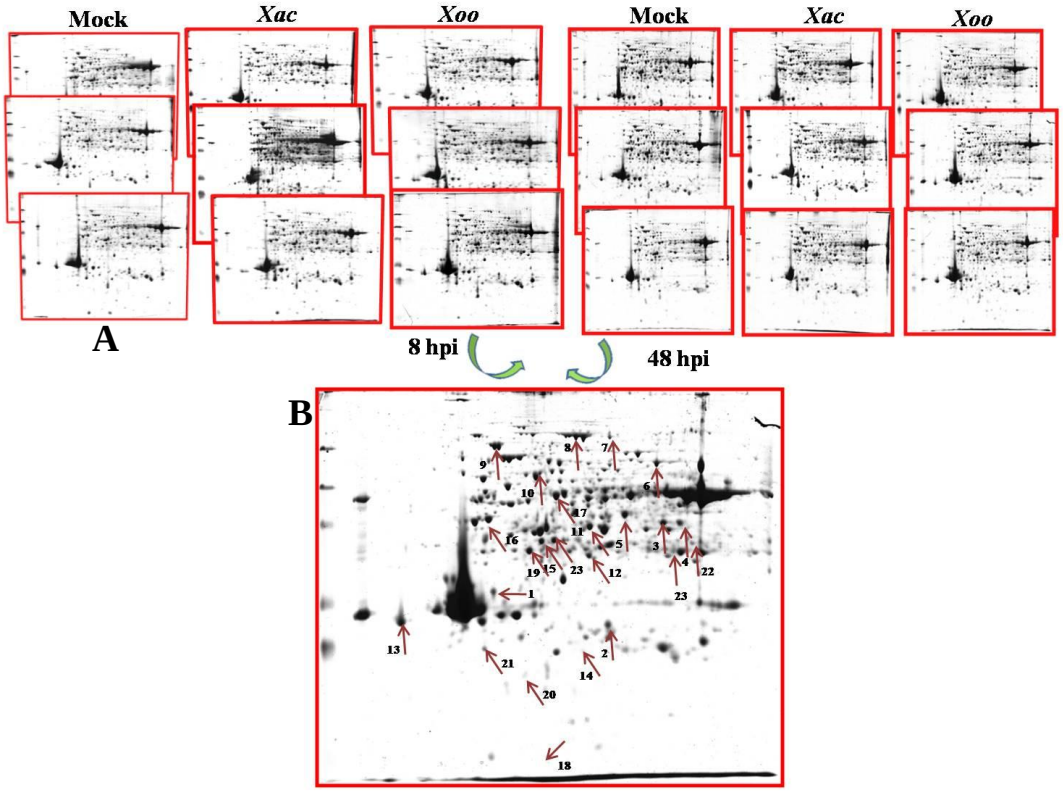

Fig 3.5: Comparative total proteome of citrus during *Xanthomonas* interaction and the representative two-dimensional gel electrophoresis

The total leaf proteins were isolated from the mock and pathogen (*Xac* and *Xoo*) challenged citrus leaves. An equal amount (600µg) of protein from each time point was separated by two-dimensional gel electrophoresis. Three replicate gels for each time point (A) were compared using ImagePlatinum 2D software and differentially regulated proteins were indicated by arrows in the standard gels (B).

Table 3.1: Differentially regulated proteins during citrus-*Xanthomonas* interaction identified in 2 DE

Spot no.	Accession	Description	*Xac*/Con 8 hpi	*Xoo*/Con 8 hpi	*Xac*/Con 48 hpi	*Xoo*/Con 48 hpi
1.	gi|11596188	lectin-related protein precursor	**1.83**	**1.68**	0.52	**2.58**
2.	gi|255547634	Carbonic anhydrase	**1.63**	**0.42**	**0.49**	0.58
3.	gi|350538241	GDP-mannose 3',5'-epimerase	0.86	1.18	**1.52**	1.02
4.	gi|319739579	NAD-dependent epimerase	**1.52**	1.42	1.38	1.03
5.	METK_BRARP	S-adenosylmethionine synthase	1.32	**1.67**	0.84	0.88
6.	gi|255546341	malic enzyme, putative	1.03	**1.54**	**0.49**	1.60
7.	gi|169160465	phospholipase D alpha	**1.71**	**2.35**	**2.34**	**2.19**
8.	CX295644	Lipoxygenase	**1.54**	**2.37**	0.95	**2.10**
9.	gi|381144430	Hsp90	1.25	**1.90**	1.14	1.15
10.	gi|357110700	chaperonin 60 subunit beta 1 or RUBISCO	**0.44**	**0.49**	1.19	0.79
11.	EFTU1_SOYBN	Elongation factor Tu	1.25	0.79	1.36	**0.39**
12.	EL891182	ATPase synthase	**1.63**	0.83	1.19	**0.45**
13.	ACA1_ARATH	Ca+2-transporting ATPase1	**0.49**	**0.43**	**0.46**	1.09
14.	GLNA2_DAUCA	Glutamine synthetase	1.08	1.43	**0.39**	**0.48**
15.	KPPR_SPIOL	Phosphoribulokinase	0.75	0.61	**0.43**	0.69
16.	RCA_CUCSA	RUBISCO activase	1.04	0.69	**0.48**	0.75
17.	ATPA_DAUCA	ATP synthase subunit alpha	**1.52**	0.99	1.09	**0.44**
18.	HS17A_ARATH	17.6 kDa heat shock protein	**0.31**	0.86	0.79	**1.98**
19.	RCA_CUCSA	RUBISCO activase	0.86	**0.39**	**0.48**	0.51
20.	CN182164	Chlorophyll a-b binding protein	**5.46**	**3.14**	1.05	0.78
21.	CB2B_PINSY	Chlorophyll a-b binding protein type 2 member 1B	**1.72**	**1.93**	**3.01**	**2.12**
22.	gi|2218152	type IIIa membrane protein cp-wap13	1.47	**1.54**	**3.60**	**2.41**
23.	KPPR_SPIOL	Phosphoribulokinase	1.04	0.56	**0.44**	0.71

Fold change values of significantly regulated proteins during *Xac* vs. Control and *Xoo* vs. Control interaction were indicated by bold. hpi-hours post inoculation.

host interactions, non-gel-based proteomics was adopted along with gel-based proteomics. The non-gel-based proteome profiling was carried out by performing 1-DE for a time sufficient for the protein samples to run into the gel, later the gel band was cut and trypsin-digested. The proteins were identified by separating the digested peptides by nano LC-MS/MS, followed by searching obtained spectra against the NCBI database using Mascot server. Four independent replicates for each treatment, and for each time points, were used for quantitative analysis of the whole leaf protein by Progenesis software. A 2-fold threshold value for increased/decreased proteins was selected to extract proteins that changed during citrus-*Xanthomonas* interaction. Through this technique, 863 proteins were identified. The molecular mass of the identified proteins ranged from 2.09 to 405.71 kDa, with 65% of these proteins ranging from 23 to 80 kDa. The pI values also ranged from 4 to 11.

A total of 137 and 280 proteins were differentially expressed at 8 and 48 hpi, respectively, during citrus-*Xanthomonas* interaction. During early interaction *i.e.*, at 8 hpi, 14 proteins were up-regulated and 11 proteins were down-regulated commonly during both the interactions. But, the regulation of these proteins was at different amplitudes. Whereas, 38 proteins in *Xoo* and 20 proteins in *Xac* interaction with citrus were up-regulated. Among the down-regulated proteins, 26 were in *Xoo* and 18 were in *Xac*-citrus interaction. At 48 hpi (late hours of interaction), proteins commonly up-regulated during both host and non-host interactions were 59, while 37 were down-regulated. Whereas, 53 proteins in *Xoo* and 52 proteins in *Xac* interaction were induced. Sixty proteins in *Xoo* interaction and 19 proteins during *Xac* challenge were down-regulated. We have also compared the dataset of differentially expressed proteins at 8 hpi with the dataset of 48 hpi. Only 27 differentially regulated proteins have temporal variation at both 8 and 48 hpi (Table 3.2).

To have an insight in to the function of the differentially expressed proteins, we have classified the proteins in to 13 functional categories. Relatively large numbers of proteins were not assigned function. The largest functional category of whole leaf proteins was unknown proteins (318 proteins, 36.8%), followed by metabolism-related proteins (287 proteins, 33.25%) and energy-related proteins (103 proteins, 11.9%).

3.2.2.1. Metabolism-related proteins:

In citrus-*Xanthomonas* interaction a total of 9 and 35 proteins were differentially regulated during 8 and 48 hpi, respectively (Table 3.2). At 8 hpi, lipoxygenase was down-regulated during both *Xac* and *Xoo* interactions, where as acyl-CoA oxidase-like protein was down-regulated only during *Xoo* interaction. Six proteins corresponding to inorganic pyrophosphatase, ferredoxin-dependent glutamate synthase 1, chloroplastic ACC oxidase, aldehyde dehydrogenase family 2 member B4, mitochondrial glycine dehydrogenase, mitochondrial glycine cleavage system P protein, glycine decarboxylase and cysteine synthase, O-acetyl-L-serine (thiol)-lyase were up-regulated. At 48 hpi, 18 and 17 proteins were differentially regulated during *Xac* and *Xoo* interaction, respectively. Among these differentially regulated proteins, sucrose synthase, putative 4-methyl-5(b-hydroxyethyl)-thiazol monophosphate biosynthesis enzyme, acetohydroxyacid synthase, Os12g0566300, 3-ketoacyl-CoA thiolase B, Phospho-2-dehydro-3-deoxyheptonate aldolase 1, 3-deoxy-D-arabino-heptulosonate7-phosphate synthase, DAHP synthase 1 and phospho-2-keto-3-deoxyheptonate aldolase 1 were up-regulated during both interactions. Two proteins, thiazole biosynthetic enzyme and glutamine synthetase were down-regulated during both interactions.

3.2.2.2. Energy-related proteins:

Several proteins related to photosynthesis, Calvin cycle and electron transfer cycle were differentially regulated during both interactions. Among these proteins, the proteins belonging to photosynthesis and Calvin cycle were up-regulated more in *Xac* interaction compared to *Xoo* interaction at 8 hpi (Table 3.3). Whereas at 48 hpi, most of the energy related proteins like ribulose-1,5-bisphosphate carboxylase/oxygenase (RUBISCO) large subunit, carbonic anhydrase and NAD-dependent formate dehydrogenase were down-regulated during both interactions. Six proteins corresponding to three isomers of glyceraldehyde-3-phosphate dehydrogenase and 3 isoforms of RUBISCO were up-regulated during both *Xac* and *Xoo* interactions at 8 hpi, and the same proteins decreased during both interactions at 48 hpi.

3.2.2.3. Defense/disease-related proteins:

Differentially regulated proteins in the defense category include proteins related to

Table 3.2: Metabolism-related proteins differentially regulated during citrus-*Xanthomonas* interaction

Accession	Description	*Xac*/Con	*Xoo*/Con
	Proteins regulted at 8 hpi		
gi|2245030	Acyl-CoA oxidase like protein	0.43 (0.024)	0.51 (0.043)
gi|255554527	Inorganic pyrophosphatase	1.99 (0.034)	2.19 (0.001)
gi|225424691	Aldehyde dehydrogenase family 2 member B4, mitochondrial	1.77 (0.047)	2.03 (0.001)
	Proteins regulted at both interactions at 48 hpi		
gi|15239735	Thiazole biosynthetic enzyme	0.38 (9.05E-05)	0.41 (6.33E-05)
gi|6578120	Glutamine synthetase	0.37 (0.002)	0.37 (0.001)
gi|6683114	Sucrose synthase	2.43 (1.46E-05)	2.27 (0.0135)
gi|171854671	4-methyl-5(b-hydroxyethyl)-thiazol monophosphate biosynthesis enzyme	3.01 (0.014)	2.88 (0.023)
gi|115489130	Os12g0566300	2.04 (0.001)	2.08 (0.009)
gi|1129145	3-ketoacyl-CoA thiolase B	5.56 (0.022)	3.92 (0.010)
	Proteins regulted during *Xac* interactions at 48 hpi		
gi|255584279	2-deoxyglucose-6-phosphate phosphatase	0.49 (0.049)	0.54 (0.014)
gi|3127890	Cysteine synthase, O-acetyl-L-serine (thiol)-lyase	0.36 (0.002)	0.63 (0.062)
gi|70609690	Glutamate decarboxylase	2.09 (0.019)	1.80 (0.074)
gi|15241945	GDP-mannose 3,5-epimerase	2.51 (0.002)	1.49 (0.051)
gi|12232032	ACC oxidase	2.51 (0.002)	1.82 (0.073)
gi|3075507	Acetohydroxyacid synthase	2.90 (0.000)	2.53 (0.052)
gi|464734	Adenosylhomocysteinase	3.38 (0.000)	5.00 (0.075)
gi|417745	Adenosylhomocysteinase	2.32 (0.013)	4.30 (0.156)
gi|21586064	Cytosolic phosphoglucomutase	6.72 (0.008)	12.23 (0.104)
gi|6651031	γ-glutamylcysteine synthetase	2.22 (0.005)	2.06 (0.072)
	Proteins regulted during *Xoo* interactions at 48 hpi		
gi|4210334	2-oxoglutarate dehydrogenase, E3 subunit	1.06 (0.764)	2.00 (0.018)
gi|34099833	O-acetylserine (thiol)lyase	14.56 (0.112)	13.71 (0.040)
gi|1346526	Methionine adenosyltransferase 2; S-adenosylmethionine synthase 2	2.32 (0.059)	3.01 (0.033)
gi|2351580	Thymidine diphospho-glucose 4-6-dehydratase homolog	1.61 (0.005)	2.18 (0.002)
gi|59380482	Methionine synthase	3.17 (0.054)	4.36 (0.039)
gi|169160465	Phospholipase D alpha	8.17 (0.105)	5.25 (0.027)
gi|114193	Phospho-2-dehydro-3-deoxyheptonate aldolase 1, chloroplastic	2.73 (0.050)	3.77 (0.032)
gi|187960379	Lipoxygenase 2	1.19 (0.514)	0.49 (0.000)

Fold change values of *Xac* vs. Control and *Xoo* vs. Control were given with *P*- value in the paranthesis. hpi-hours post inoculation.

Table 3.3: Energy-related proteins differentially regulated during citrus-*Xanthomonas* interaction

Accession	Description	*Xac*/Con	*Xoo*/Con
	Proteins regulated at 8 hpi		
gi|394932822	RUBISCO large subunit	3.31 (0.008)	3.75 (0.020)
gi|141448056	Chloroplast ferredoxin-NADP+ reductase	2.99 (0.015)	2.77 (0.030)
gi|1750330	RUBISCO large subunit	5.29 (0.020)	6.34 (0.072)
gi|53748417	RUBISCO SSU	2.73 (0.044)	1.11 (0.760)
gi|30523254	RUBISCO SSU	10.22 (0.038)	2.59 (0.324)
gi|1169586	Fructose-1,6-bisphosphatase, cytosolic	2.75 (0.0379)	2.02 (0.173)
gi|552834	RUBISCO	3.23 (0.036)	2.63 (0.171)
gi|3790102	Pyrophosphate-dependent phosphofructokinase alpha subunit	0.43 (0.016)	0.53 (0.001)
gi|373938261	Carbonic anhydrase	3.25 (0.089)	2.66 (0.005)
gi|131390	OEE2	2.09 (0.077)	2.30 (0.028)
gi|449459892	RUBISCO activase 1	2.07 (0.051)	2.16 (0.008)
gi|225446775	OEE2	1.96 (0.080)	2.23 (0.036)
gi|1488652	Fumarase	1.63 (0.077)	2.02 (0.016)
gi|7260200	RUBISCO	1.51 (0.129)	2.01(0.012)
gi|2499497	Phosphoglycerate kinase	1.31 (0.396)	2.12 (0.009)
gi|188037483	RUBISCO large subunit	1.13 0.747	2.01(0.037)
	Proteins regulated at 48 hpi at both interactions		
gi|125991565	RUBISCO large subunit	0.47 (0.006)	0.36 (0.002)
gi|66735765	RUBISCO large subunit	0.46 (0.000)	0.33 (0.000)
gi|9909955	RUBISCO	0.47 (0.011)	0.41 (0.006)
gi|12240092	RUBISCO SSU	0.37 (0.034)	0.26 (0.016)
gi|125857787	RUBISCO large subunit	0.43 (0.032)	0.35 (0.016)
gi|3980216	RUBISCO large subunit	0.48 (0.004)	0.41 (0.004)
gi|30523254	RUBISCO SSU	0.34 (0.033)	0.11 (0.003)
gi|449459892	RUBISCO activase 1	0.47 (0.021)	0.34 (0.008)
gi|188037483	RUBISCO large subunit	0.45 (0.004)	0.33 (0.002)
gi|323460960	RUBISCO large subunit	0.46 (0.004)	0.33 (0.003)
gi|2499497	Phosphoglycerate kinase, chloroplastic	0.38 (0.009)	0.60 (0.013)
gi|373938261	carbonic anhydrase	0.43 (0.036)	0.38 (0.027)
gi|1351030	RUBISCO large subunit-binding protein subunit α	0.45 (0.036)	0.30 (0.014)
gi|37927472	Putative photosystem I reaction center subunit N precursor	0.37 (0.006)	0.48 (0.002)
gi|225463817	Ferredoxin-thioredoxin reductase	0.27 (0.031)	0.35 (0.049)
gi|429560257	RUBISCO large subunit	43.67 (0.038)	32.72 (0.005)
gi|10798652	Malate dehydrogenase	18.81 (0.008)	19.05 (0.034)
gi|356536264	Fructose-bisphosphate aldolase 3	4.00 (0.021)	4.59 (0.012)
	Proteins regulted during *Xac* interactions		
gi|209970299	RUBISCO large subunit	0.45 (0.026)	0.54 (0.057)
gi|114329669	Cytochrome f	0.49 (0.029)	0.67 (0.444)

(Table 3.3 continued)

Accession	Description	*Xac*/Con	*Xoo*/Con
gi|357451633	Phosphoglycerate kinase	0.35 (0.011)	0.50 (0.124)
gi|18405061	Thylakoid lumen 18.3 kDa protein	0.47 (0.019)	0.64 (0.265)
gi|4760553	NAD-dependent formate dehydrogenase	0.41 (0.029)	0.81 (0.375)
gi|225445692	Carbonic anhydrase, chloroplastic	25.99(0.03)	29.4 (0.065)
gi|231586	ATP synthase subunit beta, mitochondrial	2.06(0.02)	2.75 (0.06)
gi|156617025	Glyceraldehyde 3-phosphate dehydrogenase	2.20 (0.003)	2.27 (0.066)
	Proteins regulted during *Xoo* interactions		
gi|168207	RUBISCO large subunit	0.56 (0.003)	0.35 (0.001)
gi|1448981	Ribulose 1,5-bisphosphate carboxylase	0.58 (0.028)	0.39 (0.003)
gi|296033256	RUBISCO large subunit	0.55 (0.001)	0.41 (0.000)
gi|440233632	RUBISCO large subunit	0.51 (0.000)	0.42 (0.000)
gi|45862244	RUBISCO large subunit	0.58 (0.021)	0.49 (0.006)
gi|440233652	RUBISCO large subunit	0.56 (0.019)	0.46 (0.010)
gi|156857837	RUBISCO large subunit	0.56 (0.021)	0.45 (0.007)
gi|255581400	Fructose-bisphosphate aldolase	0.54 (4.79E-05)	0.47(7.55E-05)
gi|158712040	Malate dehydrogenase	0.50 (0.001)	0.42 (0.007)
gi|350538149	Chloroplast sedoheptulose-1,7-bisphosphatase	0.55 (0.002)	0.44 (0.001)
gi|218218521	RUBISCO large subunit	0.56 (0.069)	0.48 (0.026)
gi|76573375	Triosphosphate isomerase	1.51 (0.008)	2.55 (0.004)
gi|470148532	Fructokinase-2	1.92 (0.002)	2.43 (0.013)
gi|470134363	Fructose-bisphosphate aldolase	1.66 (0.001)	2.09 (0.015)
gi|1750330	Ribulose1,5-bisphosphate carboxylase	0.52 (0.249)	0.08 (0.041)
gi|552834	RUBISCO	0.43 (0.076)	0.27 (0.037)
gi|440233652	RUBISCO large subunit	0.56 (0.019)	0.4 6 (0.010)
gi|114329655	Photosystem I P700 apoprotein A2	0.55 (0.294)	0.26 (0.019)
gi|156857837	RUBISCO large subunit	0.56 (0.0206)	0.45 (0.007)
gi|255581400	Fructose-bisphosphate aldolase	0.54 (4.79E-05)	0.48 (7.55E-05)
gi|357470665	Photosystem II CP43 chlorophyll apoprotein	0.53 (0.082)	0.3 9 (0.035)
gi|340511502	RUBISCO large subunit	0.50 (0.062)	0.24 (0.017)
gi|228403	Glycolate oxidase	0.72 (0.176)	0.44 (0.022)
gi|53748417	RUBISCO SSU	0.43 (0.069)	0.21 (0.012)
gi|21320986	RUBISCO large subunit	0.62 (0.102)	0.40 (0.027)
gi|361355	Photosystem I protein	0.74 (0.546)	0.23 (0.026)
gi|895909	Fructose-1, 6-bisphosphatase	0.53 (0.087)	0.38 (0.030)
gi|131241	Photosystem Q(B) protein	0.69 (0.331)	0.20 (0.017)
gi|603221	6-phosphogluconate dehydrogenase	1.96 (0.052)	2.05 (0.002)
gi|5764653	NADP-isocitrate dehydrogenase	1.13 (0.388)	2.2 2 (0.020)
gi|585451	NAD-dependent malic enzyme 62 kDa isoform	1.16 (0.522)	2.13 (0.009)

Fold change values of *Xac* vs. Control and *Xoo* vs. Control were given with *P*- value in the paranthesis. hpi-hours post inoculation.

Table 3.4: Disease/defense-related proteins differentially regulated during citrus-*Xanthomonas* interaction

Accession	Description	*Xac*/Con	*Xoo*/Con
	Proteins regulated at 8 hpi		
gi|624674	Heat shock protein	0.11 (0.0030	0.26 (0.014)
gi|449468161	β-hexosaminidase 2	2.16 (0.069)	2.68 (0.002)
gi|4760553	NAD-dependent formate dehydrogenase	0.79 (0.572)	2.15 (0.002)
gi|357147646	: Peptidyl-prolyl cis-trans isomerase CYP38, chloroplastic-like	1.68 (0.024)	2.38 (0.000)
gi|87299375	Miraculin-like protein 1	0.67 (0.378)	0.25 (0.044)
gi|1220144	Chitinase	0.42 (0.011)	0.60 (0.035)
gi|32401095	Class I heat shock protein	0.39 (0.016)	0.54 (0.031)
gi|11990130	17.9 kDa heat-shock protein	0.36 (0.015)	0.76 (0.368)
gi|376341420	Small heat shock protein	0.27 (0.021)	0.62 (0.238)
gi|10944737	Luminal binding protein	0.17 (0.048)	0.27 (0.073)
gi|145355337	Heat Shock Protein 70, cytosolic	0.15 (0.048)	0.46 (0.196)
	Proteins regulated at 48 hpi		
gi|87299377	Miraculin-like protein 2	0.36 (0.014)	0.28 (0.021)
gi|119367468	Miraculin-like protein 2	0.41 (0.014)	0.19 (0.002)
gi|31126793	Glycine hydroxymethyltransferase	0.47 (5.28E-05)	0.47 (7.05E-05)
gi|473983421	Heat shock cognate 70 kDa protein 1	0 (0.035)	0 (0.034)
gi|10944737	Putative luminal binding protein	15.06 (0.011)	17.689 (0.006)
gi|3264769	Late embryogenesis-like protein	3.63 (0.011)	1.19 (0.778)
gi|340343788	Miraculin-like protein 2	0.48 (0.034)	0.44 (0.077)
gi|99906997	Class III peroxidase	0.40 (0.011)	0.80 (0.538)
gi|23496447	Acidic class II chitinase	6.08 (0.057)	3.66 (0.000)
gi|41584275	Heat shock cognate protein 70	1.47 (0.001)	2.87 (0.012)
gi|110007377	Peroxidase	1.95 (0.067)	3.24 (0.002)
gi|343887285	Heat shock protein	1.72 (0.329)	3.67 (0.031)
gi|32401095	Class I heat shock protein	1.36 (0.165)	4.12 (0.004)
gi|255582806	Heat shock protein	1.11 (0.334)	2.01 (0.003)
gi|145355337	Heat Shock Protein 70	7.61 (0.201)	64.36 (0.034)
gi|11990130	17.9 kDa heat-shock protein	1.40 (0.163)	2.78 (0.004)
gi|376341420	Small heat shock protein	1.54 (0.181)	6.18 (0.003)
gi|384253238	Heat Shock Protein	1.46 (0.060)	2.43 (0.032)
gi|15221275	Stress-inducible protein	1.51 (0.029)	2.20 (0.015)
gi|3451147	Chitinase	3.48 (0.052)	2.02 (0.044)
gi|4151199	Class I extracellular chitinase	62.64 (0.120)	18.22 (0.000)

Fold change values of *Xac* vs. Control and *Xoo* vs. Control were given with *P*- value in the paranthesis. hpi-hours post inoculation.

Table 3.5: Protein synthesis-related proteins differentially regulated during citrus-*Xanthomonas* interaction

Accession	Description	*Xac*/Con	*Xoo*/Con
gi|225426522	50S ribosomal protein L11	2.40 (0.049)	1.66 (0.002)
gi|75313851	30S ribosomal protein S5	13.16 (0.025)	5.00 (0.088)
gi|357167856	NAC domain-containing protein 100	0.27 (0.017)	0.48 (0.067)
gi|1184989	NTGB2, partial	1.14 (0.522)	0.44 (0.021)
gi|37780996	40S ribosomal protein S5	0.70 (0.230)	0.46 (0.024)
gi|227937359	Translation elongation factor	0.49 (0.077)	0.49 (0.049)
gi|2662343	EF-1 alpha	3.86 (0.000)	4.00 (0.030)
gi|303844	Eukaryotic initiation factor 4A	2.16 (0.001)	2.04 (0.019)
gi|2500980	Glutamate--tRNA ligase	2.31 (0.007)	3.06(3.6E-05)
gi|159485314	Plastid ribosomal protein L3	7.94 (0.011)	6.57 (0.006)
gi|396582353	Pentatricopeptide repeat-containing protein	0.37 (0.041)	0.0 8 (0.000)
gi|225439460	40S ribosomal protein S4	2.07 (0.013)	0.94 (0.490)
gi|32400861	40S ribosomal protein	2.03 (0.004)	1.17 (0.489)
gi|464630	60S ribosomal protein L27	0.74 (0.164)	0.35 (0.007)
gi|225237	Ribosomal protein S19	0.58 (0.001)	0.43 (0.000)
gi|20022	Ribosomal protein S6	0.82 (0.354)	0.40 (0.023)
gi|1173045	60S ribosomal protein L37a	0.95 (0.789)	0.46 (0.020)
gi|52220845	Ribosomal protein S8	0.46 (0.059)	0.2 5 (0.007)
gi|12323890	Ribosomal protein S9	0.53 (0.047)	0.37 (0.008)
gi|585876	60S ribosomal protein L23a	0.86 (0.479)	0.34 (0.003)
gi|11276604	Ribosomal protein S13	0.54 (0.034)	0.38 (0.009)
gi|449440632	Elongation factor Tu, chloroplastic	0.87 (0.543)	0.38 (0.025)

Fold change values of *Xac* vs. Control and *Xoo* vs. Control were given with *P*- value in the paranthesis. hpi-hours post inoculation.

Table 3.6: Protein destination and storage-related proteins differentially regulated during citrus-*Xanthomonas* interaction

Accession	Description	*Xac*/Con	*Xoo*/Con
	Proteins regulated at 8 hpi		
gi|356539340	Serine carboxypeptidase-like 51-	2.33 (0.040)	2.63 (7.11E-05)
gi|52783176	Non-specific lipid-transfer protein	5.23 (0.041)	2.56 (0.394)
gi|26224736	Serpin-like protein	0.25 (0.044)	0.37 (0.082)
gi|547500	H-protein	2.18 (0.099)	2.33 (0.004)
gi|22947842	20S proteasome alpha 6 subunit	0.73 (0.270)	0.46 (0.034)
	Proteins regulated at 48 hpi		
gi|356508308	Aspartic proteinase nepenthesin-1-like	2.33 (0.001)	2.21 (0.000)
gi|402171768	β-amylase 5	5.41 (0.034)	4.24 (0.004)
gi|26224736	Serpin-like protein	2.30 (0.001)	2.45 (0.049)
gi|255539116	Prolyl endopeptidase	2.90 (0.009)	2.65 (0.013)
gi|52783176	Non-specific lipid-transfer protein	0.33(0.005)	0.28 (0.003)
gi|15229866	TCP-1/cpn60 chaperonin family protein	3.05 (0.000)	1.65 (0.083)
gi|22947842	20S proteasome alpha 6 subunit	3.33 (0.011)	2.40 (0.147)
gi|4235430	Latex-abundant protein	6.50 (5.51E-06)	5.8 2 (0.181)
gi|225446742	ATP-dependent Clp protease proteolytic subunit 4	0.45 (0.041)	0.57 (0.170)
gi|470126676	Chaperone protein ClpB1	1.76 (3.93E-05)	4.91 (0.024)
gi|1009712	Calreticulin	3.36 (0.054)	3.99 (0.020)
gi|297880	Ubiquitin conjugating enzyme	1.61 (0.007)	2.50 (0.021)
gi|225447176	Protein disulfide isomerase	1.69 (0.031)	2.65 (0.007)
gi|470107656	Peptidyl-prolyl cis-trans isomerase FKBP62	0.86 (0.771)	3.10 (0.038)
gi|15242093	TCP-1/cpn60 chaperonin	0.73 (0.023)	0.45 (0.002)

Fold change values of *Xac* vs. Control and *Xoo* vs. Control were given with *P*- value in the paranthesis. hpi-hours post inoculation.

Table 3.7: Secondary metabolism-related proteins differentially regulated during citrus-*Xanthomonas* interaction at 48 hpi

Accession	Description	*Xac*/Con	*Xoo*/Con
gi|7430935	Cinnamyl-alcohol dehydrogenase	1.22 (4.8E-07)	14.19 (0.000)
gi|100234	Phenylalanine ammonia-lyase	4.03 (0.001)	4.34 (0.014)
gi|11386015	2C-methyl-D-erythritol 2,4-cyclodiphosphate synthase	2.42 (0.022)	2.73 (0.039)
gi|15994	Resveratrol synthase	1.92 (0.317)	2.60 (0.044)
gi|126201	3-isopropylmalate dehydrogenase	0.45 (0.011)	0.54 (0.015)
gi|373939378	Isoflavone reductase-like protein	0.83 (0.185)	4.47 (0.004)
gi|122894098	Cinnamyl alcohol dehydrogenase	1.29 (0.251)	2.48 (0.002)

Fold change values of *Xac* vs. Control and *Xoo* vs. Control were given with *P*- value in the paranthesis. hpi-hours post inoculation.

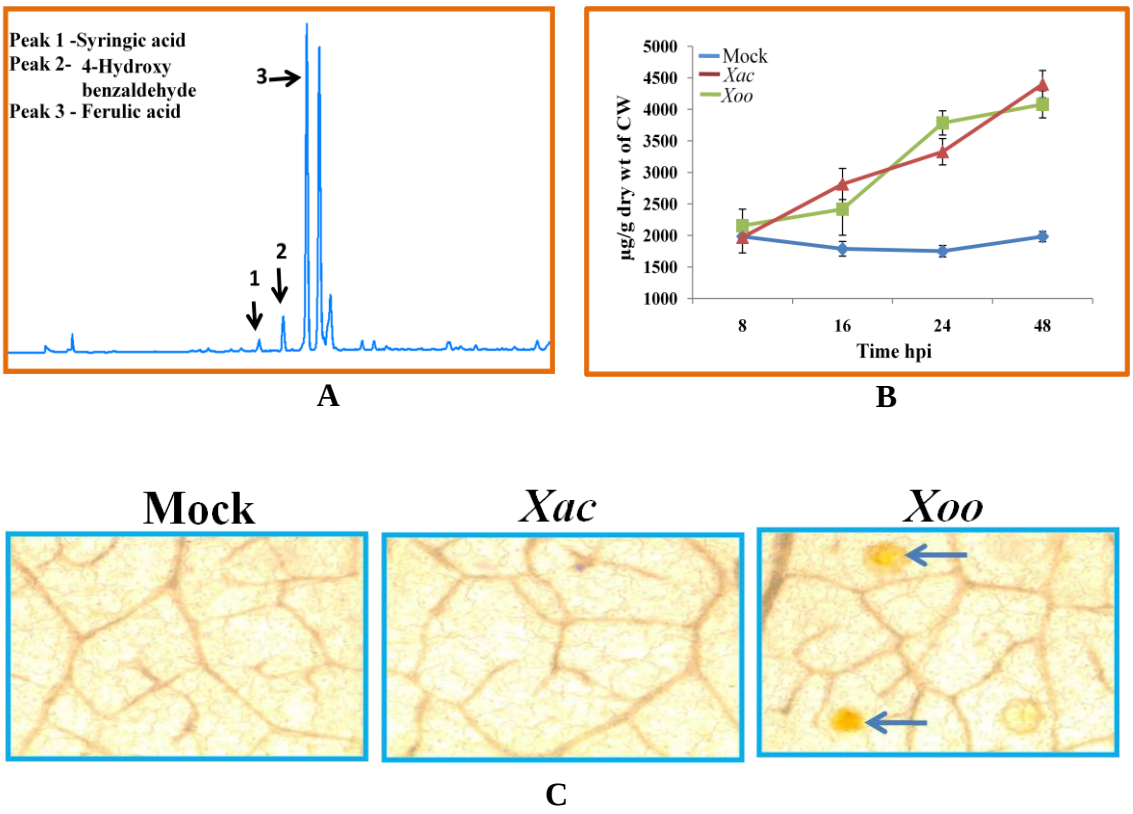

Fig 3.6: Analysis of cell wall bound phenols and lignin deposition during citrus-*Xanthomonas* interaction

A) Cell wall-bound phenols identified in citrus leaves (shown with arrows), B) Ferulate levels at different hpi were quantified as µg/g dry weight of cell wall. Error bars indicate standard deviation of the mean from three independent experiments. hpi-hours post inoculation , and C) Staining with phloroglucinol at 72 hpi. Lignin deposition was indicated by arrows.

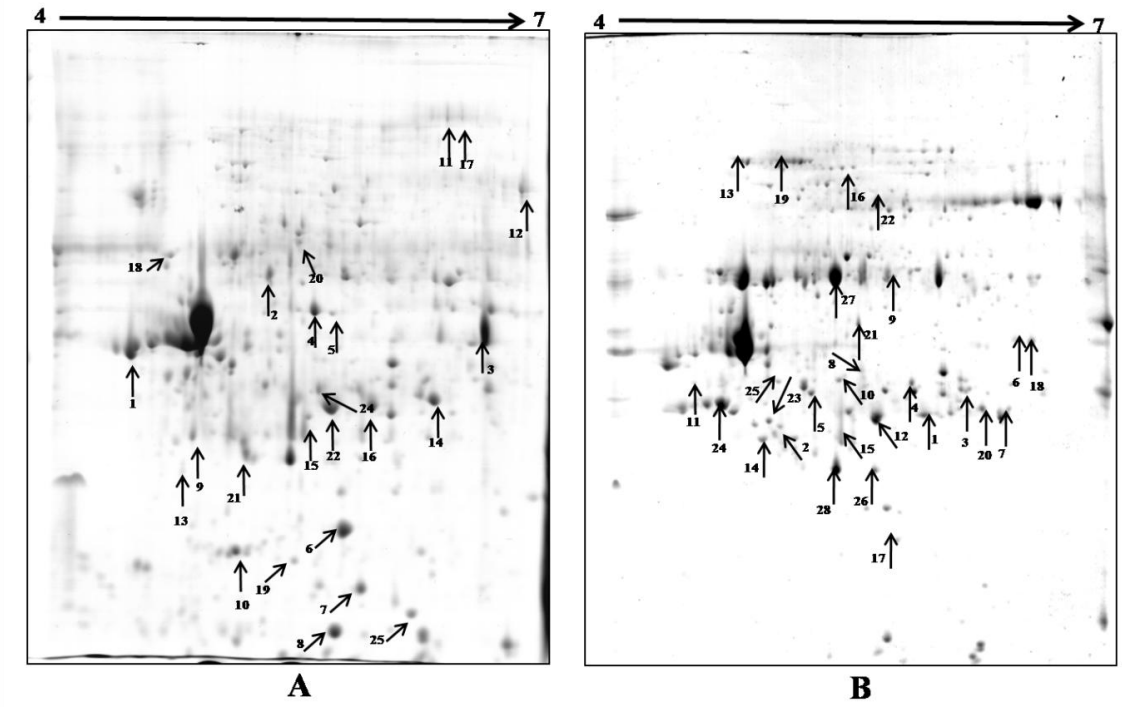

Fig 3.8: Representative images of 2D gels of citrus leaf ECM proteome in response to *Xac* or *Xoo* challenge

Proteome separated by 2-DE and visualized by colloidal coomassie blue. Representative images of A) WE fraction from *Xac* inoculated leaves, B) SE fraction from *Xoo* inoculated leaves. Arrows and numbers represent the protein spots that altered significantly ($P<0.05$) and selected for MS/MS analyses.

different isoforms of chitinase, heat shock proteins (HSP), peroxidase and miraculin-like proteins (MIR). MIR I was down-regulated only during *Xoo* interaction at 8 hpi whereas, another isoform of MIR 2 was down-regulated during both interactions at 48 hpi (Table 3.4). A cell death regulator cysteine protease was up-regulated during both interactions at 8 hpi while, cystatin-like protein was up-regulated only during *Xac* interaction at 48 hpi (Table 3.14). A pathogenesis-related (PR) protein, chitinase was repressed at 8 hpi during *Xac* interaction whereas, at 48 hpi, an acidic class II chitinase and class I extracellular chitinase, were up-regulated only during *Xoo* interaction. HSPs like class 1 HSP, HSP 70 and 17.9 kDa HSP were down-regulated during *Xac* interaction at 8 hpi but up-regulated during *Xoo* interaction at 48 hpi. Class III peroxidise was up-regulated during both the interactions at early interaction, and was repressed at 48 hpi during *Xac* interaction. Peroxidase was induced at 48 hpi only during *Xoo* interaction.

3.2.2.4. Protein synthesis and protein destination and storage:

Three proteins corresponding to protein synthesis and 3 related to protein destination and storage was differentially regulated at 8 hpi. At 48 hpi, 15 proteins related to protein synthesis (Table 3.5) and 16 related to protein destination and storage-related proteins were regulated (Table 3.6). Protein synthesis-related proteins like ribosomal proteins, and elongation factor Tu were down-regulated during *Xoo* interaction at both 8 and 48 hpi (Table 3.14).

3.2.2.5. Secondary metabolism-related proteins:

Proteins-related to phenylproponoid biosynthetic pathway were differentially regulated during citrus-*Xanthomonas* interaction. Two proteins corresponding to benzyl alcohol O-benzoyl transferase and cinnamyl-alcohol dehydrogenase were up-regulated during both interactions at 8 hpi. At 48 hpi, 5 proteins were up-regulated during both interactions whereas, 2 proteins were induced only at non-host interaction and 2 proteins decreased during host pathogen interaction (Table 3.7). Among the differentially expressed secondary metabolism-related proteins, cinnamyl-alcohol dehydrogenase increased during both the interactions at both the time points. A low quality protein: benzyl alcohol O-benzoyl transferase decreased at 8 hpi during *Xac* interaction and up-regulated during both interactions at 48 hpi.

3.2.2.6. Cell structure-related proteins:

Cell structure-related proteins like lectin, pectin esterase, β-D-xylosidase, histone, actin, β-galactosidase, β-mannosidase, UDP-glucose 6-dehydrogenase and type IIIa membrane protein cp-wap13 were induced during both interactions at late hours of interaction. CW remodelling proteins like xyloglucan endotransglycosylase/hydrolase, endo-xyloglucan transferase and β-galactosidase were induced only during *Xoo* interaction at 8 hpi (Table 3.8).

3.2.2.7. Proteins related to signalling, transcription and transport:

Four proteins related to signalling like 14-3-3 protein 32 kDa endonuclease, acid phosphotase, small ras-related protein and LRR-family protein were differentially regulated (Table 3.9). Transcription-related proteins like zinc finger protein, RNA-binding glycine-rich protein and G-box binding factor were differentially regulated (Table 3.10). Proteins involved in transport like adenine nucleotide translocator, nucleotide-binding subunit of vacuolar ATPase and dicarboxylate/tricarboxylate carrier proteins were differentially regulated (Table 3.11). Proteins related to DNA repair, DNA binding and transcription were regulated at both the time points of interactions.

Antioxidant protein monodehydroascorbate reductase was induced during both interactions. Other ROS metabolising proteins Cu/Zn SOD, and hydroxyacylglutathione hydrolase were induced during *Xoo* interaction, while glutathione S-transferase and catalase were repressed. Proteins related to antioxidant status and intracellular trafficking were differentially regulated during pathogen challenge (table 3.12 and 3.13).

3.2.3. Analysis of cell wall-bound phenols and lignin deposition during citrus-*Xanthomonas* interaction:

Cell wall-bound phenols of citrus leaf were extracted at different time points after *Xanthomonas* challenge and profiled using HPLC. Though there was no qualitative difference in the peaks of pathogen and mock-challenged leaves, quantitative difference in the peak intensity was identified. Three phenols syringic acid, 4-hydroxybenzaldehyde and ferulic acid were identified in the wall-bound samples (Fig 3.6A). Further, ferulate levels at different hpi were quantified. Equal concentration of ferulate was detected in citrus-*Xac/Xoo* interactions at 48 hpi (Fig 3.6B). Lignin deposition was visible as

Table 3.8: Cell structure-related proteins differentially regulated during citrus-*Xanthomonas* interaction

Accession	Description	*Xac*/Con	*Xoo*/Con
	Proteins regulated at 8 hpi		
gi|379987825	Xyloglucan endotransglycosylase/hydrolase	2.15 (0.053)	3.58 (0.024)
gi|2244732	Endo-xyloglucan transferase	1.61 (0.071)	2.53 (0.028)
gi|508808	ADP-glucose pyrophosphorylase small subunit	1.55 (0.021)	2.03 (0.012)
gi|255538780	β-galactosidase	1.13 (0.368)	2.02 (0.004)
gi|24250746	Thermostable pectinesterase	0.49 (0.032)	0.80 (0.099)
gi|11596188	Lectin-related protein precursor	7.91 (0.010)	7.23 (0.036)
gi|2098711	Pectinesterase	2.47 (0.000)	2.33 (0.003)
gi|57014097	Pectinesterase 3	38.99 (0.002)	1.26 (5.69E-09)
gi|356573297	UDP-glucose 6-dehydrogenase	3.43 (0.000)	3.74 (0.022)
gi|255115691	Actin 1	3.30 (0.002)	4.77 (0.029)
gi|2218152	Type IIIa membrane protein cp-wap13	3.34 (0.009)	2.92 (0.003)
gi|15237736	β-D-xylosidase 4	3.22 (0.019)	3.17 (0.034)
gi|18397283	Carbamoyl phosphate synthetase B	4.52 (0.018)	5.03 (0.023)
gi|356511309	Pectinesterase/pectinesterase inhibitor 6	0.66 (0.008)	0.44 (0.000)
gi|3021483	Histone H2B-2	0.64 (0.117)	0.41 (0.037)

Fold change values of *Xac* vs. Control and *Xoo* vs. Control were given with *P*- value in the paranthesis. hpi-hours post inoculation.

Table 3.9: Signal transduction-related proteins differentially regulated during citrus-*Xanthomonas* interaction

Accession	Description	*Xac*/Con	*Xoo*/Con
	Proteins regulated at 8 hpi		
gi|307135855	LRR-family protein	3.99 (0.016)	9.74 (0.002)
gi|89212810	14-3-3-like protein	0.33 (0.004)	0.43 (0.007)
gi|34394047	Acid phosphatase-like	0.59 (0.222)	0.34 (0.010)
	Proteins regulated at 48 hpi		
gi|34394047	Acid phosphatase-like	3.79 (0.049)	3.01 (0.072)
gi|429162	14-3-3 protein 32kDa endonuclease	1.52 (0.093)	2.12 (0.004)
gi|495731	Small ras-related protein	1.92 (0.012)	2.39 (0.000)

Fold change values of *Xac* vs. Control and *Xoo* vs. Control were given with *P*- value in the paranthesis. hpi-hours post inoculation.

Table 3.10: Transcription-related proteins differentially regulated during citrus-*Xanthomonas* interaction

Accession	Description	*Xac*/Con	*Xoo*/Con
	Proteins regulated at 8 hpi		
gi|225450527	Uncharacterized protein At1g09340	2.09 (0.045)	1.85 (0.001)
gi|21309	28kD RNA binding protein	1.64 (0.045)	2.17 (0.010)
gi|357484973	G-box-binding factor	0.35 (0.004)	0.42 (0.009)
	Proteins regulated at 48 hpi		
gi|255562029	Zinc finger protein	5.58 (0.000)	4.31 (0.021)
gi|469070	RNA-binding glycine-rich protein-1a	2.32 (0.000)	2.31 (0.162)
gi|11138076	Coatmer β subunit	2.18 (0.010)	1.04 (0.877)
gi|188526460	Maturase K	0.50 (0.004)	0.44 (0.013)

Fold change values of *Xac* vs. Control and *Xoo* vs. Control were given with *P*- value in the paranthesis. hpi-hours post inoculation.

Table 3.11: Transporters-related proteins differentially regulated during citrus-*Xanthomonas* interaction

Accession	Description	*Xac*/Con	*Xoo*/Con
	Proteins regulated at 8 hpi		
gi|166627	Nucleotide-binding subunit of vacuolar ATPase	0.41(0.070)	0.32 (0.031)
gi|124360831	H+-transporting two-sector ATPase, α/β	2.25 (0.014)	1.13 (0.674)
gi|460414021	ABC transporter C family member 8	0.24 (0.002)	0.5 2 (0.048)
	Proteins regulated at 48 hpi		
gi|168035911	ATP-binding cassette transporter	2.16 (0.003)	2.3 2 (0.007)
gi|225454680	Uncharacterized protein LOC100264930 isoform 1	3.97 (0.002)	3.66 (0.033)
gi|3334115	ADP,ATP carrier protein 1	0.77 (0.039)	0.46 (0.000)
gi|37964368	Dicarboxylate/tricarboxylate carrier	0.76 (0.178)	0.39 (0.000)
gi|111154399	Vacuolar H+-ATPase subunit C	1.02 (0.953)	2.09 (0.040)

Fold change values of *Xac* vs. Control and *Xoo* vs. Control were given with *P*- value in the paranthesis. hpi-hours post inoculation.

Table 3.12: Antioxidant-related proteins differentially regulated during citrus-*Xanthomonas* interaction

Accession	Description	*Xac*/Con	*Xoo*/Con
	Proteins regulated at 8 hpi		
gi|255566325	Glutathione transferase	5.88 (0.034)	5.98 (0.011)
gi|221327589	Ascorbate peroxidase 2	2.57 (0.080)	2.33 (0.026)
gi|225441864	NADPH-dependent thioredoxin reductase 3-like	1.92 (0.034)	2.85 (0.023)
gi|75324751	Peroxiredoxin Q, chloroplastic	2.26 (0.035)	1.67 (0.019)
	Proteins regulated at 48 hpi		
gi|146432261	Monodehydroascorbate reductase	2.30 (5.12E-05)	2.27 (0.011)
gi|34786892	Phospholipid hydroperoxide glutathione peroxidase	5.82 (0.041)	11.02 (0.169)
gi|2274917	Cu/Zn superoxide dismutase	17.83 (0.084)	24.03 (0.000)
gi|319739583	L-galactose-1-phosphate phosphatase	1.34 (0.156)	2.09 (0.019)
gi|417093	Glutathione S-transferase	0.50 (0.063)	0.25 (0.007)
gi|262192812	Catalase	0.75 (0.249)	0.48 (0.040)
gi|71534880	Hydroxyacylglutathione hydrolase	1.69 (0.057)	2.21 (0.005)
gi|20902	Superoxide dismutase	0.44 (0.169)	0 (0.016)
gi|146747426	Catalase	0.50 (0.003)	0.43 (0.002)

Fold change values of *Xac* vs. Control and *Xoo* vs. Control were given with *P*- value in the paranthesis. hpi-hours post inoculation.

Table 3.13: Intracellular traffic-related proteins differentially regulated during citrus-*Xanthomonas* interaction

Accession	Description	*Xac*/Con	*Xoo*/Con
	Proteins regulated at 8 hpi		
gi|350539281	Calnexin-like protein	0.30 (0.013)	0.45 (0.002)
gi|6714425	Putative exportin1 (XPO1)	0.21 (0.007)	0.45 (0.041)
gi|18532	Actin	2.07 (0.041)	1.52 (0.070)
gi|6016683	Clathrin heavy chain	0.46 (0.022)	0.59 (0.050)
	Proteins regulated at 48 hpi		
gi|19569135	Tubulin β-1	2.28 (0.000)	1.76 (0.003)
gi|449469885	Tubulin β-1	2.86 (0.035)	0.87 (0.839)
gi|464840	Tubulin α-1 -1 chain	2.22 (0.000)	1.47 (0.019)
gi|225460010	Dynamin-2B	3.39 (0.017)	1.46 (0.367)
gi|449438187	Annexin D2	2.44 (0.057)	2.4 6 (6.94E-05)
gi|357492745	Clathrin heavy chain	1.06 (0.874)	0.2 1 (0.031)
gi|89276295	Actin depolymerizing factor 8	1.67 (0.206)	3.54 (0.006)

Fold change values of *Xac* vs. Control and *Xoo* vs. Control were given with *P*- value in the paranthesis. hpi-hours post inoculation.

Table 3.14: Proteins regulated at both 8 and 48 hpi during citrus-*Xanthomonas* interaction

Accession	Description	*Xac*/Con 8 hpi	*Xoo*/Con 8 hpi	*Xac*/Con 48 hpi	*Xoo*/Con 48 hpi	Function
gi|2598579	L-ascorbate oxidase	0.41 (0.028)	0.59 (0.02)	3.46 (0.003)	1.83 (0.006)	Antioxidant
gi|119507461	Pectin methylesterase	5.21 (0.034)	6.58 (0.001)	0.65 (0.182)	0.36 (0.000)	Cell structure
gi|255545176	Heat shock protein	0.36 (0.015)	0.41 (0.016)	5.74 (0.008)	5.00 (0.032)	Disease/defense
gi|6911551	Heat shock protein 70	0.44 (0.033)	0.44 (0.030)	2.73 (0.0060	3.33 (0.003)	Disease/defense
gi|11596186	Cystatin-like protein	0.08 (0.019)	0.19 (0.034)	3.12 (0.024)	2.20 (0.464)	Disease/defense
gi|169821633	RUBISCO large subunit	2.06 (0.036)	2.13 (0.021)	0.41 (0.003)	0.26 (0.004)	Energy
gi|460385509	Glyceraldehyde-3-phosphate dehydrogenase	2.25 (0.010)	2.03 (0.006)	0.47 (0.003)	0.48 (0.002)	Energy
gi|4580920	Vacuole-associated annexin	0.39 (0.002)	0.59 (0.013)	3.26 (0.019)	2.69 (0.056)	Intracellular traffic
gi|18461098	Lipoxygenase	0.44 (0.031)	0.42 (0.031)	0.86 (0.591)	0.41 (0.035)	Metabolism
gi|7430935	Cinnamyl-alcohol dehydrogenase	1.93 (0.028)	4.55 (0.003)	1.22 (4.8E-07)	14.19 (0.000)	Secondary Metabolism
gi|357154587	LOW QUALITY PROTEIN: benzyl alcohol O-benzoyl transferase	2.88 (0.030)	2.04 (7.51E-05)	0.44 (0.047)	0.75 (0.350)	secondary Metabolism
gi|18418688	Uncharacterized protein	0.26 (0.011)	0.35 (0.025)	5.69 (0.067)	6.62 (0.044)	Unknown
gi|482548801	Hypothetical protein CARUB_v10025984mg	0.25 (0.001)	0.42 (0.004)	2.25 (0.012)	4.06 (4.68E-05)	Unknown proteins
gi|147770771	Hypothetical VITISV_008875	0.15 90.006)	0.14 (0.005)	3.55 (0.014)	0.44 (0.258)	Unknown proteins
gi|225442247	Uncharacterized protein LOC100244649	2.84 (0.047)	2.22 (0.002)	0.41 (0.040)	0.55 (0.120)	Unknown proteins

Fold change values of *Xac* vs. Control and *Xoo* vs. Control were given with *P*- value in the paranthesis. hpi-hours post inoculation.

reddish brown spots in *Xoo*-challenged citrus leaves at 72 hpi, whereas, in *Xac*- and mock-challenged leaves there were no such signs (Fig 3.6C).

3.3. ECM-associated proteome changes during citrus-*Xanthomonas* interactions using gel-based proteomics approach:

To obtain exhaustive coverage of ECM-associated proteins, both destructive- and non-destructive extraction methods were used. Wall-bound ECM (WE) fraction was isolated by rupturing the cells, purifying cell wall (CW) *via* differential centrifugation followed by excessive water washes. Subsequently, CW bound proteins were sequentially extracted with salts. Soluble ECM (SE) fractions were isolated by vacuum infiltration and centrifugation without breaking the cell.

3.3.1. Assessment of cytosolic contamination:

Catalase activity in the WE fraction was negligible compared to the total protein extract (Fig 3.7A). In addition, immunoblot analysis using fructose 1,6 *bis* phosphatase (FBPase) antibody showed the signal only in total protein fraction confirming that the WE fraction was free of cytosolic proteins (Fig 3.7B). Cytosolic contamination in SE fractions collected at different centrifugal forces was assessed through malate dehydrogenase (MDH) assay and immunoblot analysis with the antibody of rubisco larger subunit. MDH activity was low in the SE fraction and negligible in SE-fractions collected below 5000 g (Fig 3.7C). The signal for rubisco was detected in all the fractions except in the fractions collected at 1200 g and 1000 g (Fig 3.7D). Therefore, SE fraction extracted at 1200 g was used for proteomic analysis.

3.3.2. 2-DE and protein expression profiling:

To understand the dynamic changes occurring at the ECM of citrus during its interaction with host (*Xac*) and non-host (*Xoo*) pathogen, the proteome-level differences were examined in both WE and SE fractions. A total of 220 protein spots in WE and 192 in SE fractions were reproducibly detected in 2-DE gels. Although some protein spots were present in both WE and SE fractions, large qualitative differences were also detected in the spot profile. Three biological replicate gels were run separately for WE and SE proteins isolated from mock-, *Xac*- and *Xoo*- challenged leaves at 8, 16, 24 and 48 hpi

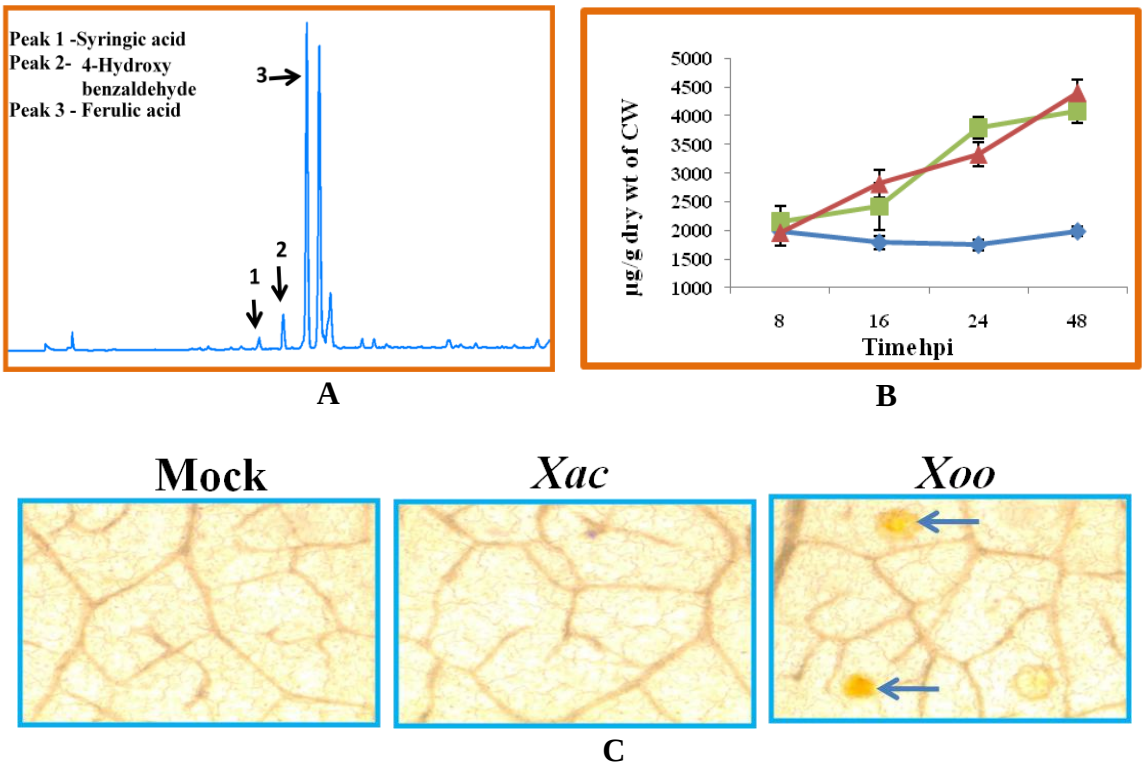

Fig 3.6: Analysis of cell wall bound phenols and lignin deposition during citrus-*Xanthomonas* interaction

A) Citrus cell wall-bound phenols extracted and profile during HPLC and with three standard phenols (shown with arrows), B) Ferulate levels at different hpi were quantified as µg/g dry weight of cell wall. Error bars indicate standard deviation of the mean from three independent experiments. hpi-hours post inoculation , and C) Staining with phloroglucinol at 72 hpi. Lignin deposition was indicated by arrows.

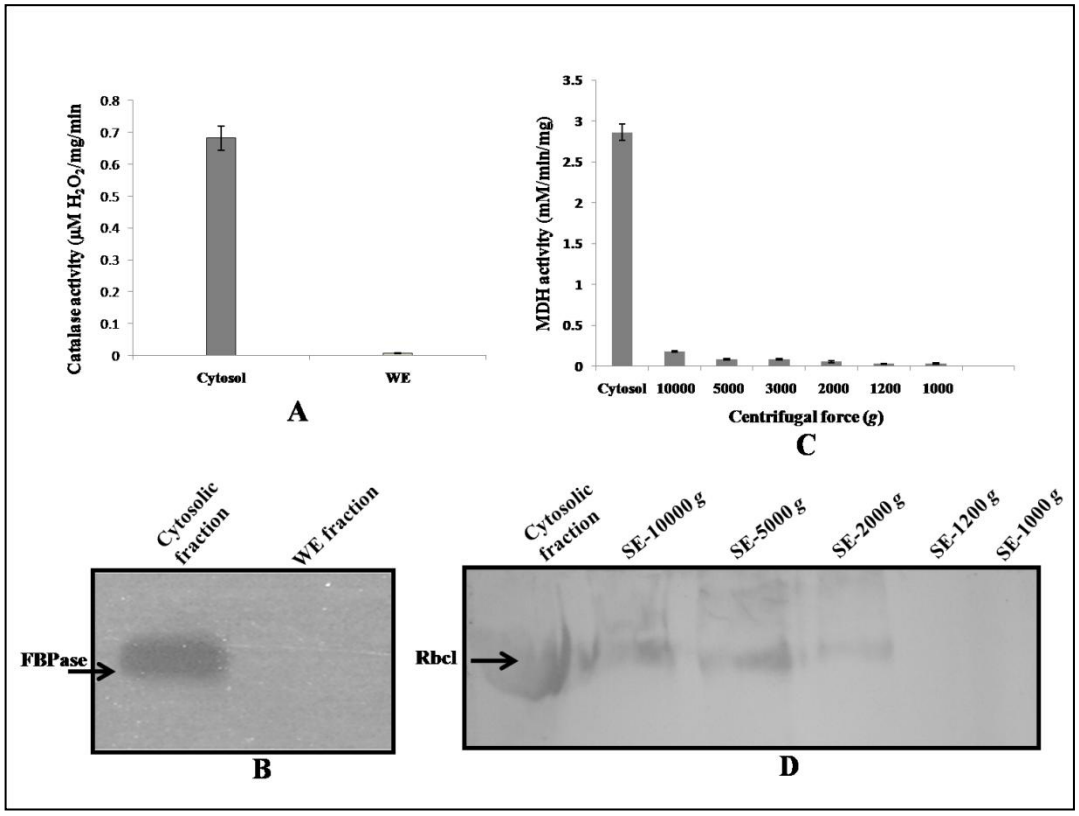

Fig 3.7: Assessment of purity of WE and SE fractions through cytosolic enzyme activity and immunoblot

A) Catalase activity in cytosolic and WE fractions, B) cytosolic and WE fraction proteins separated by SDS-PAGE and immunodetected with anti-FBPase antibody, C) malate dehydrogenase activity in cytosolic fraction and in SE fractions collected under different centrifugal force (x-axis), and D) detection of rubisco larger subunit (Rbcl) in cytosolic and SE fractions collected at different centrifugal force with anti-Rbcl polyclonal antibody.

ECM proteome. The average biological % of co-efficient of variance (% CV) for the SE fraction was < 19% and for WE fraction was < 22%. Based on % CV of WE and SE fractions, an orbitrary cut-off for quantitative difference with ±50% variance in a spot ratio (*i.e.,* spot ratio of ≥1.5-fold for upregulated and ≤ 0.5 for downregulated proteins) was selected. The gels were analysed to detect the proteins that had changed in abundance at least at one time point during any one or both the pathogen interactions. The expression of 25 proteins of WE fraction and 28 proteins of SE fraction was significantly different in response to *Xac* and *Xoo* challenge (Fig 3.8A and B). The differentially expressed proteins were analysed by MALDI-TOF MS/MS analysis, with 92% (23 out of 25 spots) of WE proteins and 75% (21 out of 28 spots) of SE proteins were successfully indentified (Table 3.15-3.17). The rest of the proteins from WE fraction (spots WE-20 and -25) and SE fraction (spots SE-9, -10, -15, -16, -19 and -25) did not show significant hits in the plant and *Xanthomonas* database and hence were not considered. Among the 44 identified proteins many of the proteins were identified with the same protein ID. In them, 2 spots were identified as chitinases, 2 as lectins and 2 spots as heat shock proteins and 3 spots as glutationine lyase and these proteins are different as they were identified each with different accession numbers. Three spots were identified as Cu/Zn SOD and among these two were same as they have same accession number and the third is different as it was identified with different accession number. Two protein spots were identified as oxygen-evolving enhancer protein 2 (OEE2), 2 as triose phosphate isomerase, 3 as xyloglucan endotranshydrolase/glucosylase (XTH) and 2 as α-xylosidase and these proteins were identified with same accession number. The expression levels of the identified proteins with standard deviation, *P*-value and putative function were listed in tables 3.15, 3.16 and 3.17.

3.3.3. Differential expression of proteins in citrus upon *Xac* and *Xoo* challenge:

3.3.3.1. The WE fraction:

The 23 differentially expressed WE fraction proteins identified in response to *Xac* and *Xoo* pathogens correspond to 16 different protein entities (Table 3.15 and Fig 3.8A). Miraculin, Cu/Zn SOD and lactoylglutathione lyase proteins were present as multiple hits in the list. Curculin-like (mannose-binding) lectin, concanavalin A-like lectin kinase-like protein and Fe SOD (spots WE-12, -13 and -15, respectively) were up-regulated

during *Xoo* interaction and significantly decreased during *Xac* interaction. α-xylosidase (spots WE-11, -17) and cys-peroxiredoxin were up-regulated during *Xac* challenges and were repressed during *Xoo* interaction. The peptidyl-prolyl *cis*-trans isomerase (spot WE-18) was up-regulated during both *Xac* and *Xoo* interactions. Two protein spots, annotated as Cu/Zn SOD (HS087559), were up-regulated during *Xoo* interaction and another protein corresponding to Cu/Zn SOD (CX672497) was induced during *Xac* interaction. Five protein spots corresponding to two isoforms of lectin-like protein, two isoforms of OEE2 and unknown predicted protein were up-regulated only during *Xoo* challenge and no significant changes occurred during *Xac* interaction. Four spots corresponding to miraculin-like proteins (MIR, MIR1 and MIR2) were differentially regulated in WE fraction. Expression of MIR-2 (spot WE-16 and -22) was identified only in WE fraction and the expression levels increased during *Xoo* challenge. Whereas the other two isoforms of miraculin were also identified to be differentially regulated in SE fraction.

3.3.3.2. The SE fraction:

Analysis of the SE fraction proteome in response to *Xac* and *Xoo* inoculation revealed changes in the expression of 28 spots (Fig 3.8B), of which 21 were identified successfully (Table 3.16). These 21 spots corresponded to 13 different protein entities. XTH and two isoforms of miraculin were present as multiple spots and differentially expressed during pathogen challenge. Two spots SE-8 and -28 were identified as MIR1, and SE-1, -12, -20 and -26 were identified as MIR. In citrus-*Xoo* interaction, two heat shock proteins, S-ribonuclease, chitinase, CHI1, cysteine and aspartyl protease were up-regulated and ascorbate peroxidase (APX) was down-regulated. During *Xac* interaction, expression of thaumatin, APX, glucan 1,3 β-glucosidase and endochitinase increased, while chitinase and aspartyl protease decreased.

3.3.3.3. In both WE and SE fraction:

Though WE and SE fractions protein profile was dissimilar, four proteins corresponding to miraculin, lactoylglutathione lyase activity protein, XTH and triosephosphate isomerase were differentially expressed in both the fractions during pathogen challenge (Table3.17). Four spots of WE and six spots of SE fraction corresponded to three isoforms of miraculin protein. The multiple spots of miraculin had different pIs and/ or MWt in the 2-DE gels. Protein spots WE-4 and -5 and SE-21 corresponded to

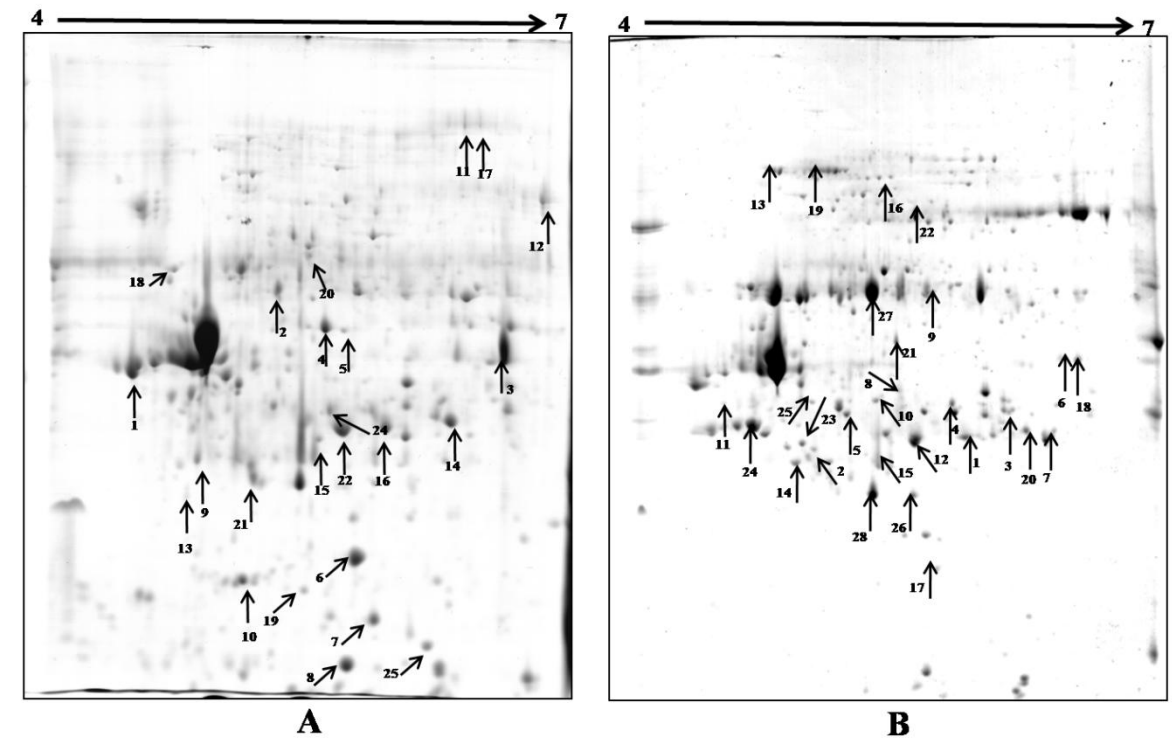

Fig 3.8: Representative images of 2D gels of citrus leaf ECM proteome in response to *Xac* and *Xoo* challenge

Proteome separated by 2-DE and visualized by colloidal coomassie blue. A) WE fraction, B) SE fraction. Arrows and numbers represent the protein spots that altered significantly (P<0.05) and selected for MS/MS analyses.

Table 3.15: Proteins differentially expressed only in wall-bound ECM-fraction during *Xac* and *Xoo* challenge

Spot no.[a]	Homologous protein	Fold Change at Time[b] (hpi)							
		Xac				*Xoo*			
		8	**16**	**24**	**48**	**8**	**16**	**24**	**48**
WE-1	Lectin-related protein precursor	0.65 (0.002)	1.15 (0.123)	0.76 (0.021)	1.06 (0.552)	1.50 (0.004)	1.71 (0.045)	1.42 (0.167)	1.24 (0.184)
WE-2	Unknown predicted protein	0.96 (0.689)	1.19 (0.221)	1.22 (0.177)	1.28 (0.352)	1.33 (0.144)	1.96 (0.007)	1.58 (0.033)	1.42 (0.072)
WE-6	Cu/Zn-superoxide dismutase SOD2	1.35 (0.005)	1.22 (0.046)	1.41 (0.023)	1.00 (0.962)	2.14 (0.002)	1.75 (0.007)	2.16 (0.018)	1.47 (0.038)
WE-7	Cu/Zn-superoxide dismutase SOD2	0.80 (0.283)	1.47 (0.027)	1.36 (0.046)	1.01 (0.085)	1.78 (0.019)	1.90 (0.030)	1.93 (0.001)	1.41 (0.024)
WE-8	Cu/Zn-superoxide dismutase SOD2	1.02 (0.035)	2.58 (0.018)	1.13 (0.066)	1.27 (0.057)	1.41 (0.075)	1.09 (0.047)	1.24 (0.186)	1.15 (0.005)
WE-9	2-Cys-Peroxiredoxin	1.26 (0.020)	1.34 (0.055)	1.69 (0.008)	1.24 (0.125)	0.91 (0.145)	0.43 (0.006)	1.03 (0.046)	1.12 (0.070)
WE-10	Oxygen-evolving enhancer protein 2	0.92 (0.176)	1.08 (0.098)	1.13 (0.085)	0.97 (0.073)	1.26 (0.075)	1.60 (0.047)	1.24 (0.016)	1.45 (0.151)
WE-11	Alpha-xylosidase	1.40 (0.090)	1.18 (0.065)	1.32 (0.010)	1.53 (0.014)	1.21 (0102)	1.43 (0.008)	0.81 (0.061)	1.25 (0.029)
WE-12	curculin-like (mannose-binding) lectin	0.83 (0.214)	0.95 (0.074)	0.49 (0.004)	0.97 (0.055)	1.78 (0.012)	2.80 (0.005)	1.46 (0.036)	1.20 (0.021)
WE-13	concanavalin A-like lectin kinase	0.69 (0.023)	0.46 (0.044)	0.61 (0.017)	0.95 (0.132)	1.70 (0.015)	1.87 (0.013)	1.39 (0.050)	1.20 (0.106
WE-15	Fe-superoxide dismutase	1.02 (0.237)	0.49 (0.015)	0.95 (0.166)	1.37 (0.225)	1.50 (0.107)	1.68 (0.028)	1.55 (0.041)	0.63 (0.263)
WE-16	Miraculin-like protein 2	0.96 (0.374)	0.81 (0.183)	1.22 (0.341)	1.18 (0.057)	1.52 (0.002)	1.23 (0.26)	1.36 (0.295)	0.90 (0.021)
WE-17	Alpha-xylosidase	1.29 (0.000)	1.05 (0.170)	1.36 (0.004)	1.59 (0.015)	1.10 (0.077)	0.85 (0.032)	0.92 (0.018)	1.37 (0.049)
WE-18	Peptidyl-prolyl cis-trans isomerase	1.22 (0.276)	1.62 (0.009)	2.54 (0.048)	1.27 (0.095)	1.60 (0.039)	1.52 (0.020)	1.09 (0.258)	1.46 (0.223)
WE-19	Oxygen-evolving enhancer protein 2	1.19 (0.331)	1.32 (0.163)	1.26 (0.125)	1.15 (0.177)	1.43 (0.163)	1.71 (0.018)	1.37 (0.224)	1.40 (0.068)
WE-21	lectin-related protein precursor	1.38 (0.018)	1.13 (0.164)	1.27 (0.133)	0.82 (0.062)	1.62 (0.007)	1.44 (0.003)	1.37 (0.068)	1.26 (0.015)
WE-22	Miraculin-like protein 2	1.15 (0.332)	1.40 (0.091)	1.46 (0.186)	1.05 (0.727)	1.77 (0.011)	1.69 (0.009)	2.02 (0.069)	1.43 (0.025)

[a] Spot no., spot number as given in Fig. 3.8A [b]Fold change time represents average of relative fold change of either *Xac* and *Xoo* challenge compared with the mock-inoculated plants at 8, 16, 24 and 48 hours post inoculation (hpi) ± standard error. Data in parentheses denote *P*- values of student's t-test.

Table 3.16: Proteins differentially expressed only in soluble ECM-fraction during *Xac* and *Xoo* challenge

Spot no.[a]	Homologous protein	Fold Change at Time (hpi)							
		Xac				*Xoo*			
		8	**16**	**24**	**48**	**8**	**16**	**24**	**48**
SE-2	Thaumatin like-protein	1.50 (0.049)	1.01 (0.116)	0.63 (0.042)	0.86 (0.257)	1.05 (0.103)	1.44 (0.304)	1.35 (0.417)	1.24 (0.054)
SE-4	Ascorbate peroxidase 2	1.60 (0.019)	1.55 (0.040)	1.28 (0.137)	0.75 (0.066)	0.56 (0.002)	0.34 (0.025)	0.49 (0.020)	1.25 (0.361)
SE-7	Chitinase CHI1	0.53 (0.002)	0.91 (0.106)	0.47 (0.005)	1.09 (0.081)	1.86 (0.009)	1.34 (0.074)	1.79 (0.002)	1.47 (0.060)
SE-11	Cysteine protease	1.40 (0.324)	0.97 (0.053)	1.28 (0.194)	0.86 (0.227)	1.02 (0.086)	1.55 (0.014)	1.88 (0.015)	1.40 (0.023)
SE-13	Heat shock protein	1.39 (0.017)	1.15 (0.086)	1.22 (0.129)	1.14 (0.083)	1.78 (0.024)	1.51 (0.006)	1.35 (0.097)	1.23 (0.060)
SE-14	S-like ribonuclease	1.01 (0.083)	0.49 (0.015)	0.37 (0.003)	1.22 (0.179)	2.27 (0.006)	0.99 (0.031)	1.36 (0.001)	0.70 (0.107)
SE-17	Heat shock protein	1.27 (0.121)	1.10 (0.095)	1.34 (0.068)	1.22 (0.079)	1.76 (0.019)	1.54 (0.054)	1.30 (0.145)	1.39 (0.003)
SE-22	Glucan 1,3-beta-glucosidase 2	1.36 (0.047)	1.42 (0.029)	1.77 (0.0002)	2.03 (0.011)	1.14 (0.237)	0.59 (0.010)	0.50 (0.004)	1.24 (0.076)
SE-23	Chitinase	1.07 (0.586)	0.50 (0.006)	0.96 (0.782)	0.49 (0.022)	2.27 (0.032)	2.32 (0.007)	1.89 (0.031)	1.40 (0.070)
SE-24	Endochitinase	1.74 (0.035)	1.46 (0.049)	1.35 (0.074)	1.04 (0.062)	1.81 (0.003)	2.43 (0.004)	2.08 (0.018)	1.43 (0.131)
SE-27	Aspartyl protease	0.53 (0.002)	0.67 (0.053)	0.49 (0.006)	1.07 (0.015)	1.42 (0.007)	1.53 (0.028)	1.20 (0.05)	3.69 (0.031)

[a] Spot no., spot number as given in Fig. 3.8B.

Table 3.17: Proteins differentially expressed in both wall-bound and soluble ECM-fraction during *Xac* and *Xoo* challenge

Spot no.	Homologous protein	Fold Change at Time (hpi)							
		Xac				*Xoo*			
		8	**16**	**24**	**48**	**8**	**16**	**24**	**48**
WE-3	Xyloglucan endotrans glucosylase /hydrolase	1.38 (0.117)	0.90 (0.041)	1.39 (0.086)	1.03 (0.90)	1.70 (0.092)	1.53 (0.069)	1.75 (0.003)	1.59 (0.055)
WE-4	Lactoylgluta-thione lyase	1.36 (0.238)	1.32 (0.117)	1.72 (0.009)	1.44 (0.385)	1.41 (0.116)	1.55 (0.071)	1.41 (0.003)	1.58 (0.043)
WE-5	Lactoylgluta-thione lyase	1.08 (0.045)	1.37 (0.031)	1.56 (0.002)	1.53 (0.033)	1.20 (0.076)	1.44 (0.048)	1.47 (0.059)	1.61 (0.014)
WE-14	Miraculin-like protein	1.29 (0.042)	0.77 (0.089)	1.31 (0.103)	0.26 (0.043)	1.28 (0.037)	1.42 (0.056)	1.08 (0.017)	1.23 (0.136)
WE-23	Triosephosphate isomerase	1.25 (0.085)	1.50 (0.027)	1.68 (0.004)	1.79 (0.018)	1.14 (0.056)	1.09 (0.231)	1.68 (0.074)	1.45 (0.020)
WE-24	Miraculin-like protein 1	1.38 (0.028)	2.73 (0.014)	0.87 (0.135)	1.45 (0.076)	2.62 (0.030)	2.02 (0.069)	1.66 (0.020)	1.38 (0.084)
SE-1	Miraculin-like protein	1.13 (0.094)	1.21 (0.068)	0.68 (0.029)	0.37 (0.001)	1.42 (0.063)	1.04 (0.007	1.18 (0.045)	1.46 (0.027)
SE-5	Triosephosphate isomerase	1.06 (0.041)	1.22 (0.019)	1.54 (0.015)	1.77 (0.003)	1.19 (0.032)	1.46 (0.003)	1.50 (0.024)	1.37 (0.056)
SE-6	Xyloglucan endotrans glucosylase /hydrolase	0.86 (0.176)	1.32 (0.141)	1.25 (0.035)	0.81 (0.109)	1.16 (0.118)	1.79 (0.012)	1.94 (0.005)	1.38 (0.014)
SE-8	Miraculin-like protein 1	1.12 (0.013)	1.26 (0.046)	1.85 (0.037)	1.22 (0.065)	1.51 (0.009)	1.43 (0.002)	1.60 (0.042)	1.14 (0.046)
SE-12	Miraculin-like protein	1.34 (0.061)	1.16 (0.023)	1.07 (0.055)	0.49 (0.036)	1.02 (0.108)	1.35 (0.062)	0.96 (0.018)	1.44 (0.087)
SE-18	Xyloglucan endotransgluco-sylase/hydrolase	0.78 (0.106)	1.20 (0.035)	1.37 (0.089)	1.26 (0.066)	1.07 (0.092)	1.51 (0.013)	2.97 (0.002)	1.23 (0.057)
SE-20	Miraculin-like protein	1.29 (0.007)	0.55 (0.069)	0.32 (0.028)	1.02 (0.118)	1.36 (0.040)	0.78 (0.062)	1.04 (0.013)	0.61 (0.080)
SE-21	Lactoylgluta-thione lyase	1.45 (0.043)	1.62 (0.029)	1.08 (0.027)	1.37 (0.094)	1.12 (0.087)	1.19 (0.055)	2.04 (0.034)	1.59 (0.112)
SE-26	Miraculin-like protein	1.53 (0.116)	0.61 (0.040)	0.38 (0.07 1)	0.92 (0.085)	2.79 (0.005)	2.01 (0.036)	1.32 (0.142)	1.83 (0.068)
SE-28	Miraculin-like protein 1	0.72 (0.051)	0.76 (0.022)	0.86 (0.069)	1.15 (0.031)	1.55 (0.024)	0.81 (0.076)	1.46 (0.045)	1.42 (0.092)

[a] Spot no., spot number as given in Fig. 3.8A and B.

lactoylglutathione lyase and showed differential expression. Two of SE and one of WE fraction proteins were identified as triosephosphate isomerase, whose expression increased during both *Xac* and *Xoo* interaction.

3.3.4. Expression patterns of ECM-associated proteome during Xac and Xoo interaction:

To evaluate the pattern of expression of 44 (23 of WE and 21 of SE fractions) differentially expressed proteins over the course of time after *Xac* and *Xoo* challenge, a hierarchical clustering analysis was performed. The average fold-change expression values transformed to $\log_2$ were used for clustering in PermutMatrix software. The cluster analysis categorised 44 proteins into 3 prominent divisions and subdivided into 8 clusters (Fig 3.9). Cluster 1 and 2 represent the proteins with increased expression in citrus-*Xoo* interaction at 2 or 3 time points or at least at one time point, respectively. Whereas, proteins with induced expression, at least at one time point during *Xac* and *Xoo* interaction, correspond to clusters 3 and 4, respectively. Proteins with decreased expression in citrus-*Xac* interaction clustered as division 5. In 6 and 7 clusters, proteins that decreased during *Xac* and increased in *Xoo* interactions clustered. Cluster 8 included proteins with decreased expression in *Xoo* interaction.

3.3.4. Effect of secretory vesicle trafficking inhibition on *in planta* bacterial growth:

In planta growth of *Xac* increased by 2 log units at 3 days after inoculation (dai) in 0.5 % DMSO pre-infiltrated leaves and by 3 log units in brefeldin A treated leaves. During citrus-*Xoo* interaction, the *in planta* growth of the bacteria decreased by 1 log unit at 2 dai, and further declined by 3 dai in DMSO pre-infiltrated leaves. Whereas, in brefeldin A pre-infiltrated leaves, *Xoo* survived and increased the count at 3 dai (Fig 3.10). Cell death was not observed in *Xoo*-infiltrated in brefeldin A-treated leaves at 3 dai.

3.4. Nuclear proteome changes during citrus-*Xanthomonas* interaction:

Nuclear proteome constitutes a highly organized, complex network that plays diverse roles during cellular development and other physiological processes. These proteins are involved in different cellular functions such as cell signalling, gene regulation, structure, translation, proteolysis, physiological responsiveness and a variety of RNA-associated

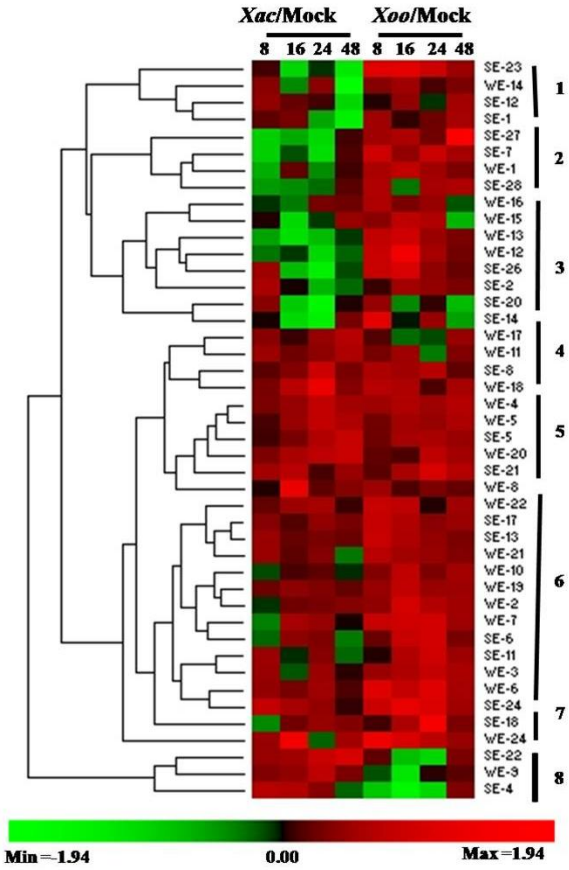

Fig 3.9: Hierarchical cluster analysis of differentially expressed proteins

The average fold-change in expression levels between mock and either *Xac* or *Xoo* interaction at 8, 16, 24 and 48 hpi were transformed in to $\log_2$ value and hierarchical clustering was performed with PermutMatrix graphical interface. Euclidean distance similarity metric and complete linkage method were used for the analysis. Each row represents fold-change levels coloured according to the scale at the bottom of the figure and spot numbers are indicated for each row. Number of clusters is indicated at the right side.

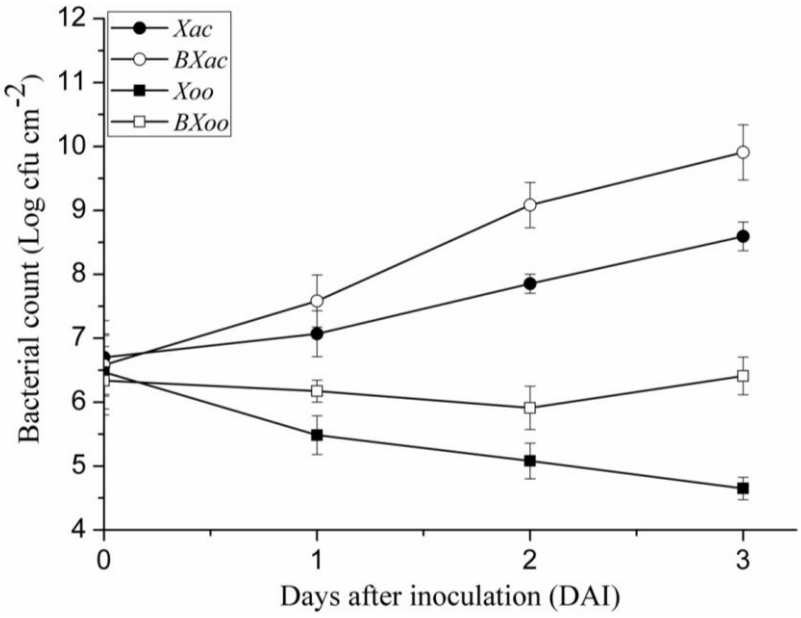

Fig 3.10: Growth of *Xac* and *Xoo* after infiltration in DMSO or brefeldin A pre-infiltrated citrus leaves

Bacterial growth in DMSO or brefeldin A pre-infiltrated citrus leaves was assessed from 0.6 cm leaf discs of *Xac* and *Xoo* infiltrated regions and bacterial number expressed as CFU cm^{-2} leaf tissue. Lines with closed and open circle represent *Xac* growth pattern in DMSO or brefeldin A pre-infiltrated leaves respectively. Whereas, closed and open square represents growth pattern of *Xoo* in DMSO or brefeldin A pre-infiltrated leaves. Values represent means of three samples; error bars represent standard deviations.

functions. We have analysed the nuclear proteome of citrus during *Xanthomonas* interaction. The integrity of a sub-cellular proteome is largely dependent on the purification of the isolated compartment away from other cellular contaminants. The separation of high-purity nuclei from plant is a difficult task as it might compromise the yield. In this study, the nuclei were isolated from citrus leaves using hyperosmotic sucrose buffer, and the nuclei-enriched pellet so obtained was washed repeatedly to separate contaminants from other organelles. The integrity of the isolated nuclei was analyzed by DAPI staining (Fig 3.11A). The nuclei were uniform spheres. These results indicate that the isolated nuclei were highly purified. The nuclear proteins were prepared from the purified nuclei using Trizol reagent (Sigma) to remove the contaminating nucleic acids which might interfere during the IEF process. The enrichment of nuclear proteins was evaluated by immunoblot analysis using specific antibodies for FBPase (Fig 3.11C). The protein profile of the nuclear fractions appeared distinct and enriched with nuclear proteins from that of the cytosolic fractions in a 1D gel (Fig 3.11B). The proteome was determined using a sequential method of organelle enrichment followed by 2-DE-based and nanoLC-MS based protein identification.

3.4.1. Gel-based proteomics of citrus nuclear proteome:

To monitor changes in citrus nuclear proteome prepared at 2, 8, 16 and 48 hpi after *Xac* or *Xoo* infiltration, 2DE was performed. 2-D map of citrus nuclear proteome was constructed on pH 4.0-7.0 range, 11 cm IPG strips and visualized through silver staining. The probability of differences being statistically significant was calculated using student's t test; changes in expression were considered significant if the calculated *p* value was < 0.05. The differentially expressed spots were manually excised from the gel and subsequently characterized by MALDI-TOF/TOF MS analysis.

The proteome analysis led to the identification of 18 differentially regulated proteins (Fig 3.12A) (out of 32 differentially expressed spots) presumably involved in a variety of functions (Table 3.18). These include 1) signalling-related proteins (F-box, Wall associated kinase 3, patatin-like phospholipase2), 2) transcription and chromosome remodelling (kinetochore protein, bHLH62, WRKY-22, SW1/SNF-related matrix-associated actin regulator of chromatin subfamily A and Cytosine-5 DNA methyltransferase DRM2), 3) defense (flavin containing monoxygenase, disease resistance protein, hypothetical selmodraft and tetrahydrocannabinolic acid synthase), 4)

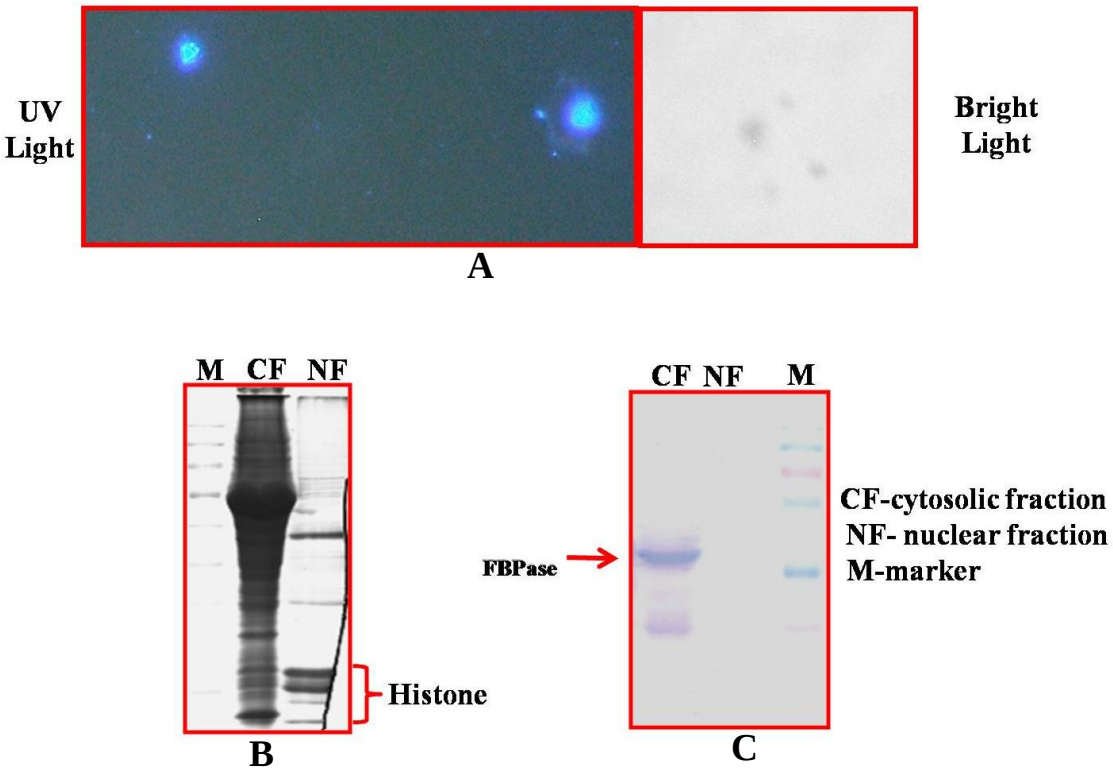

Fig 3.11: Assessment of integrity and purity of citrus nuclear proteome fraction

A) the purified nuclear fraction was stained with DAPI and visualized by microscopy. Micrograph of the DAPI-stained nuclei under UV light (left panel), and bright light (right panel), B) Enrichment of nuclear proteins was analysed by 1-DE. Aliquots of 30µg of nuclear fraction (NF) protein and 10µg of cytosolic fraction (CF)s were separated by 12.5% SDS-PAGE, and C) immunoblot analysis of extracted nuclear proteins with anti-FBPase antibody. The gel was electroblotted onto nitrocellulose membrane, and FBPase was detected using alkaline phosphatase conjugated secondary antibodies.

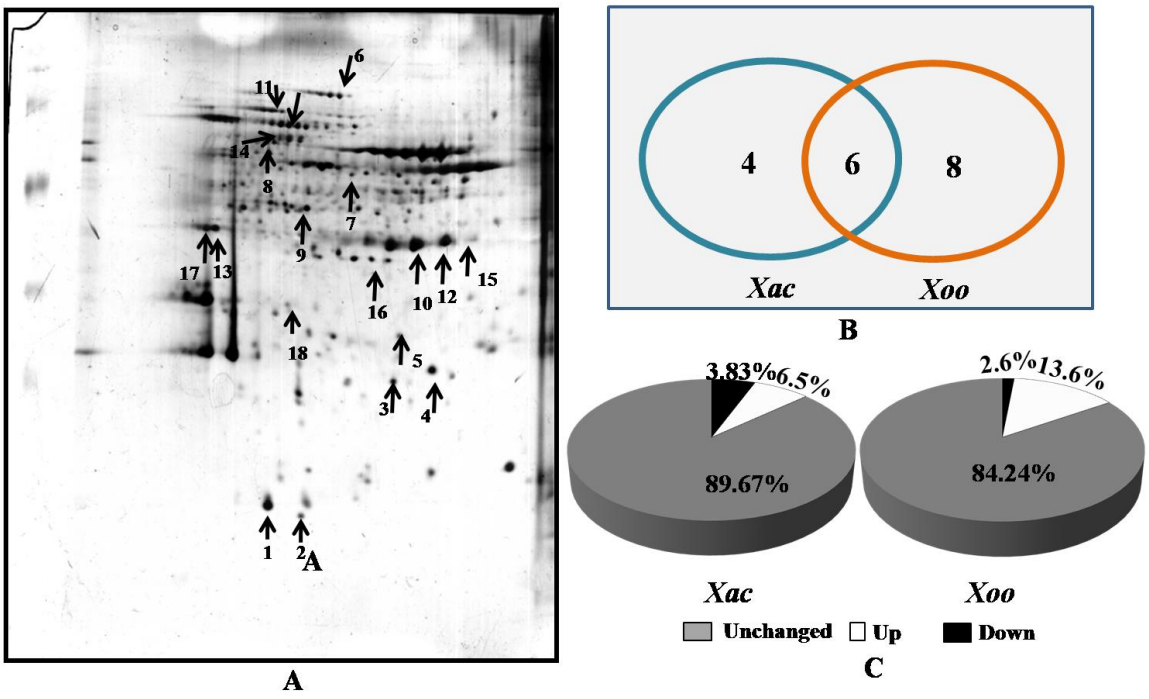

Fig 3.12: Representative image of 2D gel and diagrammatic representation of differentially expressed citrus leaf nuclear proteome in response to *Xac* and *Xoo* challenge

A) Proteome separated by 2-DE and visualized by silver staining. Arrows and numbers represent the protein spots that altered significantly ($P<0.05$) and selected for MS/MS analyses. B) Venn diagram and C) Pie analysis of the expression of differentially regulated proteins during *Xac* and *Xoo* interaction.

Table 3.18: Differentially regulated nuclear proteins during citrus-*Xanthomonas* interaction identified in 2 DE

Spot no.	Accession	Description	Organism	*Xac*/Con	*Xoo*/Con
		Proteins differentially regulated at 2 hpi			
1.	FBW2_ARATH	F-box protein	*Arabidopsis thaliana*	0.98	**1.57**
		Proteins differentially regulated at 8 hpi			
11.	WRK22_ARATH	WRKY-22	*Arabidopsis thaliana*	**1.59**	**1.82**
12.	HDG10_ARATH	Homeobox-leucine zipper	*Arabidopsis thaliana*	**1.51**	**2.09**
14.	ATPA_DAUCA	Wall associated kinase 3	Daucus carota	0.64	**1.72**
15.	PPL2_ARATH	Patatin like phospholipase2	*Arabidopsis thaliana*	1.03	**1.60**
13.	DRM2_ARATH	Cytosine-5 DNA methyltransferase DRM2	*Arabidopsis thaliana*	1.52	**1.98**
		Proteins differentially regulated at 16 hpi			
3.	gi|21311	Rieske FeS-precursor	*Spinacia oleracea*	**1.62**	1.45
4.	gi|225448101	kinetochore protein NDC80 homolog	*Vitis vinifera*	**0.29**	0.98
6.	BH062_ARATH	Transcription factor bHLH62	*Arabidopsis thaliana*	0.86	**1.50**
9.	NDHI_CITSI	NAD(P)H-quinone oxidoreductase subunit I	*Citrus sinensis*	**1.72**	1.09
10.	SM3L1_ARATH	SWI/SNF-related matrix-associated actin-dependent regulator of chromatin subfamily A member 3-like 1	*Arabidopsis thaliana*	**0.34**	1.25
13.	DRM2_ARATH	Cytosine-5 DNA methyltransferase DRM2	*Arabidopsis thaliana*	0.91	**1.50**
18.	FRS10_ARATH	FAR1 related	*Arabidopsis thaliana*	**1.84**	**2.01**
		Proteins differentially regulated at 48 hpi			
2.	RPOA_NYMAL	DNA-directed RNA polymerase subunit alpha	*Nymphaea alba*	1.48	**1.90**
5.	gi|302820319	hypothetical protein SELMODRAFT_272235	*Selaginella moellendorffii*	0.98	**2.00**
7.	THCAS_CANSA	Tetrahydrocannabinolic acid synthase	*Cannabis sativa*	1.39	**1.83**
8.	gi|16322958	disease resistance protein	*Theobroma cacao*	**0.41**	1.03
10.	SM3L1_ARATH	SWI/SNF-related matrix-associated actin-dependent regulator of chromatin subfamily A member 3-like 1	*Arabidopsis thaliana*	**2.02**	**1.69**
16.	FMO_ARATH	Flavin containing monoxygenase	*Arabidopsis thaliana*	1.02	**1.74**
17.	DHX15_ARATH	pre-mRNA-splicing factor ATP-dependent RNA helicase	*Arabidopsis thaliana*	1.45	**1.81**

Fold change values of significantly regulated proteins during *Xac* vs. Control and *Xoo* vs. Control interaction were indicated by bold. hpi-hours post inoculation.

unknown function (hypothetical protein and predicted protein), and 5) proteins with other functions (Pre-mRNA splicing factor FAR1 related, DNA directed RNA pol, ATPase subunit and Rieske Fe-S precursor).

3.4.2. Non-gel-based proteomics of citrus nuclear proteome:

NanoLC-MS/MS based expression profiling of citrus nuclear proteome of 2, 8, 16 and 48 hpi during interaction with *Xanthomonas* was examined. These time points corresponded to early interaction of pathogen with plant (2 and 8 hpi), the first visible defense response, callose deposition occurred at 16 hpi against *Xoo*, and first visible symptoms of disease occurred at 48 hpi. Twenty three proteins with significant changes of expression were identified at 2 hpi. Of these, 12 proteins were differentially expressed during *Xac* interaction and 14 protein in *Xoo* interaction. Three proteins have overlapped regulation during both *Xac* and *Xoo* interactions. At 8 and 16 hpi, 31 and 69 proteins, respectively, were differentially regulated. Among them, 4 proteins at 8 hpi and 5 at 16 hpi were differentially expressed at both the interactions. At late hours of interaction *i.e*., at 48 hpi, 120 proteins were regulated. Fourteen of these proteins had significant changes of expression during both interactions.

To understand the function of the nuclear proteins, the identified proteins were sorted into various categories, based on their putative function. However, the classification of proteins is only tentative, since the biological function of many proteins identified is not yet established experimentally. Most of the differentially expressed proteins were grouped under the unknown category. Other functional categories mentioned are as follows:

3.4.2.1. Proteins-related to signalling and gene regulation:

Recognization of pathogen ingression at the plant cell surface leads to downstream signalling pathway and regulates gene expression to induce defense responses. In the present study, the expression of proteins related to signalling and gene regulation were more at 48 hpi compared to other time points. Histones, the basic proteins of the nucleus and their variants functionally differentiate individual nucleosomes, act as key regulators of chromatin structure and function. Four histones *viz*., histone H1, histone H2B, histone H3.2, and putative histone H3 were differentially regulated, (Table 3.19). Other proteins

like F-box/kelch-repeat protein, leucine-rich repeat receptor-like serine/threonine-protein kinase, histone-lysine N-methyltransferase, pentatricopeptide repeat-containing protein, DNA topoisomerase, fructoribonuclease and aldolase were differentially regulated. Most of these proteins were induced at 48 hpi upon *Xac* challenge.

3.4.2.2. Transcription and chromosome remodelling proteins:

Transcription factors (TFs) constitute a protein superfamily that regulates the expression of many plant genes during biotic stress. MADS-box TF, DEAD-box ATP-dependent RNA helicase 3, nuclear TF, zinc finger protein and homeobox-leucine zipper protein ATHB-14 decreased at 8 hpi during *Xoo* interaction, while decreased 48 hpi during *Xac* challenge. At 2 hpi, heat stress TF A-3 had decreased expression during *Xac* challenge. Whereas at 16 hpi, structural maintenance of chromosome protein 3 was repressed during both pathogen interactions and DEAD-box ATP-dependent RNA helicase 40 was induced during *Xac* interaction (Table 3.20).

3.4.2.3. Transport-related proteins:

The transport category including nucleobase-ascorbate transporter 5, pyrophosphate-energized vacuolar membrane proton pump, aquaporin PIP-type and D-xylose-proton symporter-like 3 were repressed during *Xac* interaction at 48 hpi. Whereas, other proteins like membrane-associated protein VIPP1, phosphate transporter PHO1 and vacuolar proton ATPase decreased during both the interactions. At 16 hpi, nuclear-pore anchor and potassium transporter 7 increased during both the interactions but at 2 hpi the increased was only during *Xoo* interaction (Table 3.21). ABC transporter B family member 25 decreased during *Xoo* interaction at 16 hpi, and sugar transporter ERD6-like decreased during both interactions at 2 hpi.

3.4.2.4. Proteins related to translation and degradation:

Proteins involved in the translational machinery are known to be associated with nuclear proteome. Most of the proteins related to protein translation were regulated at 48 hpi (Table 3.22). In the present study, 30S, 40s, 50s and 60s ribosomal proteins were differentially regulated. Polyadenylate-binding protein decreased during both the interactions whereas, the same protein increased at 2 hpi during *Xac* interaction. Another

Table 3.19: Signalling and gene regulation-related proteins regulated in citrus nuclear proteome during *Xanthomonas* interaction

Accession	Description	*Xac*/Con	*Xoo*/Con
	Proteins regulated at 2 hpi		
PP148_ARATH	Pentatricopeptide repeat-containing protein	0.23 (0.013)	0.30 (0.016)
H2B3_SOLLC	Histone H2B.3	2.04 (0.031)	1.89 (0.013)
H1_EUPES	Histone H1	0.25 (0.002)	0.63 (0.021)
PGKY_TOBAC	Phosphoglycerate kinase	2.92 (0.141)	2.66 (0.005)
ALF_MAIZE	Fructose-bisphosphate aldolase	2.08 (0.039)	1.75 (0.054)
H3_VOLCA	Histone H3	3.44 (0.153)	2.85 (0.029)
CML13_ARATH	Probable calcium-binding protein CML13	1.37 (0.159)	2.25 (0.041)
PGKH_TOBAC	Phosphoglycerate kinase	1.84 (0.175)	2.077 (0.047)
	Proteins regulated at 8 hpi		
H2AV2_ORYSJ	Probable histone H2A variant 2	2.50 (0.013)	2.41 (0.013)
DHEA_NICPL	Glutamate dehydrogenase A	0.47 (0.000)	0.28 (0.000)
PGKY_WHEAT	Phosphoglycerate kinase	1.22 (0.394)	0.42 (0.003)
	Proteins regulated at 16 hpi		
PR19A_ARATH	Pre-mRNA-processing factor 19 homolog 1	2.30 (0.029)	2.15 (0.001)
PP148_ARATH	Pentatricopeptide repeat-containing protein	0.29 (0.002)	0.14 (4.37E-05)
Y2923_ARATH	leucine-rich repeat receptor-like serine/threonine-protein kinase	0.05 (0.009)	0.92 (0.933)
TBB2_ANEPH	Tubulin β-2 chain	0.49 (0.140)	0.26 (0.039)
ALFC1_PEA	Fructose-bisphosphate aldolase 1	3.36 (0.085)	4.53 (0.015)
KPPR_SPIOL	Phosphoribulokinase	2.07 (0.132)	3.96 (0.002)
GCSP_SOLTU	Glycine dehydrogenase	2.23 (0.156)	3.78 (0.012)
FBK87_ARATH	F-box/kelch-repeat protein	5.70 (0.170)	2.88 (0.045)
KPPR_PINPS	Phosphoribulokinase	2.82 (0.125)	4.44 (0.004)
H2AXA_ARATH	Probable histone H2AXa	1.51 (0.398)	0.49 (0.016)
H2AV2_ORYSJ	Probable histone H2A variant 2	1.05 (0.905)	0.40 (0.009)
	Proteins regulated at 48 hpi		
ACT1_ARATH	Actin-1	0.39 (0.009)	0.52 (0.015)
TBB1_ORYSJ	Tubulin β-1 chain	0.20 (0.000)	0.35 (0.016)
PP295_ARATH	Pentatricopeptide repeat-containing protein	6.28 (0.002)	3.41 (0.003)
ASHH4_ARATH	Putative histone-lysine N-methyltransferase ASHH4	0.12 (0.000)	0.29 (0.003)
PEN7_ARATH	Putative pentacyclic triterpene synthase 7	0.31 (0.001)	0.42 (0.005)
PPR29_ARATH	Pentatricopeptide repeat-containing protein At1g10270	0.25 (0.004)	0.42 (0.036)
ALFC2_PEA	Fructose-bisphosphate aldolase 2	0.46 (0.001)	0.59 (0.000)
CML13_ARATH	Probable calcium-binding protein CML13	0.20 (0.013)	0.33 (0.024)
H32_ARATH	Histone H3.2	14.98 (0.017)	2.75 (0.097)
H32_CICIN	Histone H3.2	82.46(2.48E-08)	21.45 (0.154)
H2A_EUPES	Histone H2A	7.17 (0.008)	3.12 (0.072)

(Table 3.19 continued)

Accession	Description	*Xac*/Con	*Xoo*/Con
PGKY_TOBAC	Phosphoglycerate kinase	9.87 (0.025)	9.25 (0.210)
TOP1_DAUCA	DNA topoisomerase	2.05 (0.001)	1.26 (0.397)
UBQ9_ARATH	Polyubiquitin 9	5.49 (0.000)	4.81 (0.197)
PP148_ARATH	Pentatricopeptide repeat-containing protein At2g04860	8.94 (0.013)	6.86 (0.199)
Y2923_ARATH	Leucine-rich repeat receptor-like serine/threonine-protein kinase	92.41 (1.5E-05)	28.34 (0.165)
SDLCA_SOYBN	Dynamin-related protein 12A	7.12 (0.002)	1.03 (0.954)
GBLP_SOYBN	Guanine nucleotide-binding protein subunit β-like protein	15.15 (0.001)	2.52 (0.386)
ACT3_TOBAC	Actin-54	0.44 (0.023)	0.59 (0.060)
GCSP_SOLTU	Glycine dehydrogenase	0.23 (0.004)	0.53 (0.171)
CALM_BRYDI	Calmodulin	0.17 (0.019)	0.41 (0.110)
PMA11_ARATH	ATPase 11, plasma membrane-type	0.01 (0.003)	0.54 (0.271)
PMA1_NICPL	Plasma membrane ATPase 1	0 (0.007)	0.60 (0.505)
K6PF5_ARATH	6-phosphofructokinase 5	0.28 (0.020)	0.59 (0.182)

Fold change values of *Xac* vs. Control and *Xoo* vs. Control were given with *P*- value in the paranthesis. hpi-hours post inoculation.

Table 3.20: Transcriptional regulators and chromatin remodelling-related proteins regulated in citrus nuclear proteome during *Xanthomonas* interaction

Accession	Description	*Xac*/Con	*Xoo*/Con
	Proteins regulated at 2 hpi		
HSFA3_ARATH	Heat stress transcription factor A-3	0.20 (0.006)	0.85 (0.473)
SMC3_ARATH	Structural maintenance of chromosomes protein 3	0.11 (0.04)	0.22 (0.062)
	Proteins regulated at 8 hpi		
RH20_ARATH	DEAD-box ATP-dependent RNA helicase 20	0.11 (0.000)	0.24 (0.000)
TOP1_DAUCA	DNA topoisomerase 1	0.72 (0.062)	0.38 (0.004)
MAD56_ORYSI	MADS-box transcription factor 56	0.57 (0.004)	0.28 (0.000)
NFYA2_ARATH	Nuclear transcription factor Y A-2	0.67 (0.141)	0.23 (0.000)
ASHH4_ARATH	Putative histone-lysine N-methyltransferase ASHH4	0.65 (0.206)	0.46 (0.029)
RH3_HELAN	DEAD-box ATP-dependent RNA helicase 3	0.70 (0.245)	0.32 (0.015)
JKD_ARATH	Zinc finger protein JACKDAW	0.51(0.106)	0.31 (0.018)
ATB14_ARATH	Homeobox-leucine zipper protein ATHB-14	0.87 (0.703)	0.09 (0.030)
	Proteins regulated at 16 hpi		
SMC3_ARATH	Structural maintenance of chromosomes protein 3	0.36(0.021)	0.19 (0.000)
RH40_ORYSJ	DEAD-box ATP-dependent RNA helicase 40	2.68 (0.019)	2.17 (0.059)
RH48_ORYSJ	DEAD-box ATP-dependent RNA helicase 48	1.49 (0.201)	2.47 (0.001)
KIN11_ARATH	SNF1-related protein kinase α	1.25 (0.671)	0 (0.000)

(Table 3.20 continued)

Accession	Description	*Xac*/Con	*Xoo*/Con
	Proteins regulated at 48 hpi		
RECA3_ARATH	DNA repair protein recA homolog 3	4.30 (0.002)	2.07 (0.022)
RH2_ARATH	DEAD-box ATP-dependent RNA helicase 2	6.97 (0.009)	3.59 (0.030)
RAD50_ARATH	DNA repair protein RAD50	5.20 (0.309)	4.23 (0.034)
SMC3_ARATH	Structural maintenance of chromosomes protein 3	9.45 (0.001)	2.85 (0.262)
DPOE2_ARATH	DNA polymerase epsilon catalytic subunit B	44.88 (0.04)	20.90 (0.241)
HPR1_ARATH	Glycerate dehydrogenase	0.39 (0.036)	0.48 (0.065)
MAD56_ORYSI	MADS-box transcription factor 56	0.28 (0.037)	0.83 (0.657)
NFYA2_ARATH	Nuclear transcription factor Y subunit A-2	0.30 (0.001)	0.88 (0.714)
RA51D_ARATH	DNA repair protein RAD51 homolog 4	0.44 (0.023)	1.04 (0.775)
CDC5L_ARATH	Cell division cycle 5-like protein	0.32 (0.044)	0.81 (0.685)
RH3_HELAN	DEAD-box ATP-dependent RNA helicase 3	0.18 (0.038)	3.42 (0.092)
ATB14_ARATH	Homeobox-leucine zipper protein ATHB-14	0.13 (0.016)	0.69 (0.480)
RPO3B_TOBAC	DNA-directed RNA polymerase 3B	0.96 (0.841)	0.41 (0.017)

Fold change values of *Xac* vs. Control and *Xoo* vs. Control were given with *P*- value in the paranthesis. hpi-hours post inoculation.

Table 3.21: Transport-related proteins regulated in citrus nuclear proteome during *Xanthomonas* interaction

Accession	Description	*Xac*/Con	*Xoo*/Con
	Proteins regulated at 2 hpi		
ERDL3_ARATH	Sugar transporter ERD6-like 3	0 (0.023)	0.28 (0.094)
NUA_ARATH	Nuclear-pore anchor	24.29 (0.344)	90.67 (7.76E-07)
HAK7_ORYSJ	Potassium transporter 7	4.24 (0.077)	10.90 (0.003)
	Proteins regulated at 8 hpi		
AB25B_ARATH	ABC transporter B family member 25	0.75 (0.000)	0.34 (0.002)
	Proteins regulated at 16 hpi		
NUA_ARATH	Nuclear-pore anchor	1083.01 (0.0372)	640.40 (0.068)
HAK7_ORYSJ	Potassium transporter 7	52.72 (0.048)	10.55 (0.128)
	Proteins regulated at 48 hpi		
VIPP1_ARATH	Membrane-associated protein VIPP1	0.17 (0.001)	0.18 (0.002)
PHO14_ARATH	Phosphate transporter PHO1 homolog 4	0.15 (0.001)	0.39 (0.025)
VHAA3_ARATH	Vacuolar proton ATPase a3	0.07 (0.006)	0.27 (0.046)
TC753_ARATH	Protein TOC75-3	3.08 (0.028)	1.42 (0.445)
VDAC1_SOLTU	Mitochondrial outer membrane protein porin of 34 kDa	73.77 (0.014)	26.91 (0.164)
VDAC2_SOLTU	Mitochondrial outer membrane protein porin of 36 kDa	19.78 (6.16E-05)	7.28 (0.109)

(Table 3.21 continued)

Accession	Description	*Xac*/Con	*Xoo*/Con
DRP1C_ARATH	Dynamin-related protein 1C	0.20 (4.97E-05)	0.66 (0.292)
PIP1_ATRCA	Aquaporin PIP-type	0.15 (0.060)	0.45 (0.13)
AVP_HORVU	Pyrophosphate-energized vacuolar membrane proton pump	0.08 (0.000)	0.49 (0.243)
NAT5_ARATH	Nucleobase-ascorbate transporter 5	0.15 (0.004)	0.99 (0.999)
XYLL3_ARATH	D-xylose-proton symporter-like	0.15(0.00)	1.18 (0.62)
COX2_ARATH	Cytochrome c oxidase subunit 2	5.58(0.09)	5.03 (0.00)
DIT1_ARATH	Dicarboxylate transporter 1	1.86(0.09)	3.44 (0.03)

Fold change values of *Xac* vs. Control and *Xoo* vs. Control were given with *P*- value in the paranthesis. hpi-hours post inoculation.

Table 3.22: Translation-related proteins regulated in citrus nuclear proteome during *Xanthomonas* interaction

Accession	Description	*Xac*/Con	*Xoo*/Con
	Proteins regulated at 2 hpi		
RL7A_ORYSJ	60S ribosomal protein L7a	3.32 (0.015)	3.25 (0.007)
PABP2_ARATH	Polyadenylate-binding protein 2	2.15 (0.047)	1.32 (0.490)
VBF_ARATH	F-box protein VBF	0.31 (0.001)	0.56 (0.009)
SYM_ORYSJ	Probable methionine--tRNA ligase	2.97 (0.215)	3.8 9 (0.003)
RL9_PEA	60S ribosomal protein L9	0.73 (0.186)	0.40 (0.015)
RK14_CITSI	50S ribosomal protein L14	1.12 (0.512)	0.43 (0.015)
RS142_MAIZE	40S ribosomal protein	1.71 (0.250)	0.48 (0.029)
RS4_GOSHI	40S ribosomal protein S4	0.94 (0.866)	0.2 8 (0.005)
	Proteins regulated at 8 hpi		
RR3_CITSI	30S ribosomal protein S3	0.43 (0.028)	1.1 9 (0.573)
RS4_GOSHI	40S ribosomal protein S4	0.45 (0.021)	1.48 (0.238)
RR7_CITSI	30S ribosomal protein S7	1.38 (0.481)	2.71 (0.022)
RK16_CARPA	50S ribosomal protein L16	1.61 (0.176)	2.44 (0.011)
RR4_ACOCL	30S ribosomal protein S4	0.88 (0.562)	2.22 (0.037)
RS142_MAIZE	40S ribosomal protein S14	0.52 (0.080)	0.33 (0.010)
RS25_SOLLC	40S ribosomal protein S25	0.54 (0.013)	0.4 3 (0.001)
	Proteins regulated at 16 hpi		
RR18_PSEMZ	30S ribosomal protein S18	2.01 (0.036)	1.01 (0.900)
RS14_CHLRE	40S ribosomal protein S14	0.49 (0.011)	0.55 (0.007)
EFTU1_SOYBN	Elongation factor Tu	0.14 (0.042)	0.58 (0.437)
RR1_SPIOL	30S ribosomal protein S1	0.43 (0.040)	1.56 (0.232)
RR8_CHLAT	30S ribosomal protein S8	4.32 (0.196)	3.37 (0.007)
RR3_STIHE	30S ribosomal protein S3	1.92 (0.016)	2.44 (0.018)
ARGJ_RICCO	Arginine biosynthesis bifunctional protein	1.19 (0.613)	2.31 (0.027)

(Table 3.22 continued)

Accession	Description	*Xac*/Con	*Xoo*/Con
	Proteins regulated at 48 hpi		
RS16_LUPPO	40S ribosomal protein S16	0.19 (0.0145)	0.39 (0.042)
RL4_PRUAR	60S ribosomal protein L4	0.25 (0.016)	0.36 (0.033)
RR12A_OLIPU	30S ribosomal protein S12-A	0.22 (0.002)	0.46 (0.036)
RS3A1_VITVI	40S ribosomal protein S3a-1	0.18 (0.001)	0.40 (0.033)
RS11_MAIZE	40S ribosomal protein S11	0.35 (0.002)	0.4 8 (0.020)
RR7_CITSI	30S ribosomal protein S7	0.33 (0.012)	0.40 (0.026)
PABP2_ARATH	Polyadenylate-binding protein 2	0.12 (0.008)	0.38 (0.038)
RL8_TOBAC	60S ribosomal protein L8	0.32 (0.004)	0.33 (0.014)
R13A1_ARATH	60S ribosomal protein L13a-1	0.13 (0.021)	0.10 (0.019)
RR18_PSEMZ	30S ribosomal protein S18	2.01 (0.036)	1.01 (0.900)
RK2_CITSI	50S ribosomal protein L2	0.35 (0.002)	0.52 (0.024)
EFTU1_SOYBN	Elongation factor Tu	0.14 (0.042)	0.58 (0.438)
RR1_SPIOL	30S ribosomal protein S1	0.43 (0.040)	1.56 (0.232)
RR3_CITSI	30S ribosomal protein S3	0.33 (0.000)	0.70 (0.119)
RS18_ARATH	40S ribosomal protein S18	0.18 (0.004)	0.47 (0.054)
RR5_SPIOL	30S ribosomal protein S5	0.29 (0.018)	0.62 (0.085)
RR8_CITSI	30S ribosomal protein S8	0.22 (0.046)	0.46 (0.132)
RR18_CITSI	30S ribosomal protein S18	0.29 (0.012)	0.45 (0.071)
RS31_ARATH	40S ribosomal protein S3-1	0.32 (0.008)	0.57 (0.081)
RL9_ORYSJ	60S ribosomal protein L9	0.32 (0.039)	0.53 (0.115)
RK14_CITSI	50S ribosomal protein L14	0.48 (0.004)	1.01 (0.922)
RR3_STIHE	30S ribosomal protein S3	0.28 (0.028)	0.47 (0.094)
RS27_CHLRE	40S ribosomal protein S27	0.33 (0.034)	0.65 (0.094)
RS17_SOLLC	40S ribosomal protein S17	0.28 (0.015)	0.57 (0.063)
RR2_ATRBE	30S ribosomal protein S2	0.27 (0.011)	0.82 (0.475)
RL10_EUPES	60S ribosomal protein L10	0.13 (0.004)	0.46 (0.057)
RLA3_MAIZE	60S acidic ribosomal protein P3	0.18 (0.033)	0.32 (0.054)
RK22_ACOAM	50S ribosomal protein L22	0.43 (0.040)	0.6 8 (0.178)
RL3_ORYSJ	60S ribosomal protein L3	0.33 (0.000)	0.59 (0.099)
RL11_MEDSA	60S ribosomal protein L11	0.16 (0.031)	0.74 (0.384)
RR4_ACOCL	30S ribosomal protein S4	0.23 (0.004)	0.42 (0.086)
RL5_SOLME	60S ribosomal protein L5	0.10 (0.007)	0.43 (0.081)
RR1_SPIOL	30S ribosomal protein S1	0.20 (0.000)	0.48 (0.107)

Fold change values of *Xac* vs. Control and *Xoo* vs. Control were given with *P*- value in the paranthesis. hpi-hours post inoculation.

important category of proteins identified was presumably involved in degradation mechanism. These include ATP-dependent zinc metalloprotease, F-box protein, U-box domain-containing protein, BTB/POZ domain-containing protein and NPL4-like protein. The expression of BTB/POZ domain-containing protein expression decreased during *Xoo* and *Xac* interactions at 8 hpi and 48 hpi, respectively (Table 3.23). Whereas, increased expression occurred during *Xac* interaction at 16 hpi. F-box proteins decreased during both the pathogen challenge.

3.4.2.5. Proteins related to ROS pathway and energy metabolism:

ROS generated during plant-pathogen interaction is involved in triggering defense responses and exert deleterious effect on the pathogens. ROS metabolising proteins like glutathione S-transferase, 2-Cys peroxiredoxin and thioredoxin H-type were down-regulated during *Xoo* challenge at 8 hpi. At 48 hpi, catalase and thioredoxin H-type decreased during *Xac* interaction (Table 3.24). Peroxisomal (S)-2-hydroxy-acid oxidase had increased expression at 16 hpi during *Xac* challenge. Energy-related proteins were significantly differentially regulated only at 48 hpi (Table 3.25). These include increased expression of ATP synthase δ chain, ATP synthase subunit α and OEE protein 1 during *Xac* interaction.

3.4.2.6. Molecular chaperones-related proteins:

Molecular chaperones interact with and stabilize proteins that are partially or totally unfolded, as is the case when proteins are in the process of being synthesized, translocated across a membrane, or damaged by conditions of cellular stress. DnaJ protein homolog ANJ1 and HSP 2 had decreased expression at 48 hpi during *Xac* challenge. Whereas, heat shock cognate 70 kDa protein 2 and chaperone protein ClpC3 decreased during both interactions. Chaperone protein ClpB1 increased during *Xac* challenge at 48 hpi and at both interactions at 16 hpi. HSP 70 kDa and HSP 2 decreased at 8 hpi during *Xoo* interaction (Table 3.26).

3.4.2.7. Metabolism-related proteins:

Several metabolism-related proteins like ribulose-phosphate 3-epimerase, MDH, kaempferol 3-O-beta-D-galactosyltransferase, arginine biosynthesis bifunctional protein

Table 3.23: Protein degradation-related proteins regulated in citrus nuclear proteome during *Xanthomonas* interaction

Accession	Description	*Xac*/Con	*Xoo*/Con
	Proteins regulated at 2 hpi		
VBF_ARATH	F-box protein VBF	0.31 (0.000)	0.55 (0.009)
	Proteins regulated at 8 hpi		
PUB25_ARATH	U-box domain- protein 25	0.85 (0.373)	0.29 (0.002)
Y2060_ARATH	BTB/POZ domain-containing protein At2g30600	0.84 (0.308)	0.32 (0.000)
	Proteins regulated at 16 hpi		
VBF_ARATH	F-box protein VBF	0.43 (0.09)	0.41 (0.000)
Y1439_ARATH	BTB/POZ domain-containing protein At1g04390	2.22 (0.006)	2.13 (0.056)
NPL4_ORYSJ	NPL4-like protein	7.35 (0.112)	14.50 (0.008)
AMPL_SOLTU	Leucine aminopeptidase	2.10 (0.127)	3.33 (0.045)
	Proteins regulated at 48 hpi		
NPL4_ORYSJ	NPL4-like protein	0.04 (0.012)	0.51 (0.230)
POB1_ARATH	BTB/POZ domain- protein POB1	10.99 (0.027)	8.90 (0.004)
FTSH2_ARATH	ATP-dependent zinc metalloprotease FTSH 2	5.89 (0.007)	4.17 (0.124)
Y1439_ARATH	BTB/POZ domain-containing protein At1g04390	0.37 (0.039)	0.57 (0.179)

Fold change values of *Xac* vs. Control and *Xoo* vs. Control were given with *P*- value in the paranthesis. hpi-hours post inoculation.

Table 3.24: ROS pathways-related proteins regulated in citrus nuclear proteome during *Xanthomonas* interaction

Accession	Description	*Xac*/Con	*Xoo*/Con
	Proteins regulated at 8 hpi		
BIP4_TOBAC	Luminal-binding protein 4	0.41 (0.036)	2.16 (0.017)
BIP5_TOBAC	Luminal-binding protein 5	0.56 (0.083)	2.25 (0.022)
GSTUM_ARATH	Glutathione S-transferase U22	0.65 (0.004)	0.25 (0.001)
BAS1A_ARATH	2-Cys peroxiredoxin BAS1	0.86 (0.19)	0.29 (0.002)
TRXH_POPJC	Thioredoxin H-type	0.83 (0.750)	0.06 (0.043)
PR2_PETCR	Pathogenesis-related protein 2	0.66 (0.078)	0.18 (0.001)
GSTL1_ARATH	Glutathione S-transferase L1	0.90 (0.633)	0.44 (0.020)
	Proteins regulated at 16 hpi		
GOX_SPIOL	Peroxisomal (S)-2-hydroxy-acid oxidase	2.13 (0.002)	2.42 (0.061)
C98A8_ARATH	Cytochrome P450 98A8	2.11 (0.002)	1.95 (0.002)
SODM_CAPAN	Superoxide dismutase [Mn]	1.29 (0.029)	2.10 (0.032)
	Proteins regulated at 48 hpi		
CATA1_SOYBN	Catalase-1/2	0.28 (0.006)	0.71 (0.126)
DEF68_ARATH	Defensin-like protein 68	0.12 (0.008)	0.94 (0.832)
GME_ARATH	GDP-mannose 3,5-epimerase	0.39 (0.006)	0.46 (0.007)
TRXH_POPJC	Thioredoxin H-type	0.04 (0.001)	0.53 (0.130)

Fold change values of *Xac* vs. Control and *Xoo* vs. Control were given with *P*- value in the paranthesis. hpi-hours post inoculation.

Table 3.25: Energy metabolism- related proteins regulated in citrus nuclear proteome during *Xanthomonas* interaction

Accession	Description	*Xac*/Con	*Xoo*/Con
	Proteins regulated at 16 hpi		
FENR_MESCR	Ferredoxin--NADP reductase	1.81 (0.142)	3.83 (0.000)
ATPF_CITSI	ATP synthase subunit β	1.51 (0.689)	0 (0.004)
	Proteins regulated at 48 hpi		
PSBO_SOLTU	OEE1	3.4 (0.035)	1.54 (0.278)
ATPAM_BETVU	ATP synthase subunit α	2.49 (0.003)	1.37 (0.469)
ATPD_SPIOL	ATP synthase delta chain	13.37 (0.018)	24.97 (0.292)

Fold change values of *Xac* vs. Control and *Xoo* vs. Control were given with *P*- value in the paranthesis. hpi-hours post inoculation.

Table 3.26: Molecular chaperone-related proteins regulated in citrus nuclear proteome during *Xanthomonas* interaction

Accession	Description	*Xac*/Con	*Xoo*/Con
	Proteins regulated at 8 hpi		
HSP7J_ARATH	HSP 70-10	0.69 (0.128)	0.33 (0.011)
HSP02_PSEMZ	HSP 2	0.59 (0.006)	0.23 (0.001)
	Proteins regulated at 16 hpi		
CLPB1_ARATH	Chaperone protein ClpB1	3.41(0.001)	2.33 (0.035)
CLPB2_ORYSJ	Chaperone protein ClpB2	2.41 (0.030)	1.58 (0.114)
HSP7S_SPIOL	Stromal 70 kDa heat shock-related protein	1.13 (0.700)	2.05 (0.001)
HSP7S_PEA	Stromal 70 kDa heat shock-related protein	0.76 (0.236)	2.43 (0.010)
	Proteins regulated at 48 hpi		
CLPB1_ARATH	Chaperone protein ClpB1	4.07 (0.047)	6.90 (0.076)
HSP72_SOLLC	Heat shock cognate 70 kDa protein 2	0.41 (0.002)	0.43 (0.017)
HSP02_PSEMZ	HSP 2	0.29 (0.021)	0.71 (0.390)
CLPC3_ORYSJ	Chaperone protein ClpC3	0.20 (0.000)	0.41 (0.002)
DNJH_ATRNU	DnaJ protein homolog ANJ1	0 (0.045)	0.24 (0.143)
HS26M_ARATH	26.5 kDa heat shock protein	#DIV/0!(0.119)	#DIV/0! (0.047)

Fold change values of *Xac* vs. Control and *Xoo* vs. Control were given with *P*- value in the paranthesis. hpi-hours post inoculation.

.

ArgJ, transketolase and peroxisomal acyl-coenzyme A oxidase 1 were repressed during *Xac* challenge at 48 hpi (Table 3.27). 4-coumarate--CoA ligase, transketolase and MDH increased during *Xoo* challenge at 16 hpi. Whereas, NADP-dependent malic enzyme and tocopherol cyclase increased during *Xac* challenge. ATP-citrate synthase α chain protein, sucrose synthase and isocitrate dehydrogenase [NAD] regulatory subunit 1 decreased at 8 hpi during *Xac* interaction.

3.4.2.8. Miscellaneous-related proteins:

The miscellaneous class of proteins including formin-like protein 2, V-type proton ATPase subunit B 1, coatomer subunit β, protein disulfide isomerase, (+)-bornyl diphosphate synthase, membrane-anchored ubiquitin-fold protein 2, mitochondrial outer membrane protein porin 4 and purple acid phosphatase 18 were differentially expressed at 48 hpi. Protein GAMETE EXPRESSED 3, formin-like protein 11, putative membrane protein ycf1 and cytochrome c1 were regulated at 8 hpi. Rhicadhesin receptor protein was differentially regulated at 16 and 2 hpi (Table 3.28).

3.5. Major observations:

Upon *Xoo* challenge callose deposition, ROS accumulation, increase in ROS producing enzyme activity and HR was observed in citrus leaves. Whereas, no microscopic changes were observed in *Xac* challenged leaves, while at 48 hpi water soaked lesions, typical symptoms of canker appeared at bacterial infiltrated regions. Moreover there was increase in bacterial count at 3 dai and increase in activity of ROS catabolising enzymes. In total leaf cellular and nuclear proteome analysis, carbon metabolism and protein turnover related proteins were repressed during both the interactions. Proteins related to CW remodelling were differentially regulated in total cellular and ECM proteome analysis.

Table 3.27: Metabolism-related proteins regulated in citrus nuclear proteome during *Xanthomonas* interaction

Accession	Description	*Xac*/Con	*Xoo*/Con
	Proteins regulated at 2 hpi		
RBL_DROPA	Rubisco large chain	3.32 (0.456)	3.79 (0.029)
ODO2A_ARATH	Dihydrolipoyllysine-residue succinyl transferase component of 2-oxoglutarate dehydrogenase complex	2.17 (0.019)	2.02 (0.041)
	Proteins regulated at 8 hpi		
S17P_WHEAT	Sedoheptulose-1,7-bisphosphatase	0.62 (0.047)	0.39 (0.027)
GGT1_ARATH	Glutamate--glyoxylate aminotransferase 1	0.67 (0.160)	0.47 (0.029)
ACLA1_ARATH	ATP-citrate synthase alpha chain protein 1	0.45 (0.031)	0.19 (0.009)
SUSY_MEDSA	Sucrose synthase	0.41 (0.044)	0.73 (0.682)
IDH1_ARATH	Isocitrate dehydrogenase [NAD] regulatory subunit 1	0.46 (0.032)	0.62 (0.290)
	Proteins regulated at 16 hpi		
RCA2_LARTR	RUBISCO activase 2	2.15 (0.163)	3.84 (0.002)
MAOX_VITVI	NADP-dependent malic enzyme	3.61 (0.204)	3.92 (0.048)
MAOC_FLAPR	NADP-dependent malic enzyme	3.62 (0.118)	4.16 (0.011)
4CLL1_ORYSJ	4-coumarate--CoA ligase-like 1	4.32 (0.071)	3.54 (0.041)
RBL_VITSX	Rubisco large chain	2.36 (0.125)	3.23 (0.001)
TKTC_MAIZE	Transketolase	2.73 (0.137)	3.18 (0.015)
MDHP_MEDSA	Malate dehydrogenase	3.96 (0.089)	6.63 (0.015)
TOCC_ARATH	Tocopherol cyclise	4.71 (0.049)	2.58 (0.314)
RLC1_CITLI	(R)-limonene synthase 1	0.74 (0.416)	0.17 (0.020)
CAHC_PEA	Carbonic anhydrase	1.89 (0.025)	3.14 (0.002)
CAHC_ARATH	Carbonic anhydrase	1.75 (0.023)	2.53 (0.011)
G3PB_TOBAC	Glyceraldehyde-3-phosphate dehydrogenase B	1.74 (0.116)	2.66 (0.003)
RUB1_BRANA	RuBisCO large subunit-binding protein subunit α	1.50 (0.035)	2.16 (0.019)
MDHG_CITLA	Malate dehydrogenase	1.67 (0.331)	4.29 (0.026)
KGLT_PETHY	Kaempferol 3-O-beta-D-galactosyltransferase	1.10 (0.874)	2.57 (0.015)
PHOT1_ARATH	Phototropin-1	0.67 (0.181)	2.46 (0.023)
	Proteins regulated at 48 hpi		
RBL_ERICA	Rubisco large chain	3.50 (0.017)	4.81 (0.244)
MAOX_VITVI	NADP-dependent malic enzyme	0.43 (0.013)	0.45 (0.040)
PSAB_ACOCL	Photosystem I P700 chlorophyll a apoprotein A2	0.16 (0.008)	1.10 (0.772)
RPE_SOLTU	Ribulose-phosphate 3-epimerase	0.33 (0.002)	0.64 (0.127)
MDHC_BETVU	Malate dehydrogenase	0.20 (0.003)	0.55 (0.066)
KGLT_PETHY	Kaempferol 3-O-beta-D-galactosyltransferase	0.21 (0.010)	0.6 1 (0.211)
MDHC_MESCR	Malate dehydrogenase	0.37 (0.022)	0.69 (0.117)
ARGJ_RICCO	Arginine biosynthesis bifunctional protein	0.15 (0.001)	0.56 (0.067)

Fold change values of *Xac* vs. Control and *Xoo* vs. Control were given with *P*- value in the paranthesis. hpi-hours post inoculation.

Table 3.28: Miscellaneous relatedproteins regulated in citrus nuclear proteome during *Xanthomonas* interaction

Accession	Description	*Xac*/Con	*Xoo*/Con
	Proteins regulated at 2 hpi		
RHRE_PEA	Rhicadhesin receptor	1.09 (0.803)	2.04 (0.038)
	Proteins regulated at 8 hpi		
CY11_SOLTU	Cytochrome c1-1, heme protein	2.52 (0.015)	9.82 (0.129)
GEX3_ARATH	Protein GAMETE EXPRESSED 3	0.67 (0.077)	0.27 (0.001)
FH11_ARATH	Formin-like protein 11	0.78 (0.240)	0.28 (0.002)
YCF1_ATRBE	Putative membrane protein ycf1	0.63 (0.126)	0.17 (0.003)
	Proteins regulated at 16 hpi		
MUB2_ARATH	Membrane-anchored ubiquitin-fold protein 2	4.52 (0.020)	3.57 (0.000)
EXPA4_ORYSI	Expansin-A4	0.24 (0.002)	0.47 (0.006)
RHRE_PEA	Rhicadhesin receptor	2.94 (0.040)	2.57 (0.097)
GGT1_ARATH	Glutamate--glyoxylate aminotransferase 1	2.55 (0.030)	2.59 (0.052)
ICDHC_ARATH	Cytosolic isocitrate dehydrogen	2.84 (0.000)	2.30 (0.099)
SAHH_CATRO	Adenosylhomocysteinase	2.70 (0.012)	1.08 (0.847)
GLYM_FLAPR	Serine hydroxymethyltransferase 1	1.78 (0.123)	2.59 (0.001)
GSA_HORVU	Glutamate-1-semialdehyde 2,1-aminomutase	1.24 (0.063)	2.82 (0.020)
AROF_ARATH	Phospho-2-dehydro-3-deoxyheptonate aldolase 1	0.47 (0.061)	0.24 (0.018)
OEP37_PEA	Outer envelope pore protein 37	0.96 (0.938)	0.38 (0.027)
PPA18_ARATH	Purple acid phosphatase 18	0.76 (0.569)	0.36 (0.024)
CEMA_PHYPA	Chloroplast envelope membrane protein	0.54 (0.40)	0.07 (0.008)
	Proteins regulated at 48 hpi		
CB21_CUCSA	Chlorophyll a-b binding protein of LHCII type I	6.79 (5.99E-05)	3.96 (0.003)
PSBH_CITSI	Photosystem II reaction center protein H	14.97 (0.013)	8.92 (0.049)
BPPS_SALOF	(+)-bornyl diphosphate synthase	0.20 (0.001)	0.41 (0.009)
PPA18_ARATH	Purple acid phosphatase 18	6.33 (0.005)	3.77 (0.014)
CB23_SOLLC	Chlorophyll a-b binding protein 13	10.90 (0.049)	5.48 (0.068)
OEP37_PEA	Outer envelope pore protein 37	3.06 (0.031)	1.16 (0.584)
FH12_ORYSJ	Formin-like protein 12	21.06 (0.008)	22.69 (0.093)
NDUS7_ARATH	NADH dehydrogenase [ubiquinone] iron-sulfur protein 7	114.72 (0.000)	47.98 (0.151)
PSAA_CITSI	Photosystem I P700 chlorophyll a apoprotein A1	0.16 (0.002)	0.93 (0.879)
PSBC_AETCO	Photosystem II CP43 chlorophyll apoprotein	0.42 (0.038)	2.04 (0.330)
GAE6_ARATH	UDP-glucuronate 4-epimerase 6	0.25 (0.002)	0.75 (0.457)
PSAF_ARATH	Photosystem I reaction center subunit III	0.28 (0.025)	0.54 (0.141)
PDI14_ORYSJ	Protein disulfide isomerase-like 1-4	0.39 (0.009)	0.81 (0.267)
FH11_ARATH	Formin-like protein 11	0.42 (0.032)	1.14 (0.627)
MUB2_ARATH	Membrane-anchored ubiquitin-fold protein	0.25 (0.023)	0.55 (0.100)

(Table 3.28 continued)

Accession	Description	*Xac*/Con	*Xoo*/Con
4CLL1_ORYSJ	4-coumarate--CoA ligase	0.21 (0.049)	0.50 (0.247)
BXL7_ARATH	Probable β-D-xylosidase 7	0.17 (0.011)	0.47 (0.083)
PDI11_ARATH	Protein disulfide isomerase-like 1-1	0.23 (0.016)	0.87 (0.694)
COB21_ORYSJ	Coatomer subunit β'-1	0 (0.009)	0.38 (0.104)
PSBB_ACOAM	Photosystem II CP47 chlorophyll apoprotein	2.14 (0.241)	5.11 (0.032)
CB21_TOBAC	Chlorophyll a-b binding protein 16	10.08 (0.063)	7.46 (0.026)
CB23_ORYSI	Chlorophyll a-b binding protein	4.37 (0.078)	3.64 (8.03E-05)
CB21_SILPR	Chlorophyll a-b binding protein	7.43 (0.068)	11.95 (0.032)
CY11_SOLTU	Cytochrome c1-1, heme protein	5.81(0.083)	4.86 (0.021)

Fold change values of *Xac* vs. Control and *Xoo* vs. Control were given with *P*- value in the paranthesis. hpi-hours post inoculation.

Discussion

Plants interact with the environment in various ways and routinely face challenges from potential pathogens, but disease occurs only in limited cases as survival is a rule rather than an exception. Non-host resistance (NHR) is the most common, durable and non-specific type of resistance observed in plant-pathogen interactions. Understanding this type of resistance of great interest for agriculture. The discovery of plant molecular mechanisms responsible for pathogen defense may provide valuable information in the search for disease control alternatives. To understand the complex phenomenon of NHR, we have selected citrus-*Xanthomonas* as a model system. The compatible and non-host interactions of citrus were compared with the bacteria belonging to same genus *Xanthomonas*. Wherein, the differential response of citrus towards host pathogen *Xac* and non-host pathogen *Xoo* were characterized by performing anatomical and biochemical changes, and total cellular and sub organelle proteome analysis.

4.1. Type-II NHR in citrus-*Xoo* non-host pathosystem:

When a non-host pathogen manages to overcome constitutive defensive layers, it is subjected to the recognition at the plasma membrane that eventually activates basal resistance (Asai et al. 2002, Gomez-Gomez and Boller, 2002). Inducible defense responses, during NHR, include synthesis and accumulation of ROS, papillary callose, and phytoalexins, with or without formation of the HR (Nurnberger and Lipka, 2005). Infiltration of *Xoo* into citrus leaves lead to microscopically visible HR, within 24 hpi (Figure 3.2B), a hallmark of NHR. HR generates a physical barrier composed of dead plant cells that limit the availability of nutrients to the pathogen, thus resistricting its spread. It may also be accompanied by an oxidative burst as another defense response (Thordal-Christensen et al. 1997). Citrus leaves infiltrated with *Xoo,* accumulated H_2O_2 throughout the inoculation site. Callose deposition occurred only in *Xoo* challenged leaves. The deposition of a linear β-1,3-glucan polymer, callose, in response to pathogen attacking/wounding stresses is a basic defense mechanism that enables the plant to arrest pathogen proliferation by reinforcing the cell wall (Hardham et al. 2007; Glazebrook, 2005; Jacobs et al. 2003;). Moreover, the bacterial count of *Xoo* declined at 72 hpi in citrus leaves, indicating that the *Xoo* was unable to survive in citrus leaves and a type-II NHR occurred during citrus-*Xoo* interaction. During *Xac* challenge, the bacterial count increased by 3 log units by 72 hpi, and first visual symptoms of canker *i.e.,* water-soaking lesions appeared at 48 hpi. *Nicotiana benthamiana* plants inoculated with *Xoo*

also responded rapidly by eliciting an HR and type-II NHR (Li et al. 2012).

4.1.1. Antioxidant status of citrus during host and non-host interactions:

One of the earliest events in the plant defense response against both non-host- and host-specific pathogens is rapid and transient production of ROS (Lamb and Dixon, 1997). H_2O_2 evolution is an essential and integral part of pathogen induced programmed cell death (PCD), which occurs very rapidly in plant–bacterial interactions (Wojtaszek, 1997). Accumulation of ROS, increase in the activity of ROS producing enzymes and decrease in activity of antioxidant enzymes during citrus-*Xoo* interaction were notable changes. In lettuce-*Pseudomonas syringae* pv. *phaseolicola* non-host pathosystem, NHR was associated with increased peroxidase activity, H_2O_2 accumulation and cell death (Bestwick et al. 1998). Antioxidant enzymes like SOD, POD and APX are involved in regulation of ROS levels in plants. In pathogen inoculated barley leaves increased SOD contributed to the synthesis of H_2O_2 during the oxidative burst to prevent accumulation of O_2^- (Vanacker et al. 1998).

Oxidative stress caused by high accumulation of ROS during plant-pathogen interactions results in oxidative degradation of membrane lipids which finally leads to cell death. The effect of oxidative stress on plant-pathogen interactions was studied (Hakmaoui et al. 2012; Mittler et al. 1999). Increased ROS accumulation during non-host (*Xoo*) interaction resulted in high lipid peroxidation and cell death. Apparently, the increase in antioxidant enzymes activity has quenched the ROS levels during host pathogen interaction in citrus. Increased levels of ROS restricted the growth of non-host bacteria whereas, increase of antioxidant enzymes favoured survival of host bacteria and establishment of disease symptoms.

APX and POD together utilize H_2O_2 as electron acceptor, and therefore, compete for the same substrate. APX scavenges H_2O_2 using ascorbate as reductant and has high affinity to H_2O_2 than POD. APX could be responsible for H_2O_2 detoxification, preventing accumulation in the cell when produced in excess (De Pinto and de Gara, 2004). POD is involved in plant defense responses like lignifications, stiffening of the cell wall, detoxification of ROS and defense against pathogen penetration. In the present study, POD activity increased in non-host interaction, whereas APX activity increased during compatible interaction.

Thus, changes in oxidative metabolism constitute a general defense response of plants to pathogen attack rather than a specific response operating only against pathogens, causing a resistance reaction through HR. Our results indicate that increased ROS production, attained by either activation of ROS-generating mechanisms and/or inhibition of ROS-scavenging mechanisms, as well as up-regulation of lipid peroxidation, are the early responses of citrus leaves during interaction with non-host bacteria. The expression of such defense systems might contribute to resistance to *Xoo*.

4.2. Proteome changes in citrus leaves in response to *Xanthomonas* challenge:

One aim of this study was to focus on the early and late defense response of citrus towards *Xanthomonas*. Therefore, total citrus leaf proteome of early and late interaction (*i.e.,* 8 and 48 hpi) with *Xanthomonas* was profiled by performing gel-based and non-gel based proteomic approaches.

4.2.1. Repression of photosynthesis and carbon metabolism during citrus-*Xanthomonas* interaction:

A series of proteins related to photosynthesis were altered, suggesting dynamic influence of pathogen challenge on photosynthesis. Among the energy related proteins, more number of rubisco isoforms were regulated. Rubisco is the key enzyme in the Calvin cycle and catalyzes carbon dioxide fixation, while rubisco activase regulates rubisco activity by hydrolysing ATP to promote the dissociation of inhibitory sugar phosphates (Portis et al. 2008). Proteins related to photosynthesis, Calvin cycle, glycolysis and Krebs cycle were up-regulated at early hours of interaction whereas, down-regulated at 48 hpi in both host and non-host interactions. Down-regulation of photosynthesis-related proteins showed good agreement with the findings from previous studies (Garavaglia et al. 2010), indicating that the expression of many photosynthetic genes was repressed on encountering a biotic attack. The repression of photosynthesis-related proteins was known in incompable host-pathogen interactions (Matsumura et al. 2003). These results suggest that photosynthetic function in the host plant was compromised under biotic stress and resulted in establishment of canker in the leaves. Plants may activate an array of defense mechanisms that, although not always successful, demand a substantial reallocation of energy towards the defense response, which necessitates the modification of primary metabolism (Bolton, 2009). The light-dependent portion of photosynthesis is

carried out by two consecutive photosystems (photosystem I and photosystem II) in the thylakoid membrane of the chloroplasts. The chlorophyll a/b-binding proteins provide a system to balance excitation energy between photosystems I and II (Kundu et al. 2011). Two chlorophyll a/b-binding proteins accumulated in both compatible and non-host citrus-*Xanthomonas* interactions.

4.2.2. Redox status of citrus during *Xanthomonas* interaction:

An early event associated with the defense response is the oxidative burst, leading to generation of ROS (Dangl et al. 1996). The overproduction of ROS in plant cells under stress has deleterious effects on plant cell (Overmyer et al. 2003). To maintain homeostasis under stress, plants need to fortify the resistance mechanisms, such as ROS scavenging and cell defense. Regulation of ROS scavenging proteins like glutathione S transferase (GST), APX, catalase, SOD and peroxiredoxin in the host and non-host interactions, supports the hypothesis that oxidative stress is induced following pathogen challenge.

One of the major antioxidants and free radical scavengers like APX and other antioxidant proteins like GST and peroxiredoxin were induced at the early hours during both interactions. On the other hand, at late hours of *Xoo* interaction, catalase and GST were repressed and Cu/Zn SOD was strongly induced, and not induced by *Xac* challenge, indicating increase in H_2O_2 levels during non-host interaction. In gel-based proteomics ascorbic acid, metabolism-related proteins like GDP-mannose 3', 5'-epimerase and NAD-dependent epimerase increased only during *Xac* interaction. Thus an increase in antioxidant status during compatible interaction, favours survival of host pathogen. ROS production is also required for the HR, a type of PCD thought to limit the access of the pathogen to water and nutrients (Glazebrook, 2005).The response of citrus during non-host interaction is more complex than a simple down-regulation of all potential antioxidant proteins, especially in view of the up-regulation of monodehydroascorbate reductase and phospholipid hydroperoxide glutathione peroxidase.

4.2.3. Induction of defense responses during non-host interaction:

The synthesis and accumulation of PR proteins and resistance proteins is an ubiquitous plant response to pathogen infection (van Loon and van Strien, 1999). In the present

study quantitative change in the expression of defense-related proteins occurred at 8 and 48 hpi of citrus-*Xanthomonas* interaction. Increase of stress-inducible protein, class I extracellular chitinase, acidic class II chitinase, peroxidase and HSP (70 and 17.9kDa) occurred during late stages of interaction with non-host pathogen indicates establishment of defense response at the pathogen interaction site. Miraculin-like protein isoforms 1 and 2 were repressed during both the interactions. Peroxidases catalyse the reduction of H_2O_2 by using various molecules at the CW as a substrate, such as phenolic compounds, lignin precursors, auxin, or others, leading to polymerization reactions such as lignification, suberization, and cross-linking of CW proteins (Kristensen et al. 1999; Passardi et al. 2004).

4.2.4. Modulation of protein synthesis, folding and degradation:

Defense involves induction as well as repression of several proteins. To meet the demand, the cell modulates several components of transcriptional and translational proteins. In the present study proteins related to translation, like isoforms of 40S and 60S ribosomal proteins and elongation factor Tu, (Table 3.5) were down-regulated upon pathogen challenge at 48 hpi. The 40S ribosomal protein S3a is a structural subunit of the ribosome involved in protein translation in the cytoplasm (Carroll et al. 2008). The 60S ribosomal protein L3 is a subunit of the ribosome involved in translation. Few of these ribosomal proteins were homologues of chloroplast ribosomal proteins, suggesting that the plant is turning off energy spent on protein synthesis and redirecting energy to induce defense response to stop pathogen invasion.

Protein folding and degradation play a vital role in the regulation of metabolic processes and stress responses. The key rate-limiting enzymes and misfolded/damaged proteins are regulated by different strategies in plants. In the present study, ATP-dependent Clp protease, TCP-1/cpn60 chaperonin, peptidyl-prolyl cis-trans isomerase, ubiquitin conjugation enzymes and 20S proteasome were regulated during pathogen challenge. Correct folding and subsequent assembly into oligomers is required for functional enzymes. Plants can refold the misfolded proteins by chaperonins, which includes the TCP-1/cpn60 chaperonin protein family (Prasad and Stewart, 1992; Gatenby, 1992; Fink, 1999). It was reported that the TCP-1/cpn60 chaperonin proteins increased in response to oxygen radicals and bacterial infection and are essential for the correct folding and

assembly of polypeptides into oligomeric structures (Prasad and Stewart, 1992; Gor and Mayfield, 1992). Further, plants can remove the excess or the misfolded/damaged proteins by proteolysis, and most of the targeted intracellular proteolysis is performed by the energy-dependent Clp protease (Porankiewicz et al. 1999). Proteolysis of important regulatory proteins is a key aspect of cellular regulation in eukaryotes. There is evidence that the ubiquitin-proteasome pathway is important in implementation of the plant defense response (Austin et al. 2002; Liu et al. 2002).

4.2.5. Fortification of citrus CW during *Xoo* interaction:

A consequence of plant defense against pathogens is the modification of plant CW, which provides an important barrier against pathogen penetration (Huckelhoven, 2007). CW strengthening proteins like XTH, endo-xyloglucan transferase, ADP-glucose pyrophosphorylase and β-galactosidase were induced during non-host interaction. Xyloglucan is a structural polysaccharide cross-linked to cellulose microfibers of plant CW and act as load-bearing component (Cosgrove, 2001; Fry, 1989). Xyloglucan metabolizing enzymes, therefore, represent potentially important agents for controlling wall strength and extensibility by modifying the load-bearing xyloglucan tethers (Fry, 1989). XTH is a CW remodelling enzyme, that possesses both hydrolase and transglycosylase activity, involved in cutting and grafting of the newly synthesized xyloglucan chain to the cellulose microfibrils, increasing CW cross linking. XTH increase in incompatible tomato-*Cuscuta* and pepper-*Ralstonia solanacearum* interactions (Albert et al. 2004; Hwang et al. 2011). β-D-xylosidase participates in xylan or arabinoxylan breakdown to modify the cell wall (Itai et al. 2003).

Enzymes involved in the biosynthesis and recycling of methionine and S-adenosyl methionine (SAM) and lignin biosynthesis-related NADP-malic enzyme increased during *Xoo* interaction. SAM and NADP-malic enzyme are important methyl donors for numerous bioactive compounds including the hormone ethylene, DNA, lignin, and flavonoids (Roje, 2006). Upregulation of methionine/SAM enzymes was known during the HR and required for the acceleration of cell death (Liu et al. 2008). O-acetyl serine lyase, involved in synthesis of cysteine, was induced during *Xoo* challenge. Cysteine serves as a precursor for methionine biosynthesis. S-adenosyl-L-homocysteinase catalyses the conversion of S-adenosyl-L-homocysteine into adenosine and L-

homocysteine. S-adenosyl-L-homocysteinase and ACC oxidase were found to be upregulated during *Xac* interaction. ACC oxidase catalyzes the final step of ethylene biosynthesis. Ethylene regulates a variety of developmental processes and stress responses in plants, including cell elongation, senescence, fruit ripening and defense. The increased levels of ACC oxidase may increase ethylene promoting CW loosening and elongation during *Xac* interaction. Whereas, increase in methionine/SAM enzymes during *Xoo* interaction may associate with lignin deposition. This was further confirmed by phloroglucinol staining for lignin deposition that occurred in *Xoo*-challenged leaves.

Isoflavone reductase-like protein (one of the key enzymes of isoflavonoid biosynthesis), resveratrol synthase and cinnamyl alcohol dehydrogenase were up-regulated only during non-host interaction. Cinnamyl alcohol dehydrogenase is an enzyme which catalyses the final step in the biosynthesis of monolignols. It plays important role in lignin synthesis (Morreel et al. 2004). Thymine diphospho (dTDP)-glucose 4-6-dehydratase catalyses synthesis of dTDP-D-glucose, which is a precursor in the *de novo* synthesis of nucleotide-L-rhamnose (NDP-L-rhamnose). L-rhamnose is a component of the plant CW pectic polysaccharides rhamnogalacturonan I & II and is also present in diverse secondary metabolites including anthocyanins, flavonoids and triterpenoids. dTDP-β-L-Rhamnose and UDP-β-L-rhamnose were reported to act as sugar donors for the rhamnosylation of flavonoids (Barber and Neufeld, 1961). The accumulation of proteins involved in CW remodelling and secondary metabolism during *Xoo* challenge suggested that citrus is likely to change the composition and secretion of CW complex to make it more resistant to non-host pathogen entry. Whereas, increase in the isoforms of pectin esterase during *Xac* interaction may be involved in CW loosing and cell expansion during canker formation.

4.3. ECM-associated proteome changes in citrus leaves in response to *Xanthomonas* challenge :

NHR is a potential tool box for the development of alternative approaches for plant disease control. To elucidate the mechanism of NHR, whole cell transcriptome, total leaf proteome and comparative transcriptome between wild-type and signalling pathway mutants were analysed (Li et al. 2012; Daurelio et al. 2011; Zimmerli et al. 2004). We adopted a different, more focused approach, to identify the set of ECM-associated

proteins linked to NHR compatible (*Xac*) and non-host (*Xoo*) interaction with citrus at 8, 16, 24 and 48 hpi.

4.3.1. Induction of signalling response during NHR:

Plant defense responses, including NHR, begin with the recognization of pathogen and rapid activation of defense responses accompanied by production of ROS leading to HR (Glazebrook, 2005). In the present study, lectin-like protein, curculin-like lectin and concanavalin A-like lectin kinase proteins increased at early stages (*i.e.*, 8 and 16 hpi) of interaction during *Xoo* challenge, and decreased in *Xac*-challenged citrus leaves (Table 3.15). Accumulated evidences support the involvement of lectin and lectin-like receptor-like kinases (LecRLKs) in plant defense (Riou et al. 2002; Peumans and Damme 1995). LecRLK79 expression was induced upon inoculation with several non-host and avirulent pathogens suggesting their involvement in defense responses by recognizing PAMPs or monitoring CW integrity (Bouwmeester et al. 2008; Gouget et al. 2006). The increased levels of lectin and lectin-like kinases at the early hours of *Xoo* interaction may be involved in recognition and also in induction of downstream defense responses as part of NHR.

4.3.2. Redox status and CW remodelling of citrus during *Xanthomonas* interaction:

The redox balance in a plant cell is maintained by a tight regulation of ROS production and detoxification that involves several proteins/enzymes. APX and 2-cys-peroxiredoxin decreased at 16 and 24 hpi. Two isoforms of wall-bound SOD (Cu/Zn and Fe) increased at 8, 16 and 24 hpi in the ECM of citrus-*Xoo* interaction, and decreased in citrus-*Xac* interaction (except for Cu/Zn SOD) suggesting the importance of ECM redox status during host and non-host bacterial interactions. Silencing of glycolate oxidase in the peroxisomes delayed the onset of the HR against non-host pathogens *P. syringae* pv. *tomato* in *Nicotiana benthamiana* (Rojas et al. 2012) strongly support the role of ROS in defense. Suppression of H_2O_2 scavenging systems in plants, upon pathogen attack, may sustain H_2O_2 levels and lead to oxidative burst further suppressing the pathogen (Mittler et al. 1998). Therefore, the increase in SOD and decrease in APX, 2-cys peroxiredoxin possibly contribute to elevated H_2O_2 culminating in cell death in citrus-*Xoo* interaction.

Extracellular Cu/Zn-SOD was implicated in perceiving exogenous signals, in enhancing

CW-based defenses like H_2O_2-dependant cross-linking of CW glycoproteins, and establishment of physical barriers at the pathogen ingression site (Huckelhoven 2007; Kasai et al. 2006; Lamb and Dixon 1997). Similarly, the induced level of SOD in the WE fraction of citrus during non-host interaction may be involved in downstream signalling and CW strengthening. Proteins like glucan 1,3- β -glucosidase, α-xyloglucosidase and XTH associated with CW metabolism were differentially expressed in citrus-*Xac* and -*Xoo* interactions. Cleavage of load-bearing xyloglucan chains by hydrolytic enzymes might be a means of achieving rapid wall loosening. An endo-type of glucanase increased during fruit softening and in cells undergoing rapid expansion during *Xac* infection in citrus (Cernadas et al. 2008; Real et al. 2004). Increase of XTH in incompatible tomato-*Cuscuta* and pepper-*Ralstonia solanacearum* interactions were known (Hwang et al. 2011; Albert et al. 2004). The increase in wall loosening/elongation proteins like α-xyloglucosidase and glucan 1,3- β-glucosidase, during *Xac* interaction at late hours of interaction (24 and 48 hpi) in citrus may contribute to hypertrophy and hyperplasia. The increase in wall remodelling XTH protein during interaction with *Xoo* may be involved in formation of crosslinks between cellulose microfibrils and further strengthen the wall as a barrier to pathogen invasion.

4.3.3. Induction of defense-related proteins during NHR:

In NHR, an increased resistance was evident from up-regulation of chitinase and other PR-proteins at 8, 16 and 24 hpi. The decreased expression of chitinase during *Xac* interaction suggested the suppression of basal resistance of citrus in response to host pathogen. Similar repression of chitinase was reported in a compatible interaction of tobacco with *Pseudomonas syringae* pv. *tabaci* (Ott et al. 2006). RNase activity of PR10 was induced in pepper during incompatible interaction with *Xanthomonas campestris* pv. *vesicatoria* and resulted in induction of defense responses and cell death (Choi et al. 2012). The increase of RNase protein at 8 hpi during *Xoo* interaction in citrus may also be involved in inducing HR and defense responses.

Cysteine and aspartyl proteases were induced at two different time points in citrus-*Xoo* interaction whereas, down regulation of aspartyl protease occurred in *Xac* interaction. In tomato *Rcr3,* a secreted cysteine protease was required for *Cf-2* receptor-like protein-mediated resistance against *Avr2* carrying *Cladosporium fulvum* strains (Kruger et al.

2002). An apoplastic aspartic protease *CDR1* (constitutive disease resistance 1) activates defense signalling in *Arabidopsis thaliana* probably by generating an unknown mobile endogenous peptide elicitor (Xia et al. 2004). These two proteases are also involved in cell death as they are activated by cytochrome-c released during programmed cell death (Martinou et al. 2000). The proteases up-regulated during *Xoo* interaction may be involved in defense signalling and execution of HR, resulting in restriction of the pathogen in citrus. In contrast, the pathogen might suppress defense responses by regulating the expression of such proteases during *Xac* interaction.

Miraculin is a taste modifying protein belonging to Kunitz serine trypsin inhibitor family of proteinase inhibitors. Miraculin-like proteins contain N-terminus signal peptide for secretion to the apoplast (Tsukuda et al. 2006). In the present study, three isoforms of miraculin (MIR, MIR1 and MIR2), represented as 10 spots in the ECM proteome, were differentially regulated. The differential expression pattern of the miraculin may be due to post-translational modifications. Although a link is suggested between miraculin induction and methyl jasmonate (MeJA) (Maserti et al. 2011; Cantu et al. 2008), a more detailed investigation is required to suggest the involvement of MeJA pathway and the role of differentially expressed miraculin in execution of NHR in citrus-*Xoo* interaction.

4.3.4. Role of non-classical secretory proteins during NHR:

Proteins with signal peptide at their N-terminus are secreted in to the ECM through classical secretory pathway. In the present study, 5 non-classical secretory pathway proteins were up-regulated during citrus-*Xoo* interaction. Among these, triose phophate isomerase, glutathione lyase and peptidyl prolyl isomerase were differentially regulated during both *Xac* and *Xoo* interactions. Whereas, two proteins each of OEE2 and HSPs in the WE and SE fractions, respectively, were up-regulated only during *Xoo* interaction (Table 3.15 and 3.16), suggesting their possible role in NHR. It was proposed that phosphorylation of OEE2 by the wall-associated kinase 1, regulated by a glycine-rich protein, may lead to induction of defense genes in *Arabidopsis* (Yang et al. 2003). Kaffarnik et al. (2009) reported extracellular accumulation of a specific subset of non-classical secretory proteins in *Arabidopsis* suspension cultures during virulent bacterial interaction and other set of proteins during avirulent bacterial interaction. In the present study, the kinetics and level of up-regulation of non-classical proteins were different

during *Xac* and *Xoo* interactions.

Most of the proteins secreted through classical secretory pathway are involved in defense. Inhibition of protein secretion may compromise ECM-associated defense response in plants and may lead to the survival of non-adopted pathogens. Upon brefeldin A pretreamnet, the non-host (*Xoo*) bacterial count has not increased untill 2 dai. But, by 3 dai there was a marginal increase in bacterial cell count. However, there was no cell death (data not shown). On the other hand, multiplication of *Xac* in brefeldin A pretreated citrus leaves was rapid, compared to DMSO pretreated leaves. Upon brefeldin A treatment there was a partial compromise in the NHR of citrus against *Xoo* and increase in susceptibility to *Xac*. Therefore, the non-classical secretory proteins of ECM appear to play a role in defense against non-adopted pathogens.

4.4. Citrus nuclear proteome during Xanthomonas interaction:

The nucleus is the regulatory hub of the eukaryotic cell. It is a dynamic system and a repository of various macromolecules that serve as modulators of cell signalling dictating the cell fate. To better understand the molecular mechanisms of NHR, we developed a comprehensive nuclear proteome of citrus during interaction with *Xanthomonas*. The proteome was determined using a sequential method of organellar enrichment followed by 2DE and nano- LC -MS/MS. Nuclear proteome of plants was less explored. Therefore, information was not available about the function of the nuclear proteins during biotic stress. We have focused over discussion on general role of the identified nuclear proteins during *Xanthomonas* interaction.

4.4.1. Cell defense and rescue:

ROS generated during pathogen attack are recognized by plants as a signal for triggering defense responses. The nucleus is the reservoir of ROS accumulation, but recent reports suggested that it may also be an active source of ROS production (Pandey et al. 2008; Ashtamker et al. 2007). A significant proportion of the identified proteins were found to be linked to antioxidative/detoxifying reactions. Antioxidant proteins involved in scavenging of ROS like catalase, GDP-mannose 3,5-epimerase, thioredoxin H-type, GST and 2-Cys peroxiredoxin were repressed during *Xoo* interaction. SOD (Mn) showed an induced expression at 16 hpi of non-host interaction, indicating its role in stress-induced generation of ROS. 2-Cys peroxiredoxin is an important protein for detoxification of

H_2O_2 under normal conditions as well a under oxidative stress. Glutathione S-transferases with enzymatic glutathione peroxidase activity catalyze the conjugation of glutathione to a variety of toxic substrates arising from oxidative stress (Edwards et al. 2000). Repression of ROS-metabolizing proteins indicates occurrence of oxidative burst during non-host interaction.

4.4.2. Modulation of transcription regulators during NHR:

Transcription factors (TF) are important in regulating plant responses to environmental stress. Different members of TFs regulate the gene expression in response to biotic stress. However, many of these would have escaped detection as the expression level for TFs is generally not very high. TFs identified in this study are homeobox-leucine zipper protein, zinc finger protein, MADS-box TF, SNF1-related protein kinase, patatin-like phospholipase 2, PHD-finger family protein, WRKY-22, TF bHLH62, DEAD-box RNA helicase, pre-mRNA splicing machinery, heat shock factor-like protein, DNA-directed RNA polymerase and DNA topoisomerase. MADS-box protein was repressed at 16 hpi, during *Xoo* challenge and at 48 hpi, during *Xac* interaction. The MADS-box gene family encodes TF with a conserved DNA-binding domain, called the MADS-box. Over expression of MADS-box TF has induced biosynthesis genes for JA, ethylene, and ROS, suggesting involvement during various stresses (Lee et al. 2008). Kruppel-type zinc finger domains containing zinc finger TF is involved in cell cycle progression. The exact function of these proteins can only be predicted after extensive studies, and might be interesting for future investigations.

A DEAD-box RNA helicase with functions in modulating defense responses against pathogen infection and oxidative stress (Li et al. 2008) increased during non-host interaction, while it was repressed during host pathogen interaction. An induced expression of DEAD-box RNA helicase occurred upon JA, ACC, SA and incompatible interaction between a resistant rice genotype and the blast fungus, *Magnaporthe grisea*. Transgenic *Arabidopsis* plants overexpressing DEAD-box RNA helicase showed an enhanced disease resistance against *Alternaria brassicicola* and *Pseudomonas syringae* pv. *tomato DC3000* (Li et al. 2008). Most RNA helicases belong to helicase superfamily 2 (SF2) and are grouped into the DEAD-box subfamilies. RNA helicases perform their function mostly as parts of large macromolecular assemblies such as the pre-mRNA

splicing machinery (Jankowsky and Fairman, 2007). Several DEAD-box proteins have been shown to catalyze strand annealing, in addition to their duplex unwinding activity (Jankowsky and Fairman, 2007). RNA helicase was also reported in the nuclear proteomes of *Arabidopsis* and *Medicago truncatula* (Repetto et al. 2008; Bae et al. 2003)

Induction of plant immune responses involves significant transcription reprogramming that prioritizes defense over growth-related cellular functions. Heat-shock factor-like protein binds to the TL1 *cis* element and regulates the expression of genes containing this element in their promoters. Mutants of this TF have normal heat-shock responses but are compromised in the growth-to-defense transition upon pathogen challenge (Pajerowska-Mukhtar et al. 2012). The repression of this TF during *Xac* interaction may be the pathogen's strategy to avoid induction of defense responses.

4.4.3. Signalling-related proteins:

Signalling and nucleocytoplasmic transport are also closely linked as plants have multiple stress perception and signal transduction pathways, which cross-talk at various steps in response to adverse conditions (Knight and Knight, 2001). Many molecules have to move in and out of the nucleus at any given time. Proteins involved in signal transduction play a crucial role in nucleocytoplasmic transport as they provide the identity of these two compartments and ensure the directionality of transport (Pandey et al. 2008). Calcium ion is the most important signal entity in cell. In the present work calcium binding protein, calcium protein kinase and calmodulin were differentially regulated. Ca^{2+} binding proteins and calmodulin were down-regulated during both interactions indicating tight regulation of signalling pathways.

Serine/threonine kinase (STK) is a signal-related protein, regulates a variety of cellular processes (Canova et al. 2008). STK was involved in soybean defense responses induced by cotton worm feeding and induced by low temperature, Soybean mosaic virus, and SA (Chen et al. 2008; Jeong et al. 2005). STKs have long been implicated to play a role in signalling processes concerned with self verses non-self recognition and disease resistance (Ulker and Somssich, 2004). Down-regulation of STK during *Xac* interaction indicates repression of defense responses during compatible interaction.

In the present study, signalling-related proteins like histone (H3.2, H2A), phosphor-

glycerate kinase (PGK), dynamin, actin and aldolase were induced during *Xoo* interaction. Histones are highly conserved components of eukaryotic chromatin. Numerous studies have revealed that dynamin and dynamin-related proteins are involved in not only endocytosis but also diverse cellular membrane-remodelling events including vesicular transport, division of organelles and cytokinesis (Praefcke and McMahon, 2004).

PGK is known to function as a primer recognition protein involved in DNA synthesis and is known to possess a bipartite nuclear localization signal in the N-terminus. Aldolase was included in this category, as it was identified as a DNA-binding protein (Pandey et al. 2008). Apparently, aldolase is also located in the perinuclear space and functions as a nuclear protein in plants. Actin is a major cytoskeletal component and plays a role in gene transcription (Visa and Percipalle, 2010) while histones, besides their role in chromatin structure, signal the nature of the packaged DNA *via* their post-translational modifications (PTMs) (Shia et al. 2006; Yi et al. 2006). Access to certain genes can be granted or denied, depending on which PTMs are present on particular histones. In addition, combinations of PTMs (known as histone codes) may work together to modulate the degree of activation or repression (Shia et al. 2006). During the past decade, the roles of histone modification and histone variants in the regulation of gene expression was emphasized (Yi et al. 2006). Nemergut et al. (2001) demonstrated that H2A/H2B was involved in nuclear envelope assembly and nuclear transport through an interaction involving Ran-specific exchange factor, RCC1 (regulator of chromosome condensation 1) with chromatin. The interaction of RCC1 to H2A/H2B establishes the polarity of the Ran-GTP gradient which was proposed to be responsible for the afore mentioned functions (Nemergut et al. 2001). The differential regulation of these signalling-related proteins during citrus-*Xanthomonas* interaction indicates involvement of tight regulation of genes during pathogen challenge.

4.4.4. Protein synthesis, folding, and degradation-related proteins during citrus-*Xanthomonas* interaction:

Proteins related to translation were suppressed during both the pathogen interactions. Compared to *Xoo* interaction, more number of translation machinery-related proteins was repressed during *Xac* interaction. We identified Hsp70, HSP2, 26.5 kDa HSP, putative

chaperonin ClpB, ClpC3 and DnaJ a co-chaperone of HSP 70 which prevent protein misfolding and random aggregation in the cell. Protein folding and degradation play a vital role in the regulation of metabolic processes and stress responses. The key rate-limiting enzymes and misfolded/damaged proteins are regulated by different strategies in plants. Correct folding and subsequent assembly into oligomers is required for functional enzymes. Plants can refold the misfolded proteins by chaperonins, which include the HSP chaperonin protein family (Mogk et al. 1999). Heat-shock proteins such as HSP70 and HSP90 are important molecular chaperones that play critical roles in biotic and abiotic stress responses.

Under normal conditions, Hsp70 is present mainly in the cytosol, but translocates to the nucleus and nucleolus during physiological stress (Nollen et al. 2001). This movement of Hsp70 in and out of the nucleolus has been associated with the repair of stress-induced nucleolar damage (Pelham, 1984) by storing non-nucleolar unfolded proteins. The concentration of unfolded proteins at one locus in the nucleus reduces the damage by preventing their random aggregation with other nuclear proteins and macromolecular structures. DnaJ is a co-chaperone of HSP70 and in soyabean nuclear-localized DnaJ domain-containing HSP40 (GmHSP40.1) confired a critical role in cell death and disease resistance in soybean (Liu and Whitham, 2013). The decrease of HSP 70 and DnaJ during *Xac* interaction may be involved in repression of HR.

Further, plants can remove the excess or the misfolded/damaged proteins by proteolysis. Protein ubiquitination and degradation, last steps in protein turnover, are involved in plant defense responses. U-box domain-containing protein, BTB/POZ domain-containing protein, ATP-dependent metalloprotease, F-box protein and NLP4 were regulated in the present study. Ubiquitination is essential for ubiquitin/proteasome-mediated protein degradation in plant development and defense. A number of recent studies have investigated a possible role of U-box E3 ubiquitin ligases in PTI, ETI, as well as plant cell death and defense (Trujillo et al. 2008; Yang et al. 2006). F-box protein a component of the E3 ubiquitin ligase complex in the nucleus, involved in signal transduction through ubiquitin-dependent protein degradation (Craig and Tyers, 1999). Up-regulation of F-box proteins during salinity, desiccation and cold were reported in rice (Jain et al. 2007). The BTB/POZ domain is an evolutionarily conserved and widely distributed structural motif found in a battery of proteins involved in different biological processes,

such as transcriptional regulation, cytoskeletal organization, and formation of voltage-gated channels (Collins et al. 2001; Aravind and Koonin, 1999). This domain has been shown to homodimerize, multimerize, and heterodimerize with other BTB/POZ domains or with proteins devoid of the motif (Collins et al. 2001; Aravind and Koonin 1999; Li et al. 1999; Bardwell and Treisman, 1994). The BTB/POZ domain was also found in many animal transcriptional regulators (Collins et al. 2001).

Intracellular proteolytic processes triggered by proteases are necessary for regulation of cell viability. ATP-dependent metalloprotease was up-regulated during *Xac* challenge, while leucine amonipeptidase was upregulated in *Xoo* challenge in nuclear proteome of citrus leaves. ATP-dependent metalloprotease is encoded by nuclear genes and post-translationally imported into the membrane of chloroplasts by specific targeting sequences (Adam et al. 2006). In plant, it is light-inducible and can degrade the unassembled Rieske Fe-S proteins and D1 proteins of photosystem II during high-light acclimation and senescence (Haussuhl et al. 2001; Lindahl et al. 2000). In tomato, leucine aminopeptidase regulates defense and wound signalling acting downstream of JA biosynthesis and perception (Fowler et al. 2009), indicating possible involvement of JA pathway during NHR.

Several ribosomal proteins, isoforms of 30S, 40S, 50S, 60S and EF-Tu were differentially regulated. Most of these proteins were down-regulated during both host and non-host interaction. Protein synthesis elongation factor (EF)-Tu catalyzes the GTP-dependent binding of aminoacyl-tRNA to the A-site of the ribosome during the elongation phase of protein synthesis. However, EF-Tu acts as a molecular chaperone during stress, and it may be involved in protein folding and protection (Pandey et al. 2008). Several nuclear proteins differentially regulated during *Xanthomonas* interaction were classified as proteins with miscellaneous function and metabolism. Photosynthesis and carbon metabolism related proteins were identified to be regulated in the nuclear protein. These include rubisco large chain, malate dehydrogenase, sedoheptulose-1,7-bisphosphatase, sucrose synthase and transketolase. Identification of these proteins in the nuclear fraction might be due to the possible cytosolic contamination or these proteins might have functional role in the nucleus as moonlight proteins. As nuclear proteome of plants was not fully characterizied, it is difficult to assign specific function for these proteins.

Overview of the study:

Anatomical characterization of citrus-*Xoo* non-host pathosystem revealed occurrence of type II NHR. It is associated with decrease in non-host bacterial cell count *in planta*, callose deposition and cell death at the pathogen inoculation site in citrus. Decrease in the activity of ROS scavenging enzymes and increase in ROS producing enzymes lead to an oxidative burst that might be involved in cell death during citrus-*Xoo* interaction. Increase in the activity of ROS scavenging enzymes during *Xac* interaction might quench toxic ROS. The oxidative burst, PR proteins, cell wall synthesis and other signalling pathway related-proteins are pivotal in citrus-*Xoo* NHR. In the present study, total cellular and nuclear proteomics, many of the proteins related to protein synthesis were repressed during both the interactions. Whereas, CW strengthening and defense-related proteins were up-regulated in cellular and ECM-associated proteome during *Xoo* challenge. *Xanthomonas* attack repressed the expression of several proteins associated with photosynthesis in citrus. As the plant faces the challenge from pathogen it suspends its carbon metabolism till it can spare the resources. Thus, there was up-regulation of defense related proteins and loss of carbon metabolism-related ones. These signals are ultimately transduced to nucleus resulting in up-regulation of several defense and stress related transcription factors and down-regulation of growth and metabolism related ones.

Time course nuclear proteome analysis during citrus-*Xanthomonas* interactions has shed light on the involvement of transcriptional regulation, molecular chaperones, protein degradation, chromatin structure and remodelling, and nucleocytoplasmic transport related-proteins in plant-pathogen interactions. The TFs in turn, modulate the expression of down-stream genes resulting in metabolic modulations. Protein turn-out and trafficking are adjusted to churn out a proteome suited to serve the defensive needs. Primary metabolites are channelled to provide energy and raw materials for defense and CW remodelling to deter pathogen survival. These observations may possibly reveal protein targets/markers that are useful in the design of future diagnosis or plant protection strategies and provide new insights into the molecular mechanism of NHR in citrus.

Summary & Conclusion

In nature, plants are constantly challenged by a diverse range of microbes. However, a given plant species is normally resistant to most pathogens and susceptible to only a few pathogens. This is mainly due to the most robust form of plant immunity known as NHR. Resistance shown by an entire plant species against all strains of a pathogen that is able to infect other plant is known as NHR. Unlike R-gene-mediated resistance, which is often genetically controlled by a single gene, most non-host resistance is expected to be governed by a broad range of mechanisms that are regulated by multiple genes. Despite its great potential for providing crop plants with durable resistance, genetic and mechanistic components of non-host resistance are yet to be fully understood. Such understanding is necessary to engineer crops for durable disease resistance. To study NHR, we have selected citrus as a model plant and rice leaf blight pathogen *Xoo* as non-host pathogen. For comparative study, we selected citrus canker causing pathogen *Xac* as a host pathogen.

5.0. Overview of the study:

The thesis focuses on defense responses executed by citrus during compatible (*Xac*) and non-host (*Xoo*) interactions. To understand the type of response executed by citrus upon *Xoo* challenge, we performed anatomical studies using staining methods like aniline blue, DAB and trypan blue. To better understand the molecular mechanisms underlying in NHR, we studied antioxidant status and total leaf proteome during citrus-*Xanthomonas* interaction. To gain an in-depth understanding of defense responses, proteome changes occurring in the sub-organelles like extracellular matrix (ECM) and nucleus were studied.

5.1.1. Anatomical changes:

When a non-host pathogen manages to overcome constitutive defensive layers, inducible defense responses like accumulation of ROS, papillary callose, and HR are induced. Anatomical characterization of citrus-*Xoo* non-host pathosystem revealed CW-based defense *i.e.,* callose deposition occurred at 16 hpi. Indicating that callose deposition strengthened the CW at the bacterial penetration site resistricting the pathogen spread. ROS deposition and cell death were detected in *Xoo*-challenged leaves at 24 hpi. *In planta* bacterial count of host pathogen (*Xac*) increased by 3 log whereas, in non-host pathogen (*Xoo*) there was a decline by 1 log at 3 dai, indicating that *Xoo* was unable to

survive in citrus leaves. Further, a distinctly visible chlorotic HR-like response at 48 hpi suggested a type-II NHR in citrus-*Xoo* interaction. In *Xac*-challenged leaves, water-soaked lesion, typical of citrus canker was observed from 48 hpi and pustules formed after 8 days. Thus, the defense response in citrus was visible at 16 hpi against *Xoo,* whereas in *Xac*- challenge, disease symptoms appeared at 48 hpi. Therefore, we selected 8, 16, 24 and 48 hpi to study the biochemical changes in citrus.

5.1.2. Biochemical changes:

One of the earliest events in the plant defense response against pathogens is rapid and transient production of ROS. Subsequent to this oxidative burst, cell death and development of HR occur in the host site of attempted penetration to arrest pathogen growth. High accumulation of H_2O_2 during non-host interaction might be involved in cell death and restriction of progression of disease. Increase in SOD could be responsible for maintenance of high levels of H_2O_2 levels during *Xoo* interaction. This led to high lipid peroxidation in non-host interaction and therefore induces cell death. Marginal increase in H_2O_2 at the early interaction of *Xac* in citrus leaves might be a basal defense response of plant during compatible interaction. APX regulates ROS levels and its high activity during compatible interaction may maintain a strong antioxidative status. POD uses H_2O_2 as an oxidant to convert phenolic compounds to phenoxy radicals that are involved in cross-linking cell wall polymers. The high activity of POD at 24 hpi of *Xoo* interaction might be involved in strengthening of cell wall. The biochemical changes related to oxidative defense during citrus-*Xanthomonas* interaction reveal occurrence of oxidative burst during *Xoo* interaction. The increase in antioxidant status during compatible interaction quenches toxic H_2O_2 levels further lead to survival of pathogen and establishment of pathogenicity.

5.2. Total leaf proteome changes during *citrus-Xanthomonas* interactions:

Proteomics has been useful for studying plant-pathogen interactions. To understand the defense response of citrus against host (*Xac*) and non-host (*Xoo*) pathogens, a comparative total leaf proteome analysis was performed by gel-based and non-gel-based proteomic approach. The expression patterns of differentially expressed proteins of citrus during early (*i.e.*, at 8 hpi) and late (*i.e.*, at 48 hpi) interactions of *Xanthomonas* were identified. Proteins identified as differentially expressed in gel-based approach were also

identified in non-gel-based proteomics. The identified proteins participate in defense/disease responses, energy/carbohydrate metabolism, secondary metabolism, redox status, protein folding/turnover/cleavage/degradation, signal transduction and cell structure.

During citrus-*Xoo* interaction, defense-related proteins and ROS producing proteins were highly induced whereas, during *Xac* interaction antioxidant metabolism-related proteins were induced. Carbohydrate metabolism and protein synthesis was repressed during both interactions, indicating reallocation of energy towards defense response as a strategy of plant towards pathogen attack. Many proteins involved in defense response were induced only during non-host interaction. Cell wall (CW) remodelling proteins and proteins involved in lignin deposition were induced only during *Xoo* interaction, suggesting occurrence of CW strengthening in citrus during non-host interaction. Increase of proteins involved in CW loosening and elongation during *Xac* might be involved in canker formation. Thus, the total citrus leaf proteome study during *Xanthomonas* interaction indicates that NHR of citrus to *Xoo* was consistent with a shift in protein and energy metabolism, increased antimicrobial activities, possibly including cell wall reinforcement, increased ROS, decrease in antioxidive reactions, and occurrence of cell death. Nearly half of the regulated proteins were associated with chloroplast and cell wall physiology suggesting important roles for these organelles during NHR.

5.3. ECM-associated proteome changes in citrus during Xanthomonas interaction:

Plant ECM being a critical defense barrier, understanding its responses during interaction with non-host pathogen will provide insights into molecular events of NHR. The ECM-associated proteome was compared during interaction of citrus with pathogen *Xac* and non-host pathogen *Xoo* at 8, 16, 24 and 48 hpi. Comprehensive analysis of ECM-associated proteins was performed by extracting wall-bound- and soluble-ECM components using both destructive and non-destructive procedures. A total of 53 proteins were differentially expressed in citrus-*Xanthomonas* host and non-host interaction, out of which 44 were identified by mass spectrometry. The differentially expressed proteins were related to: 1) defense-response (5 pathogenesis-related proteins, 3 miraculin-like proteins (MIR, MIR1 and MIR2) and 2 proteases), 2) enzymes of ROS metabolism (Cu/Zn SOD, Fe-SOD, ascorbate peroxidase and 2-cysteine-peroxiredoxin), 3) signalling

(lectin, curculin-like lectin and concanavalin A-like lectin kinase), and 4) cell-wall modification (α-xylosidase, glucan 1, 3 β-glucosidase, XTH).

Glutathione lyase, XTH, miraculin were differentially expressed both in wall-bound and soluble ECM fractions, indicating possibility of isolation of these proteins by any of the ECM proteome isolation methods followed in the present study. Different isoforms of miraculin were present in both wall-bound and soluble fractions of ECM indicating possible involvement of post-translational modification. Non-classical secretory proteins like triose phosphate isomerase, OEE, glutathione lyase were differentially expressed in the ECM fraction. The decrease in ROS svanging proteins like ascorbate peroxidase and cysteine-peroxiredoxin could be involved in maintenance of ROS levels during non-host interaction. Increase in defense, cell wall remodelling and signalling proteins in citrus-*Xoo* interaction suggests an active involvement of ECM in execution of NHR. CW loosening proteins like α-xylosidase, glucan 1, 3-β-glucosidase were up-regulated during *Xac* interaction. The increase in susceptibility of citrus leaves to *Xac* and compromised NHR to *Xoo* upon brefeldin A (inhibitor of secreytory pathway) treatment, suggested a possible role for non-classical secretory proteins. Further investigations on the functional analysis of selected ECM proteins using either gene silencing or over expression will help assigning a specific role to these proteins in execution of NHR.

5.4. Nuclear proteome changes during citrus-*Xanthomonas* interaction:

Nuclear proteins constitute a highly organized, complex network that plays diverse roles during cellular development and other physiological processes. Proteomic study holds promise to understand the molecular basis of nuclear function using an unbiased comparative and differential approach. The nuclear proteome of citrus during interaction with host (*Xac*) and non-host (*Xoo*) is of particular interest as it will provide an insight into the functional role of the organelle in the acquisition of defense response. We identified a few hundred proteins that include classical and non-canonical nuclear components presumably associated with variety of cellular functions impinging on the complexity of nuclear proteome. The differentially expressed proteins were related to DNA replication/repair proteins, protein synthesis/degradation/folding, signalling, redox-status and proteins related to DNA structure and regulation. Cellular reorganization which is linked to gene regulation and signalling appears to be important in elicitation of

defense responses against *Xoo* in citrus. Several signalling proteins and transcription factors involved in triggering defense responses were induced during non-host interaction, while many ROS catabolising enzymes were induced during *Xac* interaction.

During citrus-*Xanthomonas* interaction, the complex architecture of nucleus responded differently against the two pathogens by using different set of nuclear proteins (NPs). Citrus might induce fundamental machinery of the nucleus to correctly target expressed proteins in a diverse defense-related pathway thereby barricade the non-host pathogens. The host pathogen may takeover control on the host plant defense machinery to induce favourable conditions for its survival. However, function of NPs belonging to protein folding and degradation, transcription regulation, and metabolism categories toward patho-stress needs further consideration to understand the susceptibility and NHR of plants.

5.5. Major Conclusion:

Citrus plants inoculated with *Xoo* responded by eliciting an HR response indicating a type II NHR. Proteome changes at cellular and sub-organelle (ECM and nucleus) level were characterized for the first time in citrus during host and non-host interactions. With the present study, we corroborate the accepted notion that the non-host pathogen is recognized at the early stage of interaction. We have identified at least four categories of proteins that can serve as markers for NHR. The proteins identified in this study revealed the involvement of proteins related to ROS production, defense-response PR proteins, cell death regulation, and CW structural and remodelling proteins in citrus-*Xanthomonas* interactions. Secretory pathway inhibition study with brefeldin A revealed the possible role of non-secretory pathway proteins in NHR. The exploration of the NHR-responsive nuclear protein expression patterns in citrus uncovered novel regulatory proteins, including MADS-box transcription factor, DEAD-box ATP-dependent RNA helicase 3, homeobox-leucine zipper protein, PHD-finger family protein and bHLH62 domain-containing proteins, strongly suggesting putative functions for them in plant defense response. However, the next challenging task would be to short-list the proteins identified in this study based on expression patterns, and to finally exploit and functionally identify the proteins that are truly responsible NHR.

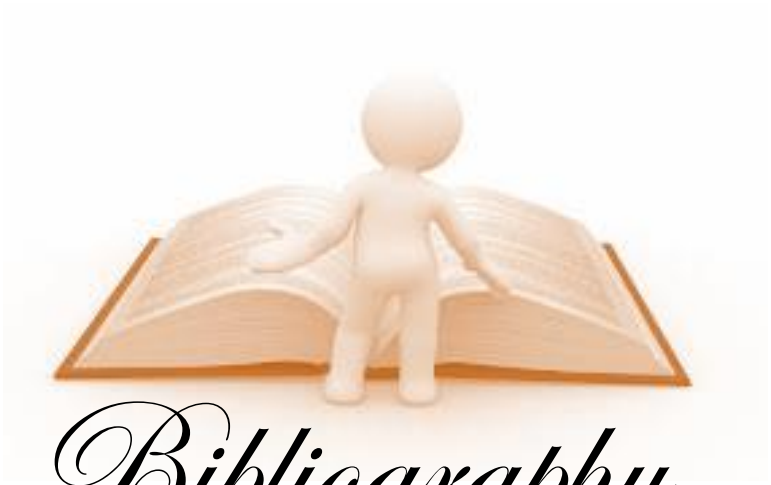

Bibliography

Abdalla KO, Baker B, Rafudeen MS (2010) Proteomic analysis of nuclear proteins during dehydration of the resurrection plant *Xerophyta viscose*. Plant Growth Regul. 62: 279-92.

Abdalla KO, Rafudeen MS (2012) Analysis of the nuclear proteome of the resurrection plant *Xerophyta viscosa* in response to dehydration stress using iTRAQ with 2DLC and tandem mass spectrometry. J. Proteomics 18: 2361-74.

Able AJ, Sutherland MW, Guest DI (2003) Production of reactive oxygen species during non-specific elicitation, non-host resistance and field resistance expression in cultured tobacco cells. Funct. Plant Biol. 30: 91-9.

Adam L, and Somerville SC (1996) Genetic characterization of five powdery mildew disease resistance loci in *Arabidopsis thaliana*. Plant J. 9: 341-56.

Adam Z, Rudella A, van Wijk KJ. (2006) Recent advances in the study of Clp, FtsH and other proteases located in chloroplasts. Curr. Opin. Plant Biol. 9: 234-40.

Afroz A, Zahur M, Zeeshan N, Komatsu S(2013) Plant-bacterium interactions analyzed by proteomics. Front Plant Sci. 4:21.

Agrawal GK, Jwa N-S, Lebrun M-H, Job D, Rakwal R (2010) Plant secretome:Unlocking secrets of the secreted proteins Proteomics 10:799-27.

Albert M, Werner M, Proksch P, Fry SC, Kaldenhoff R (2004) The cell wall-modifying xyloglucan endotransglycosylase/hydrolase *LeXTH1* is expressed during the defense reaction of tomato against the plant parasite *Cuscuta reflexa*. Plant Biol. 6: 402-07.

An C, Mou Z **(**2012) Non-host defense response in a novel *Arabidopsis- Xanthomonas citri subsp. citri* pathosystem. PLoS One 7: e31130.

Apel K, Hirt H (2004) Reactive oxygen species: metabolism, oxidative stress, and signal transduction. Annu. Rev. Plant Biol. 55: 373-99.

Arai Y, Hayashi M, Nishimura M (2008) Proteomic analysis of highly purified peroxisomes from etiolated soybean cotyledons. Plant Cell Physiol. 49: 526-39.

Aravind L, Koonin EV (1999). Fold prediction and evolutionary analysis of the POZ domain: Structural and evolutionary relationship with the potassium channel tetramerization domain. J. Mol. Biol. 285: 1353-61.

Asai T, Tena G, Plotnikova J, Willmann MR, Chiu WL, Gomez-Gomez L, et al. (2002) MAP kinase signalling cascade in Arabidopsis innate immunity. Nature 415:977-83.

Ashtamker C, Kiss V, Sagi M, Davydov O, Fluhr R (2007) Diverse subcellular locations of cryptogein-induced reactive oxygen species production in tobacco Bright Yellow-2 Cells. Plant Physiol. 143:1817-26.

Asirvatham VS, Watson BS, Sumner LW (2002) Analytical and biological variances associated with proteomic studies of *Medicago truncatula* by two-dimensional polyacrylamide gel electrophoresis. Proteomics 2: 960–68.

Assaad FF, Qiu JL, Youngs H, Ehrhardt D, Zimmerli L, Somerville CR, et al. (2004) The PEN1 syntaxin defines a novel cellular compartment upon fungal attack and is required for the timely assembly of papillae. Mol. Biol. Cell 15: 5118-29.

Austin MJ, Muskett P, Kahn K, Feys BJ, Jones JD, Parker JE (2002) Regulatory role of SGT1 in early R gene-mediated plant defenses. Science 295: 2077-80.

Bae MS, Cho EJ, Choi EY, Park OK (2003). Analysis of the *Arabidopsis* nuclear proteome and its response to cold stress. Plant J. 36: 652-63.

Barber GA, Neufeld EF (1961) Rhamnosyl transfer from TDPL-rhamnose catalyzed by a plant enzyme. Biochem. Biophys. Res. Commun. 6:44-8.

Bardwell VJ, Treisman R (1994) The POZ domain: A conserved protein-protein interaction motif. Genes Dev. 8: 1664-77.

Beauchamp C, Fridovich I (1971) Superoxide dismutase: Improved assays and an assay applicable to acrylamide gels. Anal. Biochem. 44: 276-87.

Bednarek P, Pislewska-Bednarek M, Svatos A, Schneider B, Doubsk J, Mansurova M, et al. (2009) A glucosinolate metabolism pathway in living plant cells mediates broad-spectrum antifungal defense. Science 323: 101-06.

Bestwick CS, Brown IR, Mansfield JW (1998) Localized changes in peroxidase activity accompany hydrogen peroxide generation during the development of a nonhost hypersensitive reaction in Lettuce. Plant Physiol. 118: 1067-78.

Bhushan D, Pandey A, Chattopadhyay A, Choudhary MK, Chakraborty S, Datta A, Chakraborty N (2006) Extracellular matrix proteome of chickpea (*Cicer arietinum L.*) illustrates pathway abundance, novel protein functions and evolutionary perspect. J. Proteome Res 5: 1711-20.

Blume B, Nurnberger T, Nass N, Scheel D (2000) Receptor-mediated increase in cytoplasmic free calcium required for activation of pathogen defense in parsley. Plant Cell 12:1425-40.

Bolton MD (2009) Primary metabolism and plant defense–fuel for the fire. Mol. Plant Microbe Interact. 22: 487-97.

Bolwell GP (1999) Role of reactive oxygen species and NO in plant defense responses. Curr. Opin. Plant Biol. 64: 163-76.

Bouwmeester K, Klamer S, Gouget A, Haget N, Canut H, Govers F (2008) Lectin receptor kinase 79, a putative target of the *Phytophthora infestans* effector IPI-O. In: Lorito M, Woo SL, and Scala F (eds) Biology of plant–microbe interactions St Paul MN, USA: International Society for Molecular Plant-Microbe Interactions, pp 1-6.

Broers JL, Bronnenberg NM, Kuijpers HJ, Schutte B, Hutchison CJ, Ramaekers FC (2002) Partial cleavage of A-type lamins concurs with their total disintegration from the nuclear lamina during apoptosis. Eur. J. Cell Biol. 81: 677-91.

Brugiere S, Kowalski S, Ferro M, Seigneurin-Berny D, Miras S, Salvi D et al. (2004) The hydrophobic proteome of mitochondrial membranes from *Arabidopsis* cell suspensions. Phytochemistry 65: 1693-07.

Buhr N, Carapito C, Schaeffer C, Kieffer E, Van Dorsselaer A, Viville S (2008) Nuclear proteome analysis of undifferentiated mouse embryonic stem and germ cells. Electrophoresis 29: 2381-90.

Canova MJ, Veyron-Churlet R, Zanella-Cleon I, CohenGonsaud M, Cozzone AJ, Becchi M, et al. (2008) The *Mycobacterium tuberculosis* serine/threonine kinase PknL phosphorylates Rv2175c: mass spectrometric profiling of the activation loop phosphorylation sites and their role in the recruitment of Rv2175c. Proteomics 8: 521-33.

Cantu MD, Mariano AG, Palma MS, Carrilho E, Wulff NA (2008) Proteomic analysis reveals suppression of bark chitinases and proteinase inhibitors in citrus plants affected by the citrus sudden death disease. Phytopathology 98: 1084-92.

Caraux G, Pinloche S (2005) PermutMatrix: a graphical environment to arrange gene expression profiles in optimal linear order. Bioinformatics 21:1280-81.

Carpita N, McCann M **(**2000) The cell wall. In: Buchanan BB, Gruissem W, Jones RL, (eds) Biochemistry and molecular biology of plants Rockville, MD: American Society of Plant Physiologists, pp 52-08.

Carroll AJ, Heazlewood JL, Ito J, Millar AH (2008) Analysis of the *Arabidopsis* cytosolic ribosome proteome provides detailed insights into its components and their post-translational modification. Mol. Cell Proteomics 7: 347-69.

Casasol M, Spadoni S, Lilley KS, Cervone F, De Lorenzo G, Mattei B (2008) Identification by 2-D DIGE of apoplastic proteins regulated by oligogalacturonides in *Arabidopsis thaliana.* Proteomics 8: 1042-54.

Cernadas RA, Camillo LR, Benedetti CE (2008) Transcriptional analysis of the sweet orange interaction with the citrus canker pathogens *Xanthomonas axonopodis* pv. *citri* and *Xanthomonas axonopodis* pv. *aurantifolii*. Mol. Plant Pathol. 9: 609-31.

Chance B, Maehly AC (1955) Assay of catalase and peroxidase. Methods Enzymol.2 :764-75.

Chen LR, Markhart AH, Shanmugasundaram S, Lin TY (2008) Early developmental and stress responsive ESTs from mungbean, *Vigna radiata* (L.) Wilczek, seedlings. Plant Cell Reports 27: 535-52.

Cheung AY, Reddy AS (2012) Nuclear architecture and dynamics: territories, nuclear bodies, and nucleocytoplasmic trafficking. Plant Physiol. 158: 23-5.

Chivasa S, Ndimba BK, Simon WJ, Robertson D, Yu XL, Knox JP et al. (2002) Proteomic analysis of the *Arabidopsis thaliana* cell wall. Electrophoresis 23: 1754-65.

Choi DS, Hwang IS, Hwang BK (2012) Requirement of the cytosolic interaction between PATHOGENESIS-RELATED PROTEIN10 and LEUCINE-RICH REPEAT PROTEIN1 for cell death and defense signaling in pepper. Plant Cell 24: 1675-90.

Choudhary MK, Basu D, Datta A, Chakraborty N, Chakraborty S (2009) Dehydration-responsive nuclear proteome of rice (*Oryza sativa* L.) illustrates protein network, novel regulators of cellular adaptation and evolutionary perspective. Mol. Cell. Proteomics 8: 1579-98.

Christopher-Kozjan R, Heath MC (2003) Cytological and pharmacological evidence that biotrophic fungi trigger different cell death execution processes in host and nonhost cells during the hypersensitive response. Physiol. Mol. Plant Pathol. 62: 265-75.

Coaker GL, Willard B, Kinter M, Stockinger EJ, Francis DM (2004). Proteomic analysis of resistance mediated by Rcm 2.0 and Rcm 5.1, two loci controlling resistance to bacterial canker of tomato. Mol. Plant Microbe Interact. 17: 1019-28.

Collins NC, Thordal-Christensen H, Lipka V, Bau S, Kombrink E, Qiu Jin-Long, et al. (2003) SNARE-protein-mediated disease resistance at the plant cell wall. Nature 425: 973-77.

Collins T, Stone JR, Williams AJ (2001) All in the family: The BTB/POZ, KRAB, and SCAN domains. Mol. Cell. Biol. 21: 3609-15.

Cooper B, Campbell KB, Feng J, Garrett WM, Frederick R (2011) Nuclear proteomic changes linked to soybean rust resistance. Mol. Bisys. 3: 773-83.

Cosgrove D (2001) Wall structure and wall loosening. A look backwards and forwards. Plant Physiol. 125: 131-34.

Cosgrove DJ (2005) Growth of the plant cell wall. Nature Reviews Mol. Cell Biol. 6:850-61.

Craig KL, Tyers M (1999) The F-box: a new motif for ubiquitin dependent proteolysis in cell cycle regulation and signal transduction. Prog. Biophys. Mol. Biol. 72: 299-28.

Dahal D, Pich A, Braun HP, Wydra K (2010) Analysis of cell wall proteins regulated in stem of susceptible and resistant tomato species after inoculation with *Ralstonia solanacearum*: a proteomic approach. Plant Mol. Biol. 73: 643-58.

Dahl KN, Ribeiro AJS, Lammerding J (2008) Nuclear shape, mechanics, and mechanotransduction. Circ. Res. 102: 1307-18.

Dangl JL, Dietrich RA, Richberg MH (1996) Death don't have no mercy: cell death programs in plant-microbe interactions. Plant Cell 8: 1793-07.

Dangl JL, Jones JDG (2001). Plant pathogens and integrated defence responses to infection. Nature 411: 826-33.

Dani V, Simon WJ, Duranti M, Croy RRD (2005) Changes in the tobacco leaf apoplast proteome in response to salt stress. Proteomics 5: 737-45.

Daurelio LD, Petrocelli S, Blanco F, Holuigue L, Ottado J, Orellano EG (2011) Transcriptome analysis reveals novel genes involved in nonhost response to bacterial infection in tobacco. J Plant Physiol. 168: 382-91.

Davies DR, Bindschedler LV, Strickland TS, Bolwell GP (1991) Production of reactive oxygen species in *Arabidopsis thaliana* cell suspension cultures in response to an elicitor from *Fusarium oxysporum*: implications for basal resistance**.** Mol. Plant-Microbe Interact. 4: 477-88.

De Pinto MC, De Gara L (2004). Changes in the ascorbate metabolism of apoplastic and symplastic spaces are associated with cell differentiation. J. Exp. Bot. 55: 2559-69.

Ding M-Z, Wang X, Liu W, Cheng J-S, Yang Y, Yuan Y-J (2012) Proteomic research reveals the stress response and detoxification of yeast to combined inhibitors. PLoS One 7: e43474.

Edwards R, Dixon D, Walbot B (2000) Plant glutathione S transferases: enzymes with multiple functions in sickness and in health. Trends Plant Sci. 5: 193-98.

Eichmann R, Biemelt S, Schafer P, Scholz U, Jansen C, Felk A, et al. **(**2006) Macroarray expression analysis of barley susceptibility and nonhost resistance to *Blumeria graminis.* Plant Physiol. 163: 657-70.

Eichmann R, Schultheiss H, Kogel KH, Huckelhoven R (2004) The barley apoptosis suppressor homologue BAX inhibitor-1 compromises nonhost penetration resistance of barley to the inappropriate pathogen *Blumeria graminis* f. sp. *tritici.* Mol. Plant Microbe Interactions 17: 484-90.

Erhardt M, Adamska I, Franco OL (2010) Plant nuclear proteomics – inside the cell maestro. FEBS J. 277: 3295–07.

Felix G, Boller T (2003) Molecular sensing of bacteria in plants: The highly conserved RNA-binding motif RNP-1 of bacterial cold shock proteins is recognized as an elicitor signal in tobacco. J. Biol. Chem. 278: 6201-08.

Fenn J, Mann M, Meng C, Wong S, Whitehouse C (1989) Electrospray ionization for mass spectrometry of large biomolecules. Science 246: 64-71.

Fink T, Lund P, Pilgaard L, Rasmussen JG, Duroux M, Zachar V (2008) Instability of standard PCR reference genes in adipose-derived stem cells during propagation, differentiation and hypoxic exposure. BMC Molecular Biology 9:98.

Fowler JH, Narváez-Vásquez J, Aromdee DN, Pautot V, Holzer FM, Walling LL (2009) Leucine aminopeptidase regulates defense and wound signaling in tomato downstream of jasmonic acid. Plant Cell 21: 1239-51.

Fry SC (1989) The structure and functions of xyloglucan. J. Exp. Bot. 40: 1-11.

Garavaglia BS, Thomas L, Zimaro T, Gottig N, Daurelio LD, Ndimba B et al. (2010) A plant natriuretic peptide-like molecule of the pathogen *Xanthomonas axonopodis* pv. *citri* causes rapid changes in the proteome of its citrus host. BMC Plant Biol. 10:51.

Gatenby AA (1992) Protein folding and chaperonins. Plant Mol. Biol. 19:677-87.

Glazebrook J (2005) Contrasting mechanisms of defense against biotrophic and necrotrophic pathogens. Annu. Rev. Phytopathol. 43: 205-27.

Godfrey D, Rathjen JP (2012) Recognition and response in plant PAMP-triggered immunity. eLS.

Gomez-Gomez L, Boller T (2002) Flagellin perception: a paradigm for innate immunity. Trends Plant Sci. 7: 251-56.

Gor D, Mayfield JE (1992) Cloning and nucleotide sequence of the Brucella abortus groE operon. Biochim. Biophys. Acta 1130: 120-22.

Gottwald TR, Graham JH, Civerolo EL, Barrett HC, Hearn CJ (1993) Differential host range reaction of citrus and citrus relatives to citrus canker and citrus bacterial spot determined by leaf mesophyll susceptibility. Plant Dis 77: 1004-09.

Gottwald TR, Graham JH, Schubert TS (2002) Citrus canker: The pathogen and its impact. Plant Health Progress doi:10.1094/PHP-2002-0812-01-RV.
Gouget A, Senchou V, Govers F, Sanson A, Barre A, Rouge P, et al. (2006) Lectin receptor kinases participate in protein-protein interactions to mediate plasma membrane-cell wall adhesions in *Arabidopsis*. Plant Physiol. 140: 81-90.

Graham JH, Leite RP (2004) Lack of control of citrus canker by induced systemic resistance compounds. Plant Dis 88: 745-50.

Grant M, Brown I, Adams S, Knight M, Ainslie A, John Mansfield J (2000) The *RPM1* plant disease resistance gene facilitates a rapid and sustained increase in cytosolic calcium that is necessary for the oxidative burst and hypersensitive cell death. Plant J. 23: 441-50.

Hakmaoui A, Pérez-Bueno ML, García-Fontana B, Camejo D, Jiménez A, Sevilla F, et al. . (2012) Analysis of the antioxidant response of *Nicotiana benthamiana* to infection with two strains of Pepper mild mottle virus. J. Exp. Bot. 63: 5487-96.

Hardham AR, Jones DA, Takemoto D (2007) Cytoskeleton and cell wall function in penetration resistance. Curr. Opin. Plant Biol. 10: 342-48.

Hartley RD, Morrison WH, Borneman WS, Rigsby LL, O'Neill M, Hanna WW, Akin DE (1992) Phenolic constituents of cell wall types of normal and brown midrib mutants of pearl barley (Pennisetum glaucum (L.) R Br) in relation to wall biodegradability. J. Sci. Food Agric. 59: 211-16.

Haussühl K, Andersson B, Adamska I (2001) A chloroplast DegP2 protease performs the primary cleavage of the photodamaged D1 protein in plant photosystem II. EMBO J. 20: 713-22.

Heath MC (2000) Nonhost resistance and nonspecific plant defenses. Curr. Opin. Plant Biol. 3: 315-19.

Heath RL, Packer L (1968) Photoperoxidation in isolated chloroplast. I. Kinetics and stoichiometry of fatty acid peroxidation. Arch. Biochem. Biophys. 125:189-198.

Henrich S, Cordwell SJ, Crossett B, Baker MS, Christopherson RI (2007) The nuclear proteome and DNA-binding fraction of human Raji lymphoma cells. Biochim. Biophys. Acta 1774: 413-32.

Holub EB (2001) The arms race is ancient history in Arabidopsis, the wildflower. Nat. Rev. Genet. 2:516-27.

Huckelhoven R (2007) Cell wall-associated mechanisms of disease resistance and susceptibility. Annu. Rev. Phytopathol. 45:101-27.

Huckelhoven R, Dechert C, Kogel KH (2001) Non-host resistance of barley is associated with a hydrogen peroxide burst at sites of attempted penetration by wheat powdery mildew fungus. Mol. Plant Pathol. 2: 199-05.

Hwang J, Choi Y, Kang J, Kim S, Cho M, Mihalte L, Park Y (2011) Microarray analysis of the transcriptome for bacterial wilt resistance in pepper (*Capsicum annuum* L.). Not. Bot. Horti. Agrobo. 39: 49-57.

Isaacson T, Damasceno CM, Saravanan RS, He Y, Catala C, Saladie M, Rose JKC (2006) Sample extraction techniques for enhanced proteomic analysis of plant tissues. Nat. Protoc. 1:769-774.

Itai A, Ishihara K, Bewley JD (2003) Characterization of expression, and cloning, of β-d-xylosidase and α-l-arabinofuranosidase in developing and ripening tomato (*Lycopersicon esculentum* Mill.) fruit. J. Exp. Bot 54: 2615-22.

Jacobs AK, Lipka V, Burton RA, Panstruga R, Strizhov N, et al. (2003) An Arabidopsis callose synthase, GSL5, is required for wound and papillary callose formation. Plant Cell 15: 2503-13.

Jain M, Nijhawan A, Arora R, Agarwal P, Ray S, P Sharma, et al. (2007) F-box proteins in rice. Genome-wide analysis, classification, temporal and spatial gene expression during panicle and seed development, and regulation by light and abiotic stress. Plant Physiol. 143: 4 1467-83.

Jamet E, Albenne C, Boudart G, Irshad M, Canut H, Pont-Lezica R (2008a) Recent advances in plant cell wall proteomics. Proteomics 8:893-908.

Jamet E, Boudart G, Borderies G, Charmont S, Lafitte C, Rossignol M, et al. (2008b) Isolation of plant cell wall proteins. Methods Mol. Biol. 425, 187-201.

Jankowsky E, Fairman M (2007) RNA helicases - one fold for many functions. Curr. Opin. Struct. Biol. 17: 316-24.

Jaquinod M, Villiers F, Kieffer-Jaquinod S, Hugouvieux V, Bruley C, Garin J, Bourguignon J (2007) A proteomics dissection of *Arabidopsis thaliana* vacuoles isolated from cell culture. Mol. Cell. Proteomics 6: 394-12.

Jeong RD, Lim WS, Kwon SW, Kim KH (2005) Identification of *Glycine max* genes expressed in response to Soybean mosaic virus infection. Plant Pathol. 21: 47-54.

Jonak C, Okresz L, Bogre L, Hirt H (2002) Complexity, cross talk and integration of plant MAP kinase signalling. Curr. Opin. Plant Biol. 5: 415-24.

Jones DA, Takemoto D **(**2004) Plant innate immunity–direct and indirect recognition of general and specific pathogen-associated molecules. Curr. Opin. Immunol. 16: 48-62.

Jones JDG, Dangl LJ (2006) The plant immune system. Nature 444: 323-29.

Kaffarnik FAR, Jones AME, Rathjen JP, Peck SC **(**2009) Effector proteins of the bacterial pathogen *Pseudomonas syringae* alter the extracellular proteome of the host plant, *Arabidopsis thaliana*. Mol. Cell Proteomics 8: 145-56.

Kang L, Li J, Zhao T, Xiao F, Tang X, Thilmony R, et al. (2003) Interplay of the Arabidopsis non-host resistance gene *NHO1* with bacterial virulence. Proc. Natl. Acad. Sci. 100: 3519-24.

Kanzaki H, Saitohet H, Ito A, Fujisawa S, Kamoun S, Katou S, et al. (2003) Cytosolic HSP90 and HSP70 are essential components of INF1-mediated hypersensitive response and non-host resistance to *Pseudomonas cichorii* in *Nicotiana benthamiana*. Mol. Plant Pathol. 4: 383-91.

Karas M, Hillenkamp F (1988) Laser desorption ionization of proteins with molecular masses exceeding 10,000 daltons. Anal. Chem. 60: 2299-01.

Kasai T, Suzuki T, Ono K, Ogawa K, Inagaki Y, Ichinose Y, Toyoda K, Shiraishi T (2006) Pea extracellular Cu/Zn-superoxide dismutase responsive to signal molecules from a fungal pathogen. J. Gen. Plant Pathol. 72: 265-72.

Knight H, Knight MR (2001) Abiotic stress signalling pathways: Specificity and cross-talk. Trends Plant Sci. 6: 262-67.

Knoester M, Van Loon LC, Heuvel JVD, Hennig J, Bol JF, Linthorst HJM (1998) Ethylene-insensitive tobacco lacks nonhost resistance against soil-borne fungi. Proc. Natl. Acad. Sci. 95:1933-37.

Kobayashi DY, Tamaki SJ, Keen NT (1990) Cloned avirulence genes from the tomato pathogen *Pseudomonas syringae* pv. *tomato* confer cultivar specificity on soybean. Proc. Natl. Acad. Sci. 86: 157-61.

Kobayashi Y, Yamada M, Kobayashi I, Hitoshi K (1997) Actin microfilaments are required for the expression of non-host resistance in higher plants. Plant Cell Physiol. 38: 725-33.

Kocal N, Sonnewald U, Sonnewald S (2008). Cell wall-bound invertase limits sucrose export and is involved in symptom development and inhibition of photosynthesis during compatible interaction between tomato and *Xanthomonas campestris* pv. *vesicatoria*. Plant Physiol .148: 1523-36.

Koch E, Slusarenko A (1990) *Arabidopsis* is susceptible to infection by a downy mildew fungus. Plant Cell 2:437-45.

Kristensen BK, Bloch H, Rasmussen SK (1999) Barley coleoptiles peroxidases. Purification, molecular cloning, and induction by pathogens. Plant Physiol. 120: 501-12.

Kruger J, Thomas CM, Golstein C, Dixon MS, Smoker M, Tang S, Mulder L, Jones JDG (2002) A tomato cysteine protease required for Cf-2-dependent disease resistance and suppression of autonecrosis. Science 296: 744-47.

Kundu S, Chakraborty D, Pal A (2011) Proteomic analysis of salicylic acid induced resistance to Mungbean Yellow Mosaic India Virus in *Vigna mungo*. J. Proteomics 74:337-49.

Kwon C, Neu C, Pajonk S, Yun HS, Lipka U, Humphry M, et al. (2008) Co-option of a default secretory pathway for plant immune responses. Nature 451: 835-40.

Kwon C, Bednarek P, Schulze-Lefert P (2008) Secretory pathways in plant immune responses. Plant Physiol. 147:1575-83.
Lamb C, Dixon RA (1997) The oxidative burst in plant disease resistance. Plant Mol. Biol. 48:251-75.

Lee BJ, Kwon SJ, Kim SK, Kim KJ, Park CJ, Kim YJ et al. (2006) Functional study of hot pepper 26S proteasome subunit RPN7 induced by tobacco mosaic virus from nuclear proteome analysis. Biochem. Biophy. Res. Comm. 351: 405-11.

Lee S, Woo Y-M, Ryu S, Shin Y-D, Kim WT, Park KY, et al. (2008) Further characterization of a rice AGL12 group MADS-box gene, OsMADS26. Plant Physiol 147: 156-68.

Li D, Liu H, Zhang H, Wang X, Song F (2008) *OsBIRH1*, a DEAD-box RNA helicase with functions in modulating defense responses against pathogen infection and oxidative stress. J. Exp. Bot. 59: 2133-46.

Li H, Goodwin PH, Han Q, Huang L, Kang Z (2012) Microscopy and proteomic analysis of the non-host resistance of *Oryza sativa* to the wheat leaf rust fungus, *Puccinia triticina* f. sp. *tritici.* Plant Cell Rep. 31: 637-65.

Li W, Xu YP, Zhang ZX, Cao WY, Li F, Zhou X, et al. (2012) Identification of genes required for nonhost resistance to *Xanthomonas oryzae* pv. *oryzae* reveals novel signaling components. PLoS One 7:e42796.

Li X, Peng H, Schultz DC, Lopez-Guisa JM, Rauscher III FJ, Marmorstein R (1999) Structure-function studies of the BTB/POZ transcriptional repression domain from the promyelocytic leukemia zinc finger oncoprotein. Cancer Res. 59: 5275-82.

Lindahl M, Spetea C, Hundal T, Oppenheim AB, Adam Z, Andersson B (2000) The thylakoid FtsH protease plays a role in the light-induced turnover of the photosystem II D1 protein. Plant Cell 12: 419-31.

Lipka V, Dittgen J, Bednarek P, Bhat R, Wiermer M, Schulze-Lefert P, et al. (2005) Pre- and postinvasion defenses both contribute to non-host resistance in Arabidopsis. Science 310: 1180-83.

Lipka U, Fuchs R, Lipka V (2008) Arabidopsis non-host resistance to powdery mildews. Curr. Opin. Plant Biol. 11: 1–8.

Lipka V, Panstruga R (2005) Dynamic cellular responses in plant-microbe interactions. Curr. Opin. Plant Biol. 8: 625-31.

Liu H, Wang Y, Xu J, Su T, Liu G, Ren D (2008) Ethylene signaling is required for the acceleration of cell death induced by the activation of *AtMEK5* in *Arabidopsis*. Cell Research 18: 422-32.

Liu JZ, Whitham SA (2013) Overexpression of a soybean nuclear localized type-III DnaJ domain-containing HSP40 reveals its roles in cell death and disease resistance. Plant J. 74: 110-21.

Liu Y, Schiff M, Serino G, Deng XW, Dinesh-Kumar SP (2002) Role of SCF ubiquitin-ligase and the COP9 signalosome in the N genemediated resistance response to tobacco mosaic virus, Plant Cell 14: 1483-96.

Lu M, Tang X, Zhou JM (2001) Arabidopsis *NHO1* is required for general resistance against Pseudomonas bacteria. Plant Cell 13:437-47.

Majeran W, Cai Y, Sun Q, vanWijk KJ (2005) Functional differentiation of bundle sheath and mesophyll maize chloroplasts determined by comparative proteomics. Plant Cell 17: 3111-40.

Mahmood T, Jan A, Kakishima M, Komatsu S (2006) Proteomic analysis of bacterial-blight defense-responsive proteins in rice leaf blades. Proteomics 6: 6053-65.

Maltman DJ, Gadd SM, Simon WJ, Slabas AR (2007) Differential proteomic analysis of the endoplasmic reticulum from developing and germinating seeds of castor (*Ricinus communis*) identifies seed protein precursors as significant components of the endoplasmic reticulum. Proteomics 7: 1513-28.

Martinou JC, Desagher S, Antonsson B (2000) Cytochrome c release from mitochondria: all or nothing. Nat. Cell Biol. 2: E41-E43.

Maserti BE, Del Carratore R, Croce CM, Podda A, Migheli Q, Froelicher Y, Luro F, Morillon R, Ollitrault P, Talon M, Rossignol M **(**2011) Comparative analysis of proteome changes induced by the two spotted spider mite *Tetranychus urticae* and methyl jasmonate in citrus leaves. J. Plant Physiol. 168: 392-02.

Matsumura H, Reich S, Ito A, Saitoh H, Kamoun S, Winter P, et al. (2003) Gene expression analysis of plant host-pathogen interactions by SuperSAGE. Proc. Natl. Acad. Sci. USA 100: 15718-23.

McLusky SR, Bennett MH, Beale MH, Lewis MJ, Gaskin P, Mansfield JW (1999) Cell wall alterations and localized accumulation of feruloyl 3'-tyramine in onion epidermis at sites of attempted penetration by *Botrytis allii* are associated with actin polarization, peroxidase activity and suppression of flavonoid biosynthesis. Plant J. 17: 523-34.

Mehta A, Brasileiro AC, Souza DS, Romano E, Campos MA, Grossi-de-Sá MF et al. (2008) Plant-pathogen interactions: what is proteomics telling us? FEBS J. 275: 3731-46.

Mellersh DG, Heath MC (2003) An investigation into the involvement of defense signaling pathways in components of the nonhost resistance of *Arabidopsis thaliana* to rust fungi also reveals a model system for studying rust fungal compatibility. Mol. Plant Microbe Interact. 16:398-04.

Meng X, Zhang S (2013) MAPK cascades in plant disease resistance signalling. Ann. Rev. Phytopathol. 51: DOI: 10.1146/annurev-phyto-082712-102314.

Meunier B, Dumas E, Piec I, Béchet D, Hebraud M, Hocquette JF (2007) Assessment of hierarchical clustering methodologies for proteomic data mining. J. Proteome Res. 6: 358-66.

Mittler R, Feng X, Cohen M (1998) Post-transcriptional suppression of cytosolic ascorbate peroxidase expression during pathogen-induced programmed cell death in tobacco. Plant Cell 10: 461-73.

Mittler R, Herr HE, Orvar BL, Van Camp W, Willekens H, Inzé D, Ellis BE (1999) Transgenic tobacco plants with reduced capability to detoxify reactive oxygen intermediates are hyperresponsive to pathogen infection. Proc. Natl. Acad. Sci. USA 96: 14165-70.

Mogk A, Tomoyasu T, Goloubinoff P, Rüdiger S, Röder D, Langen H, et al. (1999) Identification of thermolabile *E. coli* proteins: prevention and reversion of aggregation by DnaK and ClpB. EMBO J. 18: 6934-49.

Moresco JJ, Dong M-Q, Yates JR (2008) Quantitative mass spectrometry as a tool for nutritional proteomics. Am. J. Clin. Nutr. 88: 597-04.

Moriguchi K, Suzuki T, Ito Y, Yamazaki Y, Niwa Y, Kurata N (2005) Functional isolation of novel nuclear proteins showing a variety of subnuclear localizations. Plant Cell 17: 389-03.

Morreel K, Ralph J, Lu F, Goeminne G, Busson R, Herdewijn P, et al. (2004) Phenolic profiling of caffeic acid O-methyltransferase-deficient poplar reveals novel benzodioxane oligolignols. Plant Physiol. 136: 4023-36.

Musselman CA, Lalonde M-E, Côté J, Kutateladze TG (2012) Perceiving the epigenetic landscape through histone readers. Nat. Struct. Mol. Biol. 19: 1218-27.

Mysore KS, Ryu CM (2004) Nonhost resistance: How much do we know? Trends in Plant Science 9: 97-04.

Nakano A, Asada K (1987) Purification of ascorbate peroxidase in spinach chloroplasts: Its inactivation in ascorbate-depleted medium and reactivation by monodehydroascorbate radical. Plant Cell. Physiol. 28: 131-40.

NarulaK, Datta A, Chakraborty N, Chakraborty S (2013) Comparative analyses of nuclear proteome: extending its function. Front Plant Sci. 4: 100.

Nasir KH, Takahashi Y, Ito A, Saitoh H, Matsumura H, Kanzaki H, et al. (2005) High-throughput in planta expression screening identifies a class II ethylene-responsive element binding factor-like protein that regulates plant cell death and non-host resistance. Plant J. 43: 491-05.

Nemergut ME, Mizzen CA, Stukenberg T, Allis CD, Macara IG (2001) Chromatin docking and exchange activity enhancement of RCC1 by histones H2A and H2B. Science 292: 1540-43.

Nollen EA, Salomons FA, Brunsting JF, van der Want JJ, Sibon OC, Kampinga HH (2001) Dynamic changes in the localization of thermally unfolded nuclear proteins associated with chaperone-dependent protection. Proc. Natl. Acad. Sci. USA 98: 12038-43.

Nurnberger T, Brunner F, Kemmerling B, Piater L (2004) Innate immunity in plants and animals: striking similarities and obvious differences. Immunol. Rev. 198: 249-66.

Nurnberger T, Lipka V (2005) Non-host resistance in plants: new insights into an old phenomenon. Mol. Plant Pathol. 6:335-45.

Nurnberger T, Nennstiel D, Jabs T, Sacks WR, Hahlbrock K, Scheel D (1994) High affinity binding of a fungal oligopeptide elicitor to parsley plasma membranes triggers multiple defense responses. Cell 78: 449-60.

Nurnberger T, Scheel D (2001) Signal transmission in the plant immune response. Trends Plant Sci. 6: 372-79.

Oh IS, Park AR, Bae MS, Kwon SJ, Kim YS, Lee JE, (2005) Secretome analysis reveals an *Arabidopsis* lipase involved in defense against *Alternaria brassicicola.* Plant Cell 17: 2832-47.

Oh SK, Lee S, Chung E, Park JM, Yu SH, Ryu CM, Choi D **(**2006) Insight into Types I and II nonhost resistance using expression patterns of defense-related genes in tobacco. Planta 223: 1101-07.

Ott PG, Varga GJ, Szatmari A, Bozso Z, Klement E, Medzihradszky KF, Besenyei E, Czelleng A, Klement Z (2006) Novel extracellular chitinases rapidly and specifically induced by general bacterial elicitors and suppressed by virulent bacteria as a marker of early basal resistance in tobacco. Mol. Plant Microbe Interact. 19: 161-72.

Overmyer K, Brosche M, Kangasjarvi J (2003) Reactive oxygen species and hormonal control of cell death. Trends Plant Sci. 8: 335-42.

Pajerowska-Mukhtar KM, Wang W, Tada Y, Oka N, Tucker CL, Fonseca JP, et al. (2012) The HSF-like transcription factor TBF1 is a major molecular switch for plant growth-to-defense transition. Curr. Biol. 22: 103-12.

Pandey A, Chakraborty S, Datta A, Chakraborty N (2008) Proteomics approach to identify dehydration responsive nuclear proteins from chickpea (*Cicer arietinum* L.). Mol. Cell Proteomics 7: 88-07.

PandeyA,ChoudharyMK, Bhushan D, Chattopadhyay A, Chakraborty S, Datta A, et al. (2006). The nuclear proteome of chickpea (*Cicer arietinum* L.) reveals predicted and unex-pected proteins. J. Proteome Res. 5: 3301-11.

Passardi F, Penel C, Dunand C (2004) Performing the paradoxical: how plant peroxidases modify the cell wall. Trends Plant Sci. 9: 534-40.

Peart JR, Lu R, Sadanandom A, Malcuit I, Moffett P, Brice DC, et al. (2002) Ubiquitin ligase-associated protein SGT1 is required for host and nonhost disease resistance in plants. Proc. Natl. Acad. Sci. 99:10865-69.

Peumans WJ, van Damme EJM (1995) Lectins as plant defense proteins. Plant Physiol. 109:347-53.

Pelham HR (1984) Hsp70 accelerates the recovery of nucleolar morphology after heat shock. EMBO J 3:3095-00.

Pirondini A, Visioli G, Malcevschi A, Marmiroli N (2006) A 2-D liquid-phase chromatography for proteomic analysis in plant tissues. Journal of Chromatography B: Analytical Technologies in the Biomedical and Life Sciences 833: 91-00.

Pirovani CP, Carvalho HA, Machado RC, Gomes DS, Alvim FC, Pomella AWV, et al. **(**2008) Protein extraction for proteome analysis from cacao leaves and meristems, organs infected by *Moniliophthora perniciosa*, the causal agent of the witches' broom disease. Electrophoresis 29: 2391-01.

Porankiewicz J, Wang J, Clarke AK (1999) New insights into the ATP-dependent Clp protease: *Escherichia coli* and beyond. Mol. Microbiol. 32: 449-58.

Portis AR Jr, Li C, Wang D, Salvucci ME (2008) Regulation of Rubisco activase and its interaction with Rubisco. J. Exp. Bot. 59: 1597-04.

Praefcke GJK, McMahon HT (2004) The dynamin superfamily: universal membrane tubulation and fission molecules? Nat. Rev. Mol. Cell Biol. 5:133-47.

Prasad TK, Stewart CR (1992) cDNA clones encoding *Arabidopsis thaliana* and *Zea mays* mitochondrial chaperonin HSP60 and gene expression during seed germination and heat shock. Plant Mol. Biol. 18: 873-85.

Quirino BF, Candido ES, Campos PF, Franco OL, Krüger RH (2010) Proteomic approaches to study plant–pathogen interactions. Phytochemistry 71: 351-62.

Real MD, Company P, Garcia-Agustin P, Bennett AB, Gonzalez-Bosch C (2004) Characterization of tomato endo-β-1,4-glucanase cel1 protein in fruit during ripening and after fungal infection. Planta 220: 80-86.

Ren D, Yang H, Zhang S (2002) Cell death mediated by MAPK is associated with hydrogen peroxide production in *Arabidopsis*. J. Biol. Chem. 277: 559-65.

Repetto O, Rogniaux H, Firnhaber C, Zuber H, Küster H, Larré C, et al. (2008) Exploring the nuclear proteome of *Medicago truncatula* at the switch towards seed filling. Plant J. 56: 398-10.

Repetto O, Rogniaux H, Larré C, Thompson R, Gallardo K (2012). The seed nuclear proteome. Front Plant Sci. 3:289.

Reumann S, Babujee L, Ma C, Wienkoop S, Siemsen T, Antonicelli GE, Rasche N et al. (2007) Proteome analysis of *Arabidopsis* leaf peroxisomes reveals novel targeting peptides, metabolic pathways, and defense mechanisms. Plant Cell 19: 3170-93.

Ringli C (2010) Monitoring the outside: cell wall-sensing mechanisms. Plant Physiol. 153:1445-52.

Riou C, Hervé C, Pacquit V, Dabos P, Lescure B (2002) Expression of an Arabidopsis lectin kinase receptor gene, lecRK-a1, is induced during senescence, wounding and in response to oligogalacturonic acids. Plant Physiol. Biochem. 40: 431-38.

Rivas S (2012) Nuclear dynamics during plant innate immunity. Plant Physiol. 158: 87-94.

Robertson D, Mitchell GP, Gilroy JS, Gerrish C, Bolwell GP, Slabas AR (1997) Differential extraction and protein sequencing reveals major differences in patterns of primary cell wall proteins from higher plants. J. Biol. Chem. 272:15841-48.

Rojas CM, Senthil-Kumar M, Wang K, Ryu CM, Kaundal A, Mysore KS (2012) Glycolate oxidase modulates reactive oxygen species-mediated signal transduction during nonhost resistance in *Nicotiana benthamiana* and *Arabidopsis*. Plant Cell 24:336-352.

Roje S (2006) S-Adenosyl-l-methionine: Beyond the universal methyl group donor. Phytochemistry 67:1686-98.

Salzano AM, Paron I, Pines A, Bachi A, Talamo F, Bivi N, et al. (2006) Differential proteomic analysis of nuclear extracts from thyroid cell lines. J. Chromatogr. B Analyt. Technol. Biomed. Life Sci. 833: 41-50.

Sanchez-Vallet A, Ramos B, Bednarek P, Lopez G, Bednarek MP, Schulze-Lefert, et al. (2010) Tryptophan-derived secondary metabolites in *Arabidopsis thaliana* confer non-host resistance to necrotrophic *Plectosphaerella cucumerina* fungi. Plant J. 63:115-27.

Santoni V, Kieffer S, Desclaux D, Masson F, Rabilloud T (2000) Membrane proteomics: use of additive main effects with multiplicative interaction model to classify plasma membrane proteins according to their solubility and electrophoretic properties. Electrophoresis 21: 3329-44.

Schmelzer E (2002) Cell polarization, a crucial process in fungal defense. Trends Plant Sci. **7**: 411-15.

Schmidt UG, Endler A, Schelbert S, Brunner A, Schnell M, Neuhaus HE et al. (2007) Novel tonoplast transporters identified using a proteomic approach with vacuoles isolated from cauliflower buds. Plant Physiol. 145: 216-29.

Schulze-Lefert P, Panstruga R (2011) A molecular evolutionary concept connecting nonhost resistance, pathogen host range, and pathogen speciation. Trends Plant Sci. 16:117-25.

Senthil-Kumar M, Mysore KS (2013) Nonhost resistance against bacterial pathogens:retrospectives and prospects. Annu. Rev. Phytopathol 51:19.1–19.21.

Sharma PC, Ito A, Shimizu T, Terauchi R, Kamoun S, Saitoh H (2003) Virus-induced silencing of WIPK and SIPK genes reduces resistance to a bacterial pathogen, but has no effect on the INF1-induced hypersensitive response (HR) in *Nicotiana benthamiana*. Mol. Genet. Genomics 269: 583-91.

Sharma PD (2004) Plant pathology: Genetic basis of host: pathogen interaction. Rastogi publications 70-84.

Shia W-J, Li B, Workman JL (2006) SAS-mediated acetylation of histone H4 Lys 16 is required for H2A.Z incorporation at subtelomeric regions in Saccharomyces cerevisiae Genes & Dev. 20: 2507-12.

Snyder BA, Leite B, Hipskind J, Butler LG, Nicholson RL (1991) Accumulation of sorghum phytoalexins induced by *Colletotrichum graminicola* at the infection site. Physiol. Mol. Plant Pathol. 39: 463-70.

Snyder BA, Nicholson RL (1990) Synthesis of phytoalexins in Sorghum as a site-specific response to fungal ingress. Science 248: 1637-39.

Stein M, Dittgen J, Sanchez-Rodriguez C, Hou BH, Molina A, Schulze-Lefert P, et al. (2006) *Arabidopsis* PEN3/PDR8, an ATP binding cassette transporter, contributes to non-host resistance to inappropriate pathogens that enter plants by direct penetration. Plant Cell 18: 731-46.

Takahashi D, Kawamura Y, Yamashita T, Uemura M (2012) Detergent-resistant plasma membrane proteome in oat and rye: similarities and dissimilarities between two monocotyledonous plants. J. Proteome Res. 11: 1654-65.

Takahashi Y, Nasir KHB, Ito A, Kanzaki H, Matsumura H, Saitoh H, et al. (2007) A Novel MAPKK involved in cell death and defense signaling. Plant Signal Behav. 25: 396-98.

Takemoto D, Yoshioka H, Doke N, Kawakita K (2003) Disease stress-inducible genes of

tobacco: expression profile of elicitor-responsive genes isolated by subtractive hybridization. Physiol. Plant 118: 545-53.

Thordal-Christensen H (2003) Fresh insights into processes of non-host resistance. Curr. Opin. Plant Biol. 6: 351-57.

Thordal-Christensen H, Zhang Z, Wei Y, Collinge DB (1997) Subcellular localization of H_2O_2 in plants. H_2O_2 accumulation in papillae and hypersensitive response during the barley-powdery mildew interaction. Plant J. 11:1187-94.

Torti SD, Dearing MD, Kursar TA (1995) Extraction of phenolic compounds from fresh leaves: a comparison of methods. J. Chem. Ecol. 21: 117-25.

Trujillo M, Ichimura K, Casais C, Shirasu K (2008) Negative regulation of PAMP-triggered immunity by an E3 ubiquitin ligase triplet in *Arabidopsis*. Curr. Biol. 18: 1396-01.

Tsuchiya K, Mew TW, Wakimoto S (1982) Bacteriological and pathological characteristics of wild types and induced mutants of *Xanthomonas campestris* pv. *oryzae*. Phytopathology 72: 43-46.

Tsukuda S, Gomi K, Yamamoto H, Akimitsu K **(**2006) Characterization of cDNAs encoding two distinct miraculin-like proteins and stress-related modulation of the corresponding mRNAs in *Citrus jambhiri*. Plant Mol. Biol. 60: 125-36.

Ulker B, Somssich IE (2004) WRKY transcription factors: from DNA binding towards biological function. Curr Opin Plant Biol. 7:491-98.

Uma B, Rani TS, Podile AR **(**2011) Warriors at the gate that never sleep: non-host resistance in plants. J. Plant Physiol. 168: 2141-52.

Underwood W, Somerville SC (2013) Perception of conserved pathogen elicitors at the plasma membrane leads to relocalization of the *Arabidopsis* PEN3 transporter. doi: 10.1073/pnas.1218701110.

Varma P, Mishra RK (2011) Dynamics of nuclear matrix proteome during embryonic development in Drosophila melanogaster. J. Biosci. 36: 439-59.

Vallet C, Chabbert B, Czaninski Y, Monties B (1996) Histochemistry of lignin deposition during sclerenchyma differentiation in alfalfa stems, Ann. Bot. 78: 625-32.

Van Loon LC, Van Strien EA (1999) The families of pathogenesis-related proteins, their activities, and comparative analysis of PR-1 type proteins. Physiol. Mol. Plant Pathol. 5:85-97.

Vanacker H, Carver TLW, Foyer CH (1998) Pathogen induced changed in the antioxidant status of the apoplast in barley leaves. Plant Physiol. 117: 1103-14.

Velikova V, Yordanov I, Edreva A (2000) Oxidative stress and some antioxidant systems in acid rain-treated bean plants: protective roles of exogenous polyamines. Plant Sci. 151:59-66.

Viloria Z, Drouilard DL, Grahm JH, Grosser JW (2004) Screening triploid hybrids of 'Lakeland' Limequat for resistance to Citrus canker. Plant Dis. 88:1056-60.

Visa N, Percipalle P (2010) Nuclear functions of actin. Cold Spring Harb. Perspect. Biol. :a000620.

Vorwerk S, Somerville S, Somerville C (2004) The role of plant cell wall polysaccharide composition in disease resistance. Trends Plant Sci. 9: 203-09.

Wang K, Senthil-Kumar M, Ryu C-M, Kang L, Mysore KS (2012) Phytosterols play a key role in plant innate immunity against bacterial pathogens by regulating nutrient efflux into the apoplast. Plant Physiol. 158:1789-02.

Wang X, Li X, Li Y (2007) A modified commassie brilliant blue staining method at nanogram sensitivity compatible with proteomic analysis. Biotechnol Lett. 29: 1599-03.

Watson BS, Lei ZT, Dixon RA, Sumner LW (2004) Proteomics of *Medicago sativa* cell walls. Phytochemistry 65: 1709-20.

Whalen MC, Stall RE, Staskawicz BJ (1988) Characterization of a gene from a tomato pathogen determining hypersensitive resistance in non-host species and genetic analysis of this resistance in bean. Proc. Natl. Acad. Sci. 85: 6743-47.

Wojtaszek P (1997) The oxidative burst: a plant's early response against infection. Biochem. J. 322: 4158-63.

Wydra K, Beri H (2006) Structural changes of homogalacturonan, rhamnogalacturonan I and arabinogalactan protein in xylem cell walls of tomato species in reaction to *Ralstonia solanacearum*. Physiol. Mol. Plant Pathol. 68: 41-50.

Xia Y, Suzuki H, Borevitz J, Blount J, Guo Z, Patel K, Dixon RA, Lamb C (2004) An extracellular aspartic protease functions in *Arabidopsis* disease resistance signaling. EMBO J. 23: 980-88.

Yang CW, Gonzalez-Lamothe R, Ewan RA, Rowland O, Yoshioka H, Shenton M, et al. (2006) The E3 ubiquitin ligase activity of arabidopsis PLANT U-BOX17 and its functional tobacco homolog ACRE276 are required for cell death and defense. Plant Cell 18: 1084-98.

Yang EJ, Oh YA, Lee ES, Park AR, Cho SK, Yoo YJ, Park OK (2003) Oxygen-evolving enhancer protein 2 is phosphorylated by glycine-rich protein 3/wall-associated kinase 1 in *Arabidopsis.* Biochem. Biophys. Res. Commun. 305: 862-68.

Ye M, Jiang X, Feng S, Tian R, Zou H (2007) Advances in chromatographic techniques and methods in shotgun proteome analysis. Trends in Analytical Chemistry 26: 80–84.

Yi H-C, Sardesai N, Fujinuma T, Chan C-W, Veena, Gelvin SB (2006) Constitutive expression exposes functional redundancy between the *Arabidopsis* histone H2A gene HTA1 and other H2A gene family members. Plant Cell 18: 1575-89.

Yoshioka H, Bouteau F, Kawano T (2008) Discovery of oxidative burst in the field of plant immunity: Looking back at the early pioneering works and towards the future development. Plant Signal Behav. 3: 153–55.

Yun BW, Atkinson HA, Gaborit C, Greenland A, Read ND, Pallas JA, et al. (2003) Loss of actin cytoskeletal function and *EDS1* activity, in combination, severely compromises nonhost resistance in Arabidopsis against wheat powdery mildew. Plant J. 34:768-77.

Zhang S, Klessig DF (2001) MAPK cascades in plant defense signalling. Trends Plant Sci. 6: 520-07.

Zhou JM, Chai J (2008) Plant pathogenic bacterial type III effectors subdue host responses. Curr. Opin. Microbiol. 11: 179-85.

Zimaro T, Gottig N, Garavaglia BS, Gehring C, Ottado J (2011) Unraveling plant responses to bacterial pathogens through proteomics. J. Biomed. Biotechnol.2011: 354801.

Zimmerli L, Stein M, Lipka V, Schulze-Lefert P, Somerville S (2004) Host and non-host pathogens elicit different jasmonate/ethylene responses in *Arabidopsis*. Plant J. 40: 633-46.

Zipfel C (2009) Early molecular events in PAMP-triggered immunity. Curr. Opin. Plant Biol. 12: 414-20.

Zurbriggen MD, Carrillo N , Tognetti VB , Melzer M , Peisker M, Hause B, et al. (2009) Chloroplast-generated reactive oxygen species play a major role in localized cell death during the non-host interaction between tobacco and *Xanthomonas campestris* pv. *vesicatoria.* Plant J. 60: 962-73.

Journal of Plant Physiology 168 (2011) 2141–2152

Contents lists available at SciVerse ScienceDirect

Journal of Plant Physiology

journal homepage: www.elsevier.de/jplph

Review

Warriors at the gate that never sleep: Non-host resistance in plants

Battepati Uma, T. Swaroopa Rani, Appa Rao Podile*

Department of Plant Sciences, School of Life Sciences, University of Hyderabad, Hyderabad 500046, India

ARTICLE INFO

Article history:
Received 16 July 2011
Received in revised form
19 September 2011
Accepted 20 September 2011

Keywords:
Extracellular matrix
Non-host resistance
Oxidative burst
Plasma membrane
Vesicle trafficking

ABSTRACT

The native resistance of most plant species against a wide variety of pathogens is known as non-host resistance (NHR), which confers durable protection to plant species. Only a few pathogens or parasites can successfully cause diseases. NHR is polygenic and appears to be linked with basal plant resistance, a form of elicited protection. Sensing of pathogens by plants is brought about through the recognition of invariant pathogen-associated molecular patterns (PAMPs) that trigger downstream defense signaling pathways. Race-specific resistance, (*R*)-gene mediated resistance, has been extensively studied and reviewed, while our knowledge of NHR has advanced only recently due to the improved access to excellent model systems. The continuum of the cell wall (CW) and the CW–plasma membrane (PM)-cytoskeleton plays a crucial role in perceiving external cues and activating defense signaling cascades during NHR. Based on the type of hypersensitive reaction (HR) triggered, NHR was classified into two types, namely type-I and type-II. Genetic analysis of *Arabidopsis* mutants has revealed important roles for a number of specific molecules in NHR, including the role of SNARE-complex mediated exocytosis, lipid rafts and vesicle trafficking. As might be expected, *R*-gene mediated resistance is found to overlap with NHR, but the extent to which the genes/pathways are common between these two forms of disease resistance is unknown. The present review focuses on the various components involved in the known mechanisms of NHR in plants with special reference to the role of CW–PM components.

Contents

Abbreviations: AGP, arabinogalactose protein; AVR, avirulence; CW, cell wall; CWA, cell wall apposition; eATP, extracellular adenosine triphosphate; ECM, extracellular matrix; GPI, glycosyl phosphatidyal inositol; HR, hypersensitive reaction; LR, lipid rafts; MAPK, mitogen-activated protein kinase; NHR, non-host resistance; PAMP, pathogen associated protein kinase; PCD, programmed cell death; PEN, penetration; PM, plasma membrane; PRR, pattern recognition receptor; R, resistance; ROS, reactive oxygen species; SNARE, soluble N-ethylmalemide-sensitive factor protein receptor; WAK, wall-associated kinase.

* Corresponding author. Tel.: +91 40 2313 4503; fax: +91 40 2301 0120.
E-mail address: arpsl@uohyd.ernet.in (A.R. Podile).

0176-1617/$ – see front matter © 2011 Elsevier GmbH. All rights reserved.
doi:10.1016/j.jplph.2011.09.005

Accepted in Physiologia Plantarum

Physiologia Plantarum
An International Journal for Plant Biology

Extracellular matrix-associated proteome changes during non-host resistance in citrus-Xanthomonas interactions

Journal:	*Physiologia Plantarum*
Manuscript ID:	PPL-2013-00332.R1
Manuscript Type:	Regular manuscript - Ecophysiology, stress and adaptation
Date Submitted by the Author:	01-Aug-2013
Complete List of Authors:	T, Swaroopa Rani; university of hyderabad, plant sciences Podile, Appa Rao; University of hyderabad, plant sciences
Key Words:	Non-host resistance, Extracellular matrix, Proteome analysis, Citrus, Citrus canker